Cellular and molecular analysis of branching morphogenesis in *Drosophila melanogaster*

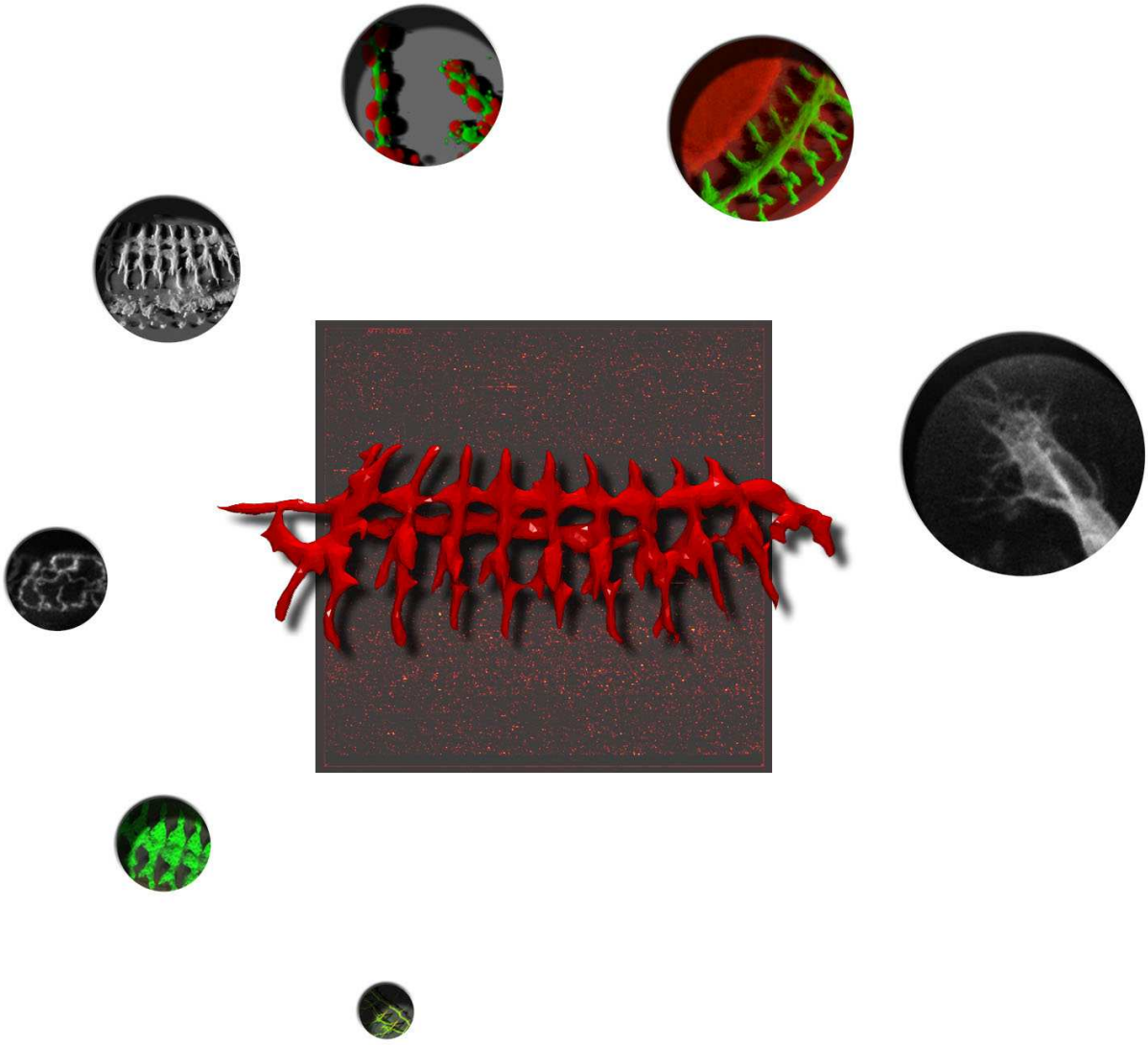

INAUGURALDISSERTATION

zur Erlangung der Würde eines Doktors der Philosophie
vorgelegt der
Philosophisch-Naturwissenschaftlichen Fakultät der Universität Basel
von

Carlos Ribeiro
aus Portugal

Ausgeführt unter der Aufsicht von Prof. Dr. Markus Affolter
Biozentrum der Universität Basel
Abteilung Zellbiologie

Basel, 2004

Genehmigt von der Philosophisch-Naturwissenschaftlichen Fakultät auf Antrag von

Prof. Markus Affolter

Prof. Walter J. Gehring

Prof. Silvia Arber

Basel, den 11. 2. 2003

Prof. Dr. Marcel Tanner
Dekan der Philosophisch-
Naturwissenschaftlichen Fakultät

This work is dedicated to my family. My mother Elvira Vidal Ribeiro (1945-1988) whose love never left us, my father Marcelino Joaquim Ribeiro whom I owe everything and my brother Marcos Ribeiro whose talents hold the possibility of a bright future.

Este traballho é dedicado a minha família. A minha mãe Elvira Vidal Ribeiro (1945-1988) cujo amor nunca nos deixou, meu pai Marcelino Joaquim Ribeiro a quem devo tudo e a meu irmão Marcos Ribeiro cujos talentos prometem a possibilidade de um grande futuro.

Thomas, because thou hast seen Me, thou hast believed. Blessed are they that have not seen and yet have believed.
- John 20:29

Success is the ability to go from failure to failure without losing your enthusiasm.
- Winston Churchill, 1874-1965

Index

Cellular and molecular analysis of branching morphogenesis in Drosophila melanogaster 1

Index *5*

Acknowledgments *8*

Abstract *10*

Preface *11*

Chapter 1 General introduction to the thesis *12*

Developmental cell biology **13**

The tracheal system as an ideal system for studying developmentally controlled cell biological processes **15**

Aim of the thesis **17**

Structure of the thesis **17**

Chapter 2 Introduction to optical and functional genomic methods in modern biology *19*

Structure and chemical properties of GFP-like proteins 20
Variants of GFP and other fluorescent proteins 22

Optical methods in modern biology **23**
In vivo imaging 24
Studying protein dynamics in living cells 25
Fluorescence Resonance Energy Transfer (FRET) 25
Fluorescence Recovery After Photobleaching (FRAP) 27
Fluorescence Correlation Spectroscopy (FCS) 27
Expressed fluorescent tags for signaling proteins 28
Evanescent field microscopy 29
Deconvolution microscopy 30
The Drosophila embryo as an excellent in vivo visualization system 31

Genomics and large scale gene expression profiling **32**
Sequencing of the Drosophila genome and its implications 32
Large scale gene expression profiling 33

Chapter 3 Signaling systems, guided cell migration and organogenesis: insights from genetic studies in Drosophila *37*

Introduction **38**

Migratory systems and their signaling mechanisms **40**
Hemocytes 40
Germ cells 40
Border cells 41
Tracheal cells 43

Comparison between the different systems **44**

Chapter 4 Regulation of cell migration during tracheal development in Drosophila melanogaster *48*

Current view of cell migration of individual cells over a two dimensional substrate **49**
Regulation of motility of cells in culture 51
An important role for small Rho GTPases in cytoskeletal reorganization required for cell migration 51
Downstream effectors of small G proteins in cell migration 52
Regulation of G protein activity by extracellular ligands 53

Regulation of migration *in vivo* **54**

The tracheal system of Drosophila melanogaster 54
Tracheal cell fate determination 54
Subdivision of the tracheal placode 56
Guided migration of primary tracheal cells 57
Additional substrates for migration 59

Cell migration in vivo: which processes are controlled by extracellular signals? 59

Chapter 5 Introduction to cellular junctions in Drosophila epithelial cells 62

Chapter 6 In vivo imaging reveals different cellular functions for FGF and Dpp signaling in tracheal branching morphogenesis 66

Introduction 67

Results 69
Formation of actin-containing cellular extensions during tracheal cell migration 69
The formation of cell extensions is a dynamic process 71
Dpp signaling is required for branch outgrowth, but not for the formation of cellular extensions 73

Discussion 77
Bnl/FGF is required and sufficient to induce the formation of cellular extensions 77
Bnl/FGF and Dpp signaling have distinct effects on the formation of dorsal tracheal branches 78
FGF signaling leads to cytoskeletal changes in other developmental contexts 80

Chapter 7 Junctional remodeling during Drosophila tracheal branching morphogenesis. 81

Introduction 82

Results 84
Dα-cetenin-GFP as a marker for junction remodeling during tracheal morphogenesis 84
Detailed analysis of the transition from a multicellular to a unicellular tube 86
Effect of tracheal Dad overexpression on AJ remodeling 88
Reintegration of dorsal buds in Dad overexpression embryos is not due to inefficient following of the dorsal Bnl spot by tracheal cells 90
Sal is responsible for the reintegration of the dorsal tracheal cells 91
Dpp signaling is not necessary for the intercalation of dorsal branch cells 93
Sal overexpression represses unicellularization 95

Discussion 96
Adherens junction remodeling during unicellularization 96
The effect of Dad overexpression is mainly visible on the AJs and reminiscent of ribbon 97
Kni/Knrl exert their function to a large extent by repressing sal 98
“Affinity group model” of tracheal branch formation 100

Chapter 8 Transcriptional profiling of different branching morphogenesis programs 103

Introduction 104

Results 104
Cell isolation and sorting 104
Oligonucleotide analysis of whole embryos expressing Dad or a constitutive active form of the Dpp receptor throughout the tracheal system 108
Overview of the differentially regulated genes obtained by the comparison of both genetic backgrounds 110
In situ hybridization of candidate genes 112

Discussion 115

Chapter 9 Final discussion, conclusions and outlook 117

Summary of the in vivo microscopy data 118
Bnl/FGF Is Required and Sufficient to Induce the Formation of Cellular Extensions 118
Bnl/FGF and Dpp Signaling Have Distinct Effects on the Formation of Dorsal Tracheal Branches 118
Intercalation of the dorsal branches is a highly complex junctional remodeling process 119
Dad overexpression inhibits reorganization of the adherens junctions but Dpp signaling is not required for unicellularization 119

Kni/Knrl exert their function to a large extent by repressing sal 120

Open questions in branching morphogenesis of the tracheal system 120
Technical challenges 121
Multiple color labeling 121
Spinning disc confocal microscopy 121
Fluorescence recovery after Photobleaching (FRAP) 122
Fluorescence resonance energy transfer (FRET) 122
New subcellular markers and protein traps 123
Biological questions 123
How is the chemoattractive signal of Bnl/FGF mediated on the cytoskeleton? 123
How do filopodia control migration? 125
Can Bnl/FGF induce migration in all ectodermal cells? 126
Why are filopodia confined to the tip cells? 126
What is the contribution of the microtubules in guiding migration in the tracheal system? 127
Is Bnl/FGF induced motility the only driving force of morphogenesis of the tracheal system? 127
How is *bnl* expression regulated? 127
How is a new tube formed? 128
How do tracheal cells interact with the surrounding tissue? 128
How does Sal control cell rearrangements? 128

Finding new factors involved tracheal morphogenesis is the way to go 129

Our Final model 130

Concluding remarks 131

Materials and methods 132

***Drosophila* Strains and Genetics 133**

Immunostainings and whole-mount in situ hybridization 134

Embryo mounting for *in vivo* visualization 134
Standard mounting of living embryos 134
"Hanging drop" mounting of living embryos 135

Time-lapse Confocal Microscopy 136

Deconvolution 136
Image collection for deconvolution 137
Deconvolution procedure using Huygens Essential 138

3D and 4D Reconstructions 141

Cell dissociation 141

Total RNA extraction from limited amount of material (according to Lydia Michaut) 142

Embryo collection and RNA extraction for array analysis 142

High-density oligonucleotide arrays and hybridization 143

Data analysis 143

References 145

Appendix 163

CURRICULUM VITAE 165

Publications 167

Acknowledgments

First, I would like to thank Markus Affolter, the driving force behind this thesis. With his enthusiasm, scientific instinct and knowledge he has strongly shaped the hereby-presented work. He has allowed me to do things in my own way while granting me all his support. Thank you very much! I also didn't think we would have to deal with vesicles and junctional proteins but that is how it went.

I am also deeply indebted to the people of the lab. Many thanks go to Andy Ebner, with whom I entered the lab and with whom I shared many projects. We spent a lot of time in the same boat and he has always been a friend. Inside and outside the lab. Alain Jung, for bad movies, enlightening fondues, J.S. Bach and for sharing the desperation of chips. Many thanks also for the critical reading of the chips section of this thesis. Marc Neumann, for joining me in the exploration of the living embryo, BMW movies, Civ and VERY CRITICAL reading of the thesis manuscript. With such a talent in the team, the tracheal system will soon have lost most of its mysteries. Britta Hartmann for the many hours in the Cargo Bar and for following me into the challenge of tango. Valérie Petit from whom I learned a lot and with whom I had many enlightening discussions. Her intelligence is only equaled by her great personality. Ute Nussbaumer, for managing the lab with an unmatched efficiency and kindness. Without her, the lab would stop working. Liliane Devaja for help fighting the monster of bureaucracy. Caroline Dossenbach, with whom I took my first salsa course. Clemens Cabernard our new fly-expert and all the remaining and former members of the lab: Jorgos Pyrowolakis, Samir Merabet, Christina Nef, Anja Jazwinska, Thomas Marty, Stephane Vincent, Alessandra Vigano and Jay Groppe. Thank you all, for making this laboratory such a great place!

Many thanks go to all the present and former members of the Department of Cell Biology. I would especially like to thank Prof. Walter Gehring. His contribution in purchasing the confocal microscope has greatly influenced the course of my work. I owe many thanks to Lydia Michaut. She was extremely competent and patient in teaching me the extraction of RNA, use of the Agilent Bioanalyzer and all aspects of Affymetrix oligonucleotide array use. Without her time and effort, these experiments would not have been possible. Special thanks also go to Greta Backhaus, Sabie Dettwiler, Isabelle Kaufmann Frédéric Prince and Simon Hippenmeyer. I would also like to thank Pia Däppen-Senn, Bernadette Bruno, Gina Evora and Karin Mauro for the never-ending supply of fly food, buffers, and clean lab ware.

Many thanks go to Markus Dürrenberger whose constant help with the microscopes is invaluable. To the people of the Reichert lab and the Genetics Pharmaceuticals Division of Hoffmann-La Roche for help in the transcript imaging project. To Mark Dessing and Annette Pickert at the defunct Basel Institute of Immunology for help with the FACS analysis. To the organizers, speakers and participants of the advanced *Drosophila* genetics course in Cold Spring Harbor. Especially: Sofia Lavista Llanos and Marco Gallio. We had a great time! To the participants of the Alp Piora retreat. Especially Mike Levine and Ernst Hafen who are not innocent in the fact

that we dared to venture into the chip project.

This work would never have been possible without the willingness of the fly community to share research material. Special thanks go to Kathy Mathews, the Bloomington *Drosophila* Stock Center at Indiana University and the FlyBase team. Thank you all!

It is needless to say that the deepest thanks go to all the people that have contributed to my thesis work by supporting me personally, and who made this chapter of my life a very enjoyable and memorable one. I feel mostly indebted to Kerstin Greve, Salome Röck, former and present flatmates, Dirk Wauschkuhn, Sara Cignacco and my family.

Abstract

In the developing tracheal system of *Drosophila melanogaster*, six major branches arise by guided cell migration from a sac-like structure. The chemoattractant Branchless/FGF (Bnl) appears to guide cell migration and is essential for the formation of all tracheal branches, while Decapentaplegic (Dpp) signaling is strictly required for the formation of a subset of branches, the dorsal and ventral branches.

The aim of this thesis was the analysis of the cellular mechanisms governing tracheal branching morphogenesis and the identification of new genes implicated in this process using large scale gene expression profiling.

Using *in vivo* confocal video microscopy, we find that Bnl/FGF and Dpp signaling affect different cellular functions required for branching morphogenesis. Bnl/FGF signaling affects the formation of dynamic filopodia, possibly controlling cytoskeletal activity and motility as such, while Dpp controls cellular functions allowing branch morphogenesis and outgrowth.

Further, we characterized the junctional remodeling events underlying cell intercalation in the dorsal branch and show that unicellularization is not induced by Dpp signaling. Dpp signaling is shown to be mainly required for the repression of *sal* in the dorsal branch. Therefore concomitant removal of Sal and Kni/Knrl leads to a rescue of dorsal branch formation. We also show that tracheal Sal controls cell-cell adhesion properties, leading to the formation of cell populations with different adhesive properties. These adhesive properties control cell rearrangements and branch formation. Based on these observations, we propose a model for tracheal morphogenesis, whose main features consist of Bnl/FGF induced cytoskeletal activity and motility, and Sal regulated cell adhesion modulation.

We also performed an oligonucleotide array screen for Sal and Kni/Knrl targets in the tracheal system. Unfortunately, due to multiple reasons discussed in this thesis, this approach was not successful and had to be abandoned.

Preface

Instead of directly binding the reprints of the publications, I authored or co-authored directly into my thesis, I have chosen to integrate these in a more coherent way into the text. I hope that this will lead to a smoother structure of this dissertation. Additionally, I have chosen to use the unabbreviated versions of the publications as I am persuaded that they are of a higher quality than the shortened printed articles. In this way, I also want to honor the excellent work of my coauthors in writing exhaustive scientific treatise of high quality.

I would also like to point out the fact that chapter 8 on the “transcriptional profiling of different branching morphogenesis programs” was kept short. This is because we were not successful in confirming the candidate genes by *in situ* hybridization and therefore no data on the function of these genes in trachea is available. Additionally, with the dissolution of the Basel Institute for Immunology, the original data of my cell sorting experiments were lost. Due to the general interest into the sorting protocol and the huge amount of effort put into this project, I have nevertheless decided to write a chapter on these studies.

For an overview on the general structure of the thesis, see the corresponding passage in chapter 1.

I hope the reader will appreciate the reading!

Chapter 1

General introduction to the thesis

Developmental cell biology

Once more during its exciting and never-ending success story, *Drosophila* research is reinventing itself. After starting its long journey through our textbooks, teaching us the logic behind heredity, genetics and development, a new chapter is starting. Developmental biologists have now begun to integrate our knowledge on fundamental cell biological processes into developmental biology. And once more *Drosophila* is proving that it is one of the best systems for performing such studies.

Since, at the beginning of the eighties, the groundbreaking studies of Christiane Nüsslein-Volhard and Eric Wieschaus (Nusslein-Volhard and Wieschaus, 1980) proved that genetics could be used to dissect the molecular mechanisms of development, innumerous screens have been performed to identify genes involved in all imaginable biological and developmental processes. These studies rapidly led to an explosion in our knowledge of the important factors involved in most of these processes.

A first climax in these efforts was the cloning of the homeotic gene *Antennapedia* in the laboratories of Matthew Scott and Walter Gehring in 1983 (described in Gehring, 1998). Homeotic mutations are mutations which can give raise to a dramatic change in the patterning of an organism, leading *e.g.* in *Drosophila* to the transformation of a segment into the likeliness of another one. These mutations had been extensively studied by Edward B. Lewis to whom we owe most of our knowledge on the genetics of this complex class of genes (Lewis, 1978). When cloned and sequenced the homeotic genes were shown to contain a common and highly conserved sequence stretch termed the homeobox, which could also be found in other essential *Drosophila* genes like *fushi tarazu* for example. The impact of this discovery went nevertheless further than the molecular characterization of the proteins for which these key players of development coded. It was the notion that homeotic genes were present, similarly organized and conserved at the sequence as well as the functional level in vertebrates, which had a major impact in the way we think of developmental biology nowadays.

Since at a first glance, vertebrates and insects develop in rather different ways, it was thought that the molecular basis of development of organisms from different phyla had to be rather different too. This idea was seriously challenged by the new discovery, which showed that such important regulators as the homeotic genes were used in most organisms in a rather similar fashion. This meant that even if detailed developmental processes could strongly differ among the different phyla, the basic strategies underlying development had remained conserved among most multicellular organisms. This discovery opened a realistic possibility that the knowledge to be gained on the molecular basis of development, would apply to the very complex process of shaping a nascent human, giving an unprecedented boost to *Drosophila*

developmental biology. Once more the gap between men and flies had shrunk.

Strikingly, most interesting phenotypes found in the major genetic screens were due to mutations in genes coding for two types of molecules: transcription factors and proteins involved in signal transduction.

The best example for the importance of transcription factors are, as outlined above, the homeotic genes, which encode homeodomain containing transcription factors. However, *Drosophila* research of the last two decades also harbors an excellent example for the discovery and dissection of signaling pathways.

Using the development of the adult eye as a model system, a handful of laboratories illuminated the logic behind the inductive determination of the omatidial cells in the eye (for an excellent review see Freeman, 1997). Triggered by the discovery of the *sevenless* gene in the Benzer laboratory and subsequent cloning, which showed that *sevenless* coded for a Receptor Tyrosine Kinase (RTK) (Hafen *et al.*, 1987) a number of genetic modifier screens proved spectacularly successful in uncovering the signal transduction pathway underlying these inductive events. These studies were the main basis on which the now widespread observation was founded that RTK signaling is mainly conveyed by the Ras pathway (reviewed by Dickson and Hafen, 1994).

One question however remains mostly unanswered: How do transcription factors and signaling pathways perform their biological role? Or alternatively stated: Which are the effector genes performing the cellular roles under the control of transcription factors and signaling pathways? In contrast to the initial spectacular success story of the characterization of the homeotic genes, the functional dissection of their target genes has been disappointing. Almost twenty years after the cloning of the first homeotic genes, very few target genes are known and we have almost no idea as to which mechanisms make a cell in a segment different from cells in other segments.

Ironically, the main strengths of fruitfly research could be the main reason for this gap. Because genetic loss of function screens, on which Drosophilists mainly rely to gain new insights, are very likely to miss the components mediating the cellular effect of transcription factors and signaling pathways. The reason might be that these components control essential cellular processes, which when mutated lead to the death of the cell (these mutations are therefore termed “cell lethals”). Additionally, the mother deposes these components in large quantities in the egg, making it more difficult to uncover their function in embryogenesis by analyzing zygotic mutants. Excellent examples for this dilemma are the genes coding for cytoskeletal proteins like actin and tubulins. No one doubts that these genes are main targets of most morphogenetic events, but it remains extremely challenging to prove this genetically.

A further problem relies in the fact that these components essential for key steps in development do not act by themselves (redundancy) and are therefore strongly buffered for

perturbations. Good examples for this phenomenon are the analysis of *Drosophila* gastrulation and germ cell migration (reviewed in Starz-Gaiano and Lehmann, 2001). Very few genes have been found to have an effect by themselves on these processes when mutated. If at all, these genes have to be expected to have a minor phenotype when mutated. We are therefore faced with the ironic situation that the genes of main interest to understand the cellular mechanisms of development, give either extremely strong or only minor phenotypes.

For all these reasons, *Drosophilists* have developed novel technical approaches to circumvent these problems. Clonal analysis and the enhancer trap technique are very good example for these tools.

Clonal analysis permits the study of mutations that otherwise lead to very early or very strong phenotypes (Golic and Lindquist, 1989; St Johnston, 2002). It is however technically trickier than the direct analysis of the zygotic phenotype and can not always be used in the context of interest (*e.g.* tracheal cells do not divide anymore and are therefore not suited for clonal analysis) strongly reducing its benefit.

Also the development of the enhancer trap technique was a major technical breakthrough and proved extremely successful in identifying novel genes (Bellen *et al.*, 1989; O'Kane and Gehring, 1987). Interestingly, the enhancer trap technique was a considerable shift in the philosophy of gene identification in *Drosophila,* as one did not start by the mutant phenotype of the gene but by its expression pattern. In a certain way, the now very fashionable use of microarrays to identify genes has also adopted this philosophy.

Nevertheless, the identification of candidate genes for a certain process does not say anything about their functional implication in the process analyzed. Consequently, *Drosophila* research is faced with a new challenge: To integrate the available and extremely valuable knowledge on the factors involved in all possible biological and developmental processes with the knowledge on other more basic cellular process gained from biochemical and cell biological studies. The fruitfly with its unchallenged panoply of techniques and one century worth of knowledge, is the ideal system to clarify in the context of a whole organism, how regulatory mechanisms act on the basic cellular machinery to shape its development. Developmental cell biology is emerging as a new major current inside classic developmental biology. New technical approaches, especially visualization techniques are helping to elucidate the cellular mechanisms underlying morphogenetic events.

The tracheal system as an ideal system for studying developmentally controlled cell biological processes

The tracheal system of *Drosophila* consists of a branched network of epithelial tubes that provides oxygen from the environment to all tissues of

the body (for reviews see Affolter and Shilo, 2000; Manning and Krasnow, 1993; Metzger and Krasnow, 1999; Shilo *et al.*, 1997). The interconnected network develops from individual clusters of ectodermal cells that invaginate into the underlying mesoderm and form 10 sacs on each side of the embryo, each containing about 80 cells. Without further cell divisions, each sac forms five to six primary branches (dorsal branch, dorsal trunk anterior and posterior, lateral branch anterior and posterior, and visceral branch) by stereotypical, directed cell migration (see Fig. 1). Each of these branches has a defined identity that specifies tube size and the subsequent determination of specialized cell fates at precise positions and in the appropriate number. Most branches differentiate a number of terminal cells, which form fine cytoplasmic extensions through which gas is exchanged with the target tissues. In addition, fusion cells at the extremity of dorsal and lateral branches and the dorsal trunk allow the interconnection of adjacent tracheal metameres, leading to the formation of a continuous luminal network (Samakovlis *et al.*, 1996).

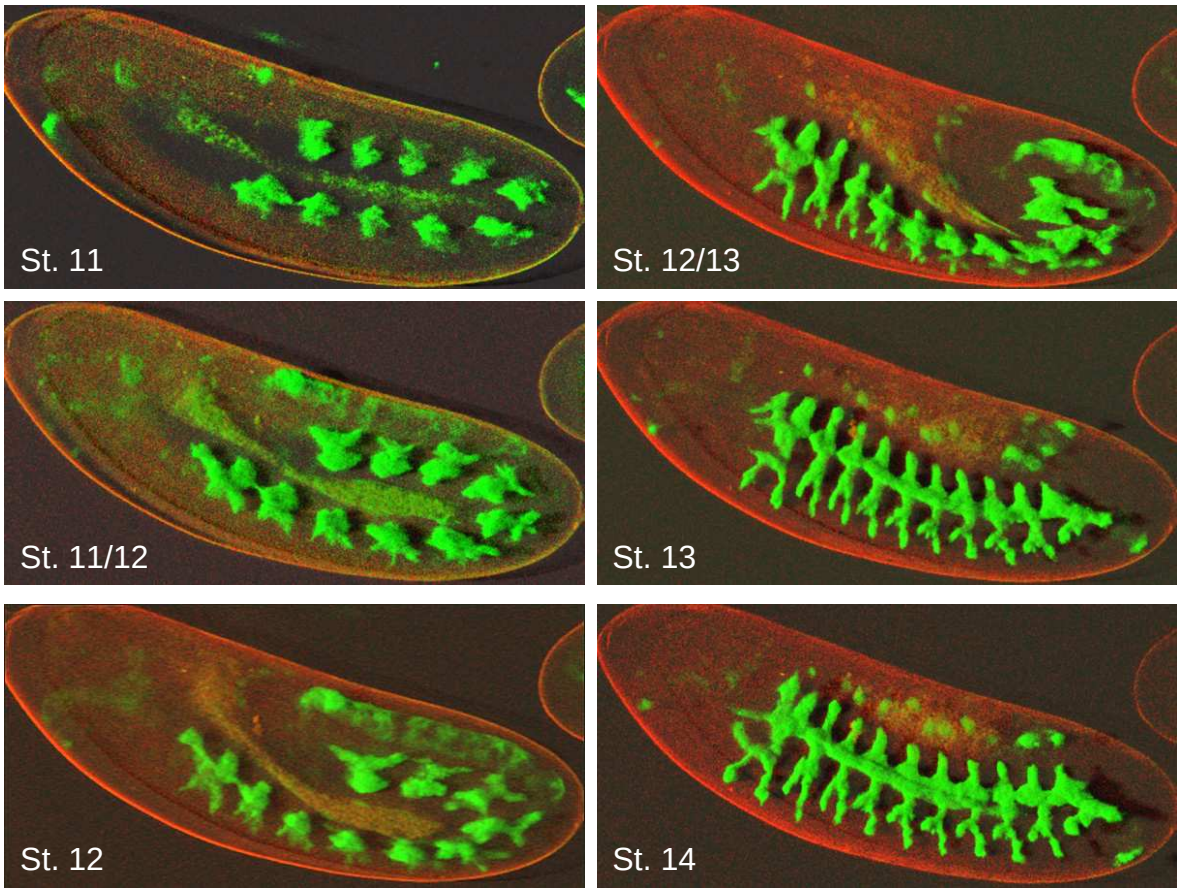

Figure 1 *Development of the tracheal system of* Drosophila melanogaster. Time-lapse 3D reconstruction of a living embryo expressing GFP in the tracheal system.

Years worth of effort have led to the identification of the primary signaling and patterning events controlling branching morphogenesis of the tracheal system. Bnl/FGF signaling acts as a chemoattractant that sculpts the tracheal system by inducing the directed outgrowth of the primary branches. Decapentaplegic (Dpp) and Wnt signaling are additionally responsible for the induction of Knirps/Knrl (Kni/Knrl) and Spalt (Sal) respectively, which are essential for branch formation by conferring branches a specific identity. It has however remained largely elusive as to which cellular processes mediate the effect of these signaling systems that lead to the formation of the esthetically very appealing shape of this larval organ.

The tracheal system therefore offers an excellent paradigm for studying how known patterning and signaling systems act on the cellular machinery to shape the form of an organ. The absence of cell division, the availability of many mutants affecting its morphogenesis, its stereotyped and well-characterized development as well as the aptitude to visualize its development *in vivo* make it the system of choice to study the cellular and molecular basis of branching morphogenesis.

Aim of the thesis

The aim of the thesis was one the one hand to identify and characterize the cellular events underlying the branching morphogenesis of the tracheal system of *Drosophila melanogaster*. On the other hand, to identify new players controlling branch identity and branch formation. To reach these goals the use of new technologies was an important factor of the hereby-presented work.

In vivo time-lapse confocal analysis of the tracheal system was established in order to analyze the effects of mutations affecting tracheal morphogenesis, at the cellular level, inside the living embryo. This approach proved to be an extremely powerful method to study the cellular basis of branching morphogenesis.

Large-scale gene expression profiling using oligonucleotide arrays was the method chosen to identify new genes controlling branch establishment and identity. Unfortunately, this method did not produce the desired results and had to be abandoned. The identification of new tracheal genes remains however a central goal for understanding the molecular basis of branching morphogenesis.

Structure of the thesis

Parts of the hereby-presented work are based upon articles published during my thesis. Due to the highly technical nature of the projects, a large introductory chapter at the beginning of the thesis deals with the optical and functional genomics

methods available nowadays in modern biological research.

The next two chapters are from two review articles, which deal with the present knowledge on migratory systems. Chapter 3 describes and compares the major migratory systems being studied in *Drosophila* while chapter 4 describes the knowledge on migration gained from cell culture studies and compares it to our current knowledge on tracheal development. For a detailed introduction to the development of the tracheal system please read the passage on the "regulation of migration *in vivo*" in chapter 4.

.

Chapter 5 gives a brief overview over our current understanding of cellular junctions in *Drosophila*.
Chapter 6, 7 and 8 represent the original scientific contributions performed during the period of the thesis. Chapter 6 and 7 deal with the dissection of the cellular events underlying branching morphogenesis using *in vivo* time-lapse confocal microscopy while chapter 8 describes the unsuccessful function genomic approach we chose to identify new genes controlling branch formation in the tracheal system.

The major points of this thesis are discussed in the concluding chapter 9. These observations are complemented by an outlook and concluding remarks.

Chapter 2

Introduction to optical and functional genomic methods in modern biology

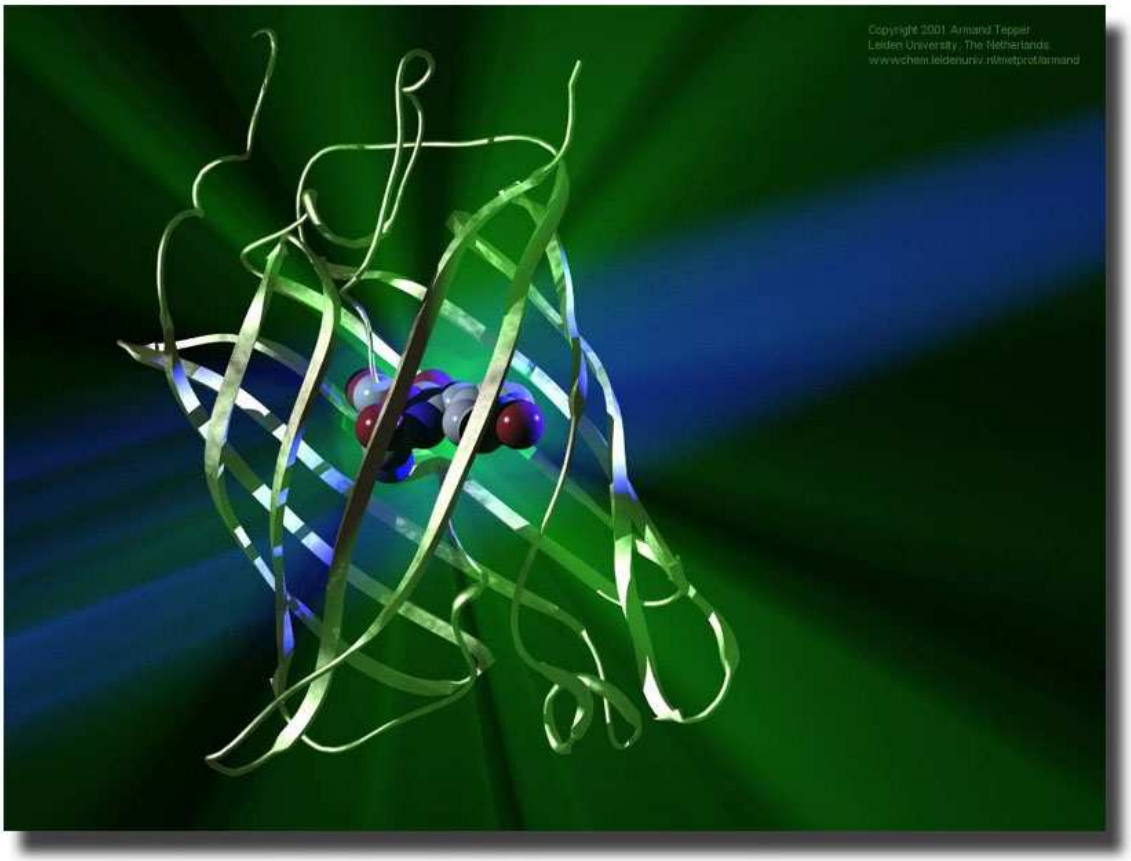

Genetically encoded fluorescent probes

The last five years have witnessed a spectacular revolution in cell biology, which is staging a small protein with astonishing properties. If *Drosophila melanogaster* is the genetic proof of god then the Green Fluorescent Protein (GFP) of the jellyfish *Aequorea victoria* is the cell biological proof of the same existence. It is by itself naturally fluorescent, functions in almost all organisms and tissues, does not require fixation for analysis, is relatively resistant to photobleaching and is small and non-toxic. Additionally, because it is compatible with the filter sets of almost all fluorescent microscopes its use does not require a change in equipment. Would any biologist have it designed differently? For an extensive review on GFP I would like to point to the excellent review by (Tsien, 1998).

Structure and chemical properties of GFP-like proteins

Members of the GFP family of proteins represent the only known biochromes, which catalyze their own synthesis from moieties of their own polypeptide chain and do therefore not require any other external agent for gaining their optical properties (Fig. 2). Additionally, as the newly synthesized pigment remains covalently attached within the protein (therefore being a *bona fide* chromophore instead of a pigment), the same protein molecule becomes the one to display the fluorescence. As a result, expression of the gene coding for a GFP-fusion protein directly leads to the appearance of fluorescence signal and therefore the location of the signal is essentially determined by the location of the mature protein.

As mentioned GFP-like proteins are astonishing enzymes as they have the capacity to perform the multiple autocatalytic reactions leading to the mature chromophore by themselves. The chromophores of GFP-like proteins however do differ notably in their covalent structures (Fig. 2). Despite this chromophore diversity, all GFP-like proteins use the same basic polypeptide fold termed “beta can” (Fig. 3) (see Matz *et al.*, 2002 for an excellent review on the biology of GFP-like proteins, their evolutionary history and the hunt for new spectral variant members of this family).
.

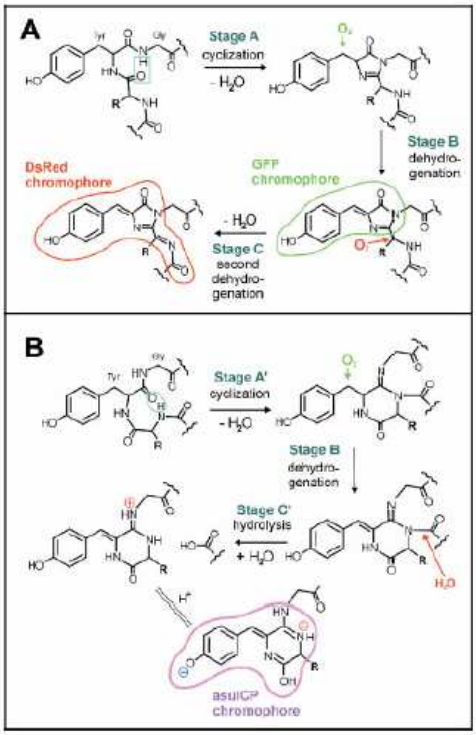

Figure 2 *Formation of chromophore in some color classes of GFP-like proteins.* Note that the substrate for the biosynthesis is three consecutive amino acids within the polypeptide chain of the same protein molecule that performs the catalysis. (A) Chromophore formation in proteins of green class represented by GFP (stages A and B) and orange-red class represented by DsRed (stages A, B and C). (B) Non-fluorescent purple class represented by asulCP.(From Matz *et al.*, 2002).

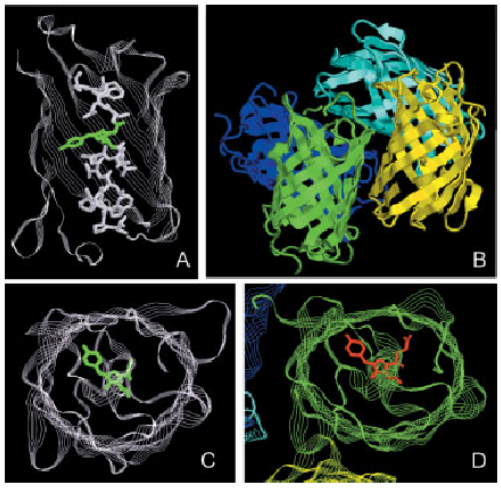

Figure 3 *Summary of the structure of GFP-like proteins*. (A) Cartoon of the beta-can of *Aequorea victoria* GFP. The front wall of the beta-can has been dissected to show the chromophore-bearing helix (sticks model) going through the middle of the can; the chromophore is green. (B) Tetramer (''four-pack'') of DsRed (C) Beta-can of GFP viewed from top, chromophore is green. (D) Monomer of DsRed viewed from top, the chromophore is red. Other monomers (blue and yellow) within the same tetrameric unit are partially visible. Note the slight deformation of the barrel in DsRed as compared to GFP. In C and D, the chromophore is shown as a sticks model, the rest of the protein is shown as strands models. The cartoons were generated using RasMol software, version 2.6 (From Matz *et al.*, 2002).

Variants of GFP and other fluorescent proteins

Due to the obvious usefulness of this class of proteins, scientists are trying to expand the available sorts of fluorescent proteins. For this effect, two main strategies have been chosen. On the one hand, they have become a favorite target for biotechnological modifications. To take full advantage of its unique "genetically encoded fluorescence", efforts have been undertaken to generate new spectral variants and to modify its folding and oligomerization properties. Additionally, a whole arsenal of fluorescent proteins with modified physical properties as, for example, pH sensitivity, degradation sensitivity and fluorescence lifetime, have been engineered (Zhang *et al.*, 2002). Targeted mutagenesis has resulted in the development of the now widely used "improved" version of GFP termed EGFP and three new spectral variants of GFP: Blue GFP (BFP, not widely used due to its bad optical properties), Cyan GFP (CFP) and Yellow GFP (YFP) (Fig. 4 and 5).

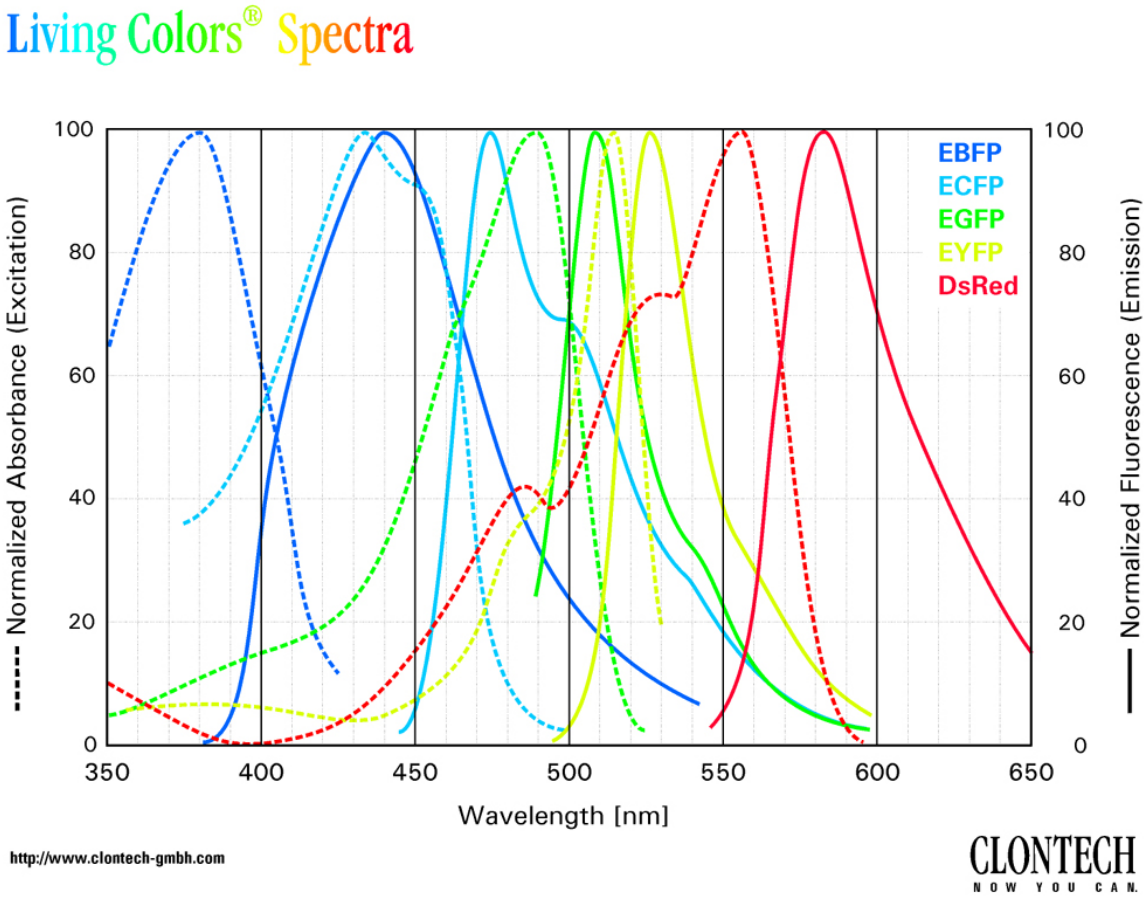

Figure 4 *Emission and absorption spectra of different GFP variants*

On the other hand a hunt for new natural spectral variants has begun (see Matz *et al.*, 2002 and Fig. 5). The discovery of new fluorescent proteins from Anthozoans for example has expanded the range of the available spectrum to the red. DsRed (*Discosoma striata*) and

HcRed (*Heteractis crispa*) were especially welcomed by the scientific community as they presented the possibility to solve the problem of autofluorescence in many biological systems, which is notably less pronounces in the long-wave region of the spectra (Matz *et al.*, 2002). The newly available palette of colors enabled for the first time *in vivo* triple-color labeling and detection. Unfortunately, the fact that these fluorescent proteins from corals were shown to form very tight oligomers (therefore they are not useful for tagging experiments) and to require a very long maturation time (approximately 30 hours), strongly reduced its use for most experimental applications and lead to a dispersal of the hopes of many scientists. But also in this case, reengineered variants of DsRed are making this tool more suitable for the scientific community. Recently a fast folding monomeric variant of DsRed was published (the result of 33 mutations!) which promises to solve most problems severely limiting its use (Campbell *et al.*, 2002). And this is surely not the last addition to the highly useful family of the fluorescent proteins.

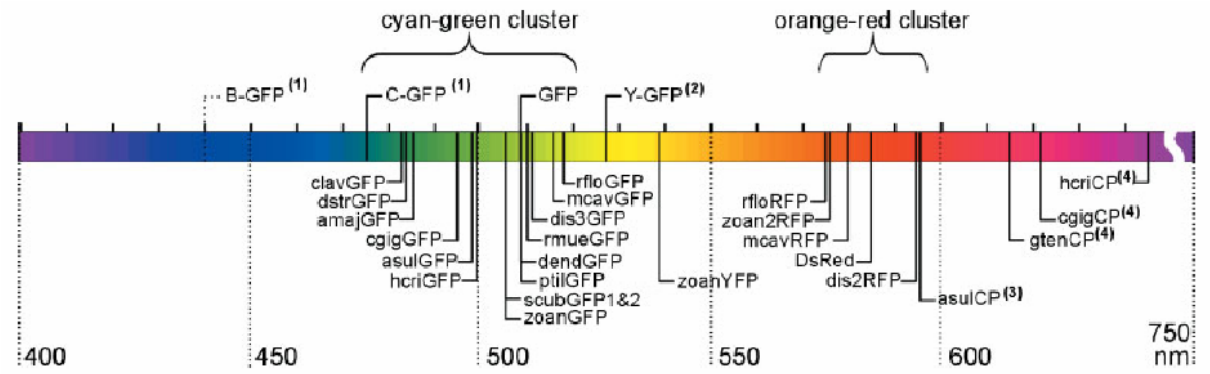

Figure 5 *Summary of the emission maxima in the current collection of GFP-like proteins and their mutant variants available for biotechnology applications.* GFP from A. victoria and its mutants are shown above the rainbow bar. (1) GFP mutants described in (Heim et al., 1994), B-GFP is indicated by dotted line due to decreased photochemical stability. (2) GFP mutant described in (Ormo et al., 1996). (3,4) Fluorescent mutant variants of originally non-fluorescent proteins of the purple-blue color class, described in (Lukyanov et al., 2000) and (Gurskaya et al., 2001) respectively. (From Matz et al., 2002)

Optical methods in modern biology

All major scientific discoveries are preceded by observations. The careful analysis and description of a problem is the basis of every scientific undertaking. As humans are strongly visual animals, pictures, diagrams and visual allegories have since the beginning of history been the strongest ally of the scientist. Biology is a good example for this. The first microscopic images of cells, for example, led Theodor Schwann to the conclusion that all living organisms are made up of cells (Harris, 1995; Schwann, 1847). Aren't we still fascinated by the drawings of Ramon y Cajal? Is there a symbol that has been used more widely to symbolize modern science than the DNA double helix? A chemical

structure turned into a visual allegory for scientific progress.

Therefore, it does not come as a surprise that advances in biology have been strongly correlated with advances in optical methods. The use of achromatic lenses, for example, strongly improved the use of the microscope by removing the chromatic artifacts of the first models built by Dutch craftsmen therefore allowing the first subcellular observations to be made. And to give a further example, it was the needs of biologists that lead to the development of the laser scanning confocal microscope (for an essay on the history of microscopy and biology see Amos, 2000).

The last years have seen an explosion in the use of optical methods in modern biology. The discovery and development of GFP, improvements in the optical equipment (especially the development of the laser scanning confocal microscope) and the urgent need to assign a functional role to the innumerous orphan proteins annotated by the genome sequencing projects have triggered a renaissance of visualization techniques in biology. This is especially the case for developmental biology. As (Lichtman and Fraser, 2001) put it "Developmental neurobiology is the study of change" and requires methodologies which allows the study of these dynamic processes inside the developing living organism.

In vivo *imaging*

In the last century, modern biology has been highly successful in deciphering many processes shaping biological systems. Approaches ranging from molecular studies to the analyses of cells *in vitro* and genetic studies have helped to narrow the focus and provide insight into developmental processes. However, sooner or later, the lessons learned from these studies must be integrated into an understanding of the intact, living organism.

In vivo imaging coupled with advances in optical methods and GFP allow the analysis of these complex processes inside the developing embryo. This approach has many advantages (Lichtman and Fraser, 2001).

First of all, these methods allow the observation of dynamic processes inside the organism. Using standard techniques developmental biologists had to rely on known morphological characteristics of the developing organism to arrange the analyzed samples into a chronological order and deduce the temporal sequence of events underlying the observed phenomenon. It is clear that this is not the method of choice. Especially because the time resolution of this method is very low (in the range of hours). However, most studies actually do not even perform such a developmental analysis but rather rely on the final phenotype of a manipulation to deduce the function of their molecule or process of interest.

Additionally, such static observations rely on histochemical manipulation of the organism, which requires the previous fixation of the animal tissue. It can however be very difficult to fix the structures of interest without loosing them. This is especially true for metastable structures as for example cellular extensions and cellular junction complexes in which developmental cell biologists have become especially interested in recent years.

Using *in vivo* visualization techniques one can overcome these hurdles and observe the cellular behavior of proteins and structures inside the living organism in three dimensions at a high temporal resolution. These methods extend further than purely descriptive approaches, as they allow the analysis of the effect of mutations and other experimental manipulations inside the living experimental system.

Studying protein dynamics in living cells

Cell biologists and optical physicists have developed methodologies, which reach widely beyond the pure observation of single tagged proteins. The integration of fluorescence resonance energy transfer (FRET), fluorescence recovery after photobleaching (FRAP) and fluorescence correlation spectroscopy (FCS) among many other techniques allow the observation of protein interactions and indirectly even biochemical processes inside the living cell (for reviews see Lippincott-Schwartz *et al.*, 2001; van Roessel and Brand, 2002). Additionally the design of new fluorescent tags for signaling processes, the use of optical tricks (evanescent field microscopy) and powerful computational approaches (deconvolution microscopy) allow for a new era in the description of biological processes.

In the following, I will give a short overview on some of the most frequently used visualization techniques.

Fluorescence Resonance Energy Transfer (FRET)

The physical basis of FRET is a quantum effect known as the Förster effect. Förster showed that a molecule (donor) emitting light (*e.g.* by fluorescence) could transfer all its emission energy to a near acceptor molecule by a nonradiative interaction leading to a shift in the emitted light from the wavelength of the donor to the wavelength of the acceptor. What makes this phenomenon especially useful for the study of protein-protein interactions is the fact that under normal circumstances this effect is very inefficient. Only when the donor and acceptor molecules get into close proximity of each other (this characteristic distance is known as

the Förster radius and is in the range of one nm) FRET occurs (Fig. 6). A FRET signal does therefore always indicate that the two molecules of interest are in close proximity. This physical process is also observed using spectral variants of GFPs (Gordon *et al.*, 1998). The following two donor/ acceptor pairs have proven especially useful for FRET based applications in vivo: CFP (donor)/ YFP (acceptor) and GFP (donor)/ DsRed (acceptor).

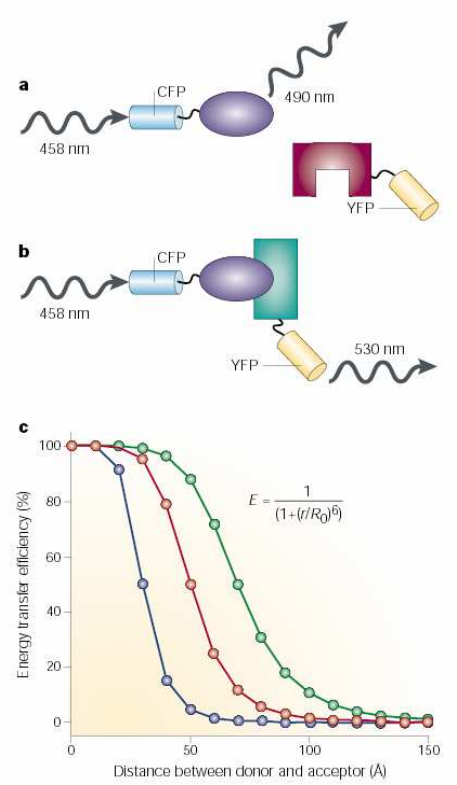

Figure 6 *Principles of FRET.* (a) No FRET is detected between two fluorescently tagged soluble proteins (blue and red) that co-localize, but do not undergo specific protein–protein interactions. Here, excitation of the donor fluorophore (CFP) results in the emission of donor fluorescence. (b) FRET occurs between two fluorescently tagged soluble proteins (blue and green) that bind one another. Here, when the donor fluorophore is excited, 'sensitized' acceptor fluorescence is observed. (c) Dependence of energy transfer efficiency *E* on the distance *r* between the donor and acceptor for proteins in solution. Plots are shown for three values of *R*0, 30 Å (blue), 50 Å (red) and 70 Å (green). Note that *E* drops off to zero at separations of > 100 Å (>2*R*0) for *R*0 = 50 Å. (From Lippincott-Schwartz *et al.*, 2001)

The confirmation of the interaction of two proteins *in vivo* is only of very moderate use. It is the possibility of measuring how, when and where these interactions happen inside a living cell that makes this method so exciting. The engineering of FRET based probes for reading out biochemical processes has proven extremely powerful in shedding light on the dynamics of biochemical processes in the living cell. We can now for example visualize the dynamics of calcium ions in living organism or see how and where small GTPases get activated and fulfill their function (Mochizuki *et al.*, 2001).

Fluorescence Recovery After Photobleaching (FRAP)

FRAP allows the assessment of the mobility of proteins inside a living cell. In this technique, fluorescent molecules in a small region of the cell are irreversibly photobleached and the subsequent movements of surrounding non-bleached fluorescent molecules into the photobleached region are recorded (Fig. 7). GFP is ideal for the use with this technique as it can be photobleached without damage to the cell. FRAP permits to retrieve qualitative and quantitative information about the dynamics of the proteins of interest. Observations on the dynamics of fluorescence reappearance allow the extrapolation of the cell biological mechanisms underlying the delivery of the protein into the photobleached region of the cells (slow appearance of signal from surrounding of the region indicates diffusion and punctuated appearance vesicular delivery). Additionally, the mobile fraction of the protein and the diffusion constant can be calculated from the rate of recovery which allows the extrapolation of the type of constrains to which the proteins are exposed inside the cell (Lippincott-Schwartz *et al.*, 2001; White and Stelzer, 1999).

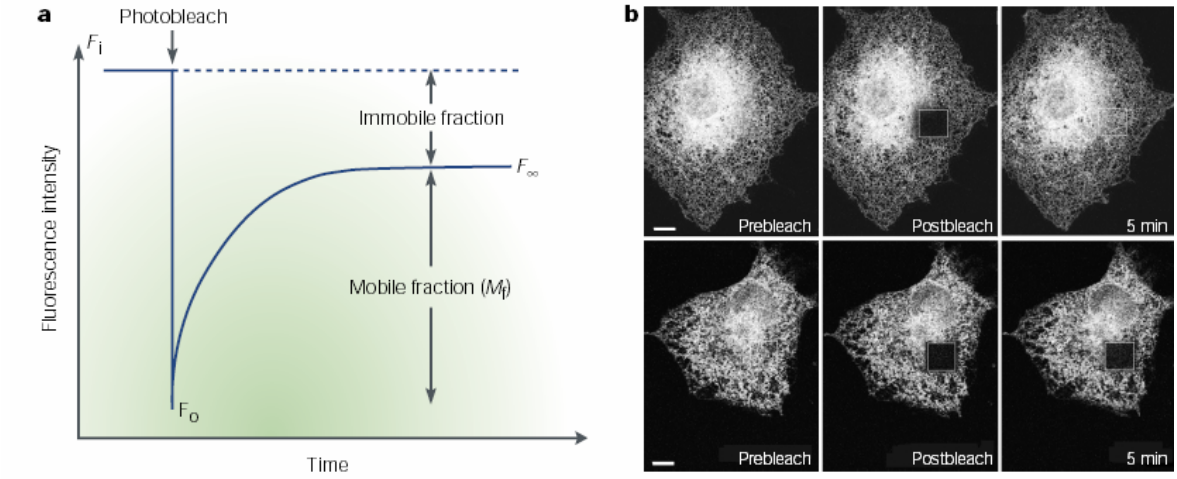

Figure 7 *Fluorescence recovery after photobleaching.* (a) Plot of fluorescence intensity in a region of interest versus time after photobleaching a fluorescent protein. The prebleach (*F*i) is compared with the asymptote of the recovery (*F*∞) to calculate the mobile and immobile fractions. Information from the recovery curve (from *F*o to *F*∞) can be used to determine the diffusion constant of the fluorescent protein. (b) Cells expressing VSVG–GFP were incubated at 40 ℃ to retain VSVG–GFP in the endoplasmic reticulum (ER) under control conditions (top panel) or in the presence of tunicamycin (bottom panel). Fluorescence recovery after photobleaching (FRAP) revealed that VSVG–GFP was highly mobile in ER membranes at 40 ℃ but was immobilized in the presence of tunicamycin. b is adapted from (Nehls *et al.*, 2000). (From Lippincott-Schwartz *et al.*, 2001)

Fluorescence Correlation Spectroscopy (FCS)

FCS is a technique, which is not used as widely as the two previously described ones, but which holds great promise for the analysis of protein dynamics *in vivo*. The ability of defining a very small sample volume by confocal microscopy has lead to the rediscovery of this technique.

FCS measures the fluctuations in the fluorescent signal resulting from labeled molecules diffusing in and out of a previously defined volume (Fig. 8). These fluctuations reflect the average number of labeled molecules in the volume, as well as the characteristic time of diffusion of each volume across it (Medina and Schwille, 2002). FCS is extremely sensitive and can theoretically even be used to measure affinity constants *in vivo*. The use of FCS in cells has only begun, but its use will be very valuable for precise observations in living cells.

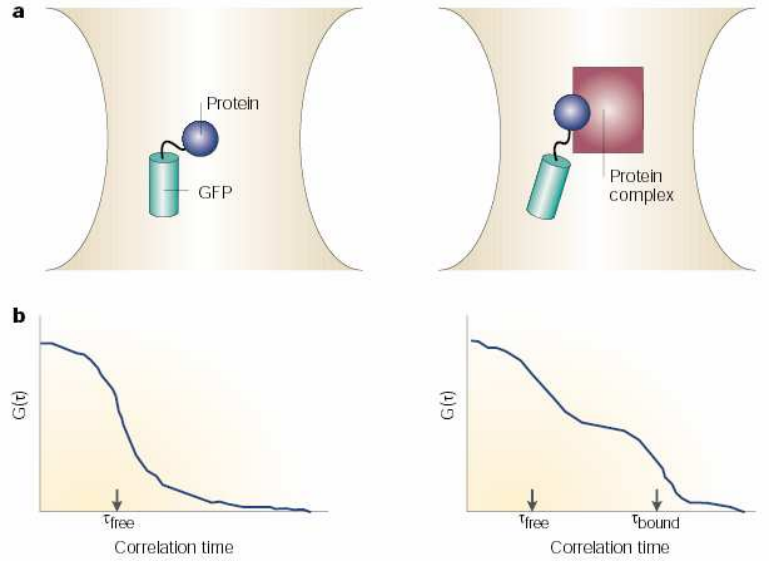

Figure 8 *Principles of fluorescence correlation spectroscopy.* (a) As a fluorescently tagged protein diffuses through the confocal volume, the attached fluorophore (here, GFP) emits photons. Individual proteins (left) diffuse faster and thus reside in the volume for less time than proteins that are bound in a complex (right). (b) From measurements of the corresponding fluctuations in fluorescence intensity over time, an autocorrelation curve can be calculated Each autocorrelation curve contains information about the average number of particles, *N*, diffusing through the volume ($G_0 = 1/N$), as well as the characteristic correlation time τ_D for this process. If several components are present, this analysis can also resolve the fraction of each (right). The correlation time τ_D is related to the diffusion constant *D* and the width of the confocal volume ω1 by $D = \omega 1^2/4\ \tau_D$. So, a shorter correlation time corresponds to a protein with faster diffusion (larger *D*).

Expressed fluorescent tags for signaling proteins

Two main strategies are available for the observation of molecules *in vivo*. On the one hand, one can label the protein of interest and observe its dynamics directly. On the other hand, one can use tags for the proteins of interest and in this way observe them indirectly (*e.g.* Tau-GFP for microtubuli or Moesin-GFP for filamentous actin). The second, so called decorative labeling, has many advantages over the direct labeling. First, it often leads to stronger signal intensities due to the fact that multiple tagging molecules can bind to one molecule of interest. Additionally, such tagging proteins can be designed to only detect specific states of the protein of interest (*e.g.* phosphorylated or oligomerized states). These tagging proteins can therefore act as sensors for the state

of a protein inside a living cell. A widely used example for this type of probes is the use of a PH domain fused to GFP. These proteins interact with phosphorylated lipid moieties and therefore translocate to the membrane upon activation of certain lipid modification pathways (Teruel and Meyer, 2000).

Evanescent field microscopy

One of the main limitations of standard confocal microscopes is that the smallest volume one can focus at, is half a micrometer wide. This is especially annoying when looking at weak signals of very small cellular structures (membranes are for example only some nanometers thick), which get obscured by the background of the enclosed cytosol. Evanescent field (EF) fluorescence microscopy overcomes this problem by enabling the observation of very small volumes. EFs can form when a beam of light traveling in a medium with a high refractive index (*e.g.* glass) encounters one of lower refractive index (*e.g.* water). When the angle of incidence is large enough (critical angel) light undergoes a total internal reflection (see Figure 9). Classic electrodynamics however does not allow an electromagnetic wave to vanish discontinuously at an interface, leading to the appearance of a thin layer (100 nm wide) of light in the water. This leads to the illumination of the fluorescent proteins at the interface leaving the surroundings in the dark. When cells are grown on a glass surface, the membrane is close enough to be illuminated by the thin layer of light without the surrounding cytosol being illuminated. This allows the membrane to be analyzed exclusively without noise from the surrounding. The situation is reminiscent of setting an actor on a theater stage into the spotlight (Steyer and Almers, 2001 and Figure 9).

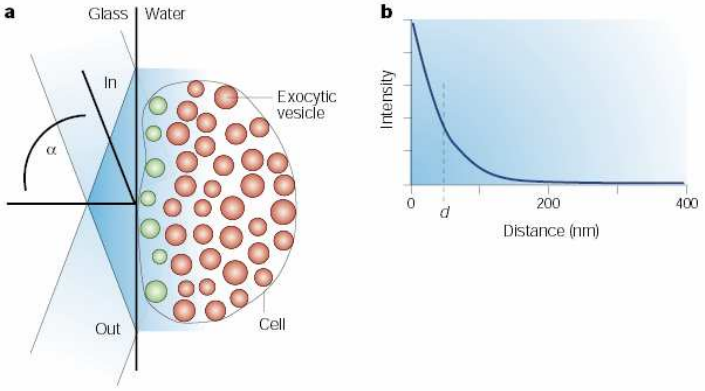

Figure 9 *Evanescent fields.* When a parallel beam of light in a medium of high refractive index (n_1) strikes an interface with a medium of lower refractive index (n_2) it suffers total internal reflection if the angle of incidence, α, exceeds the so-called critical angle. Total internal reflection generates an evanescent field in the medium of lower refractive index (a). The intensity of the evanescent field medium declines exponentially with distance from the interface (b), falling 37% within the so-called 'penetration depth' *d*. (From Steyer and Almers, 2001)

This technique has allowed unprecedented views on events occurring in the membrane and its direct environment. Studies using EF have mainly focused on secretory biology and cell adhesion studies. The fact that one is limited to the direct surface of the slide makes this technique less usable for visualization inside an organism, as most structures of interest are not located at the surface of the animal. This also holds true for *Drosophila* research although this technique could prove very valuable for the study of developmental processes in the imaginal discs.

Deconvolution microscopy

Deconvolution is a computational method used to reduce out-of-focus fluorescence in 3D microscope images. It is mainly used to reconstruct the spatial information out of conventional wide field fluorescent microscope images and to enhance the resolution and contrast of images made by confocal scanning microscopes. As a rule of thumb, the z-axis resolution for example can easily be improved by a factor of two. Deconvolution microscopy is especially useful for *in vivo* imaging, as it requires weaker signals; therefore dimmer illumination and less exposure time (see also materials and methods).

There are two main philosophies upon which deconvolution is based. In the first one, the properties of the imaging system are recorded and transformed into a function describing the optical properties of the system (called Point Spread Function (PSF)). This function is then used as a basis for the computational treatment of the data originating from the calibrated imaging system. This procedure allows the optimal use of the capacities of deconvolution microscopy. But given that the described measurements are difficult to perform and the calibration system does not always reflect the situation in which the images are going to be taken, this procedure is not simple. Especially because small mistakes in the PSF are strongly reflected in the quality of the deconvolution procedure.

In the second approach, an algorithm calculates the PSF out of the image to be deconvoluted on the fly. The so calculated PSF is less accurate than the experimentally derived one but as it is extracted from the image directly, it reflects the situation in which the image has been taken and does not require prior calibration of the system.

Given the high computational load of the algorithms required to extract the PSF on the fly and to perform the deconvolution process this method has just started to gain widespread use with the recent increase in computational power.

Deconvolution is based on the distortions due to the optical properties of the microscopes used. Theoretically, a fluorescent molecule emits light in all directions upon excitation. Confocal microscopy uses an optical trick that only allows the detection of the molecules emitting light in the plane of interest. It is nevertheless practically not possible to detect the light exclusively at the

source and therefore light is also detected in planes above and under the plane of the fluorescent molecule (Fig. 10). In other words: the signal does not appear as point anymore but as a cone. This leads to an increase in background fluorescence and a loss of resolution. However, if one knows the optical properties leading to that distortion they can be mathematically removed from the image. It is this distortion which the PSF measures.

For details on how we used deconvolution to treat our data see materials and methods. For further information on deconvolution see (McNally et al., 1999).

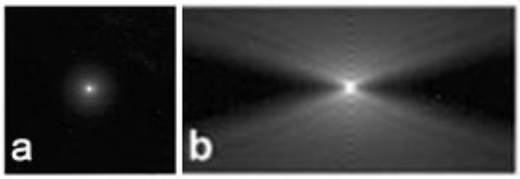

Figure 10 *Principle of deconvolution.* (a) Theoretical image of a fluorescent molecule. (b) Point spread function, representing the fluorescent molecule as seen through an objective (exaggerated).

The Drosophila *embryo as an excellent* in vivo *visualization system*

The *Drosophila* embryo is an ideal system to perform *in vivo* visualization experiments. The embryo is very robust, survives most experimental manipulations required for *in vivo* visualization and can be embedded and imaged without affecting its development. After removal of the outer chorion shell, it is almost transparent and its relatively small size allows the acquisition of most structures of interest, even if laying deeper within the organism. Sudden, random movements do not occur until late in embryonic development, allowing the assembly of smooth time-lapse videos.

Additionally, using the Gal4 system (Brand and Perrimon, 1993) it is possible to target the expression of GFP and GFP fusion proteins to specific tissues, making it very easy to mark the cells of interest.

This potential is exemplified by the study of two types of developmental processes using *in vivo* microscopy of the *Drosophila* embryo: asymmetric cell division of neuroblasts and dorsal closure.

Asymmetric partitioning of cell fate determinants is employed to generate cell type diversity in a number of different organisms. During neurogenesis in *Drosophila*, neuronal precursors (neuroblasts) divide asymmetrically. *In vivo* imaging has been extensively used to study the dynamics of this essential process (reviewed in Kaltschmidt and Brand, 2002). These studies have lead to a substantial progress in our understanding of the cellular and

molecular mechanisms controlling this important developmental step.

Dorsal closure is the other process of *Drosophila* development, which has been extensively studied, using live imaging techniques. During this process, a naturally occurring epithelial hole is sealed by the morphogenetic movement of the lateral epithelium (Jacinto *et al.*, 2001). As such this process is reminiscent of re-epithelialization of the a wound (Noselli, 2002; Wood *et al.*, 2002). The insights from these studies indicate that dorsal closure is associated with dynamic filopodia, which could play an important role in correctly positioning opposing epithelial cells for subsequent sealing (Jacinto *et al.*, 2000) and an actin cable which is thought to act in a similar way as a purse-string (Kiehart *et al.*, 2000). Additionally, the contribution of small GTPases to the dorsal closure process has also been studied using this approach (Bloor and Kiehart, 2002; Jacinto *et al.*, 2002).

Genomics and large scale gene expression profiling

Sequencing of the Drosophila *genome and its implications*

The fruitfly was the first organism to have its genome extensively studied. These groundbreaking studies performed at the beginning of the last century by the group gathered around T.H. Morgan at Columbia University in New York and later at the California Institute of Technology in Pasadena, California, have shaped in an unprecedented fashion our understanding on the genetic basis of heredity and the organization of genes on chromosomes (Morgan, 1934).

Less than hundred years later, these efforts have culminated in the almost complete sequencing of the genome of the fruitfly, setting a temporary finishing point to the chemical analysis of the molecular composition of the genomic information of *Drosophila* (Adams *et al.*, 2000). It is nevertheless also clear that it is only a further, albeit essential, step in gaining a deeper understanding in how the organization and interpretation of the genetic information governs the formation of such a complex and fascinating organism as the fruitfly. The extensive sequence information gained by this massive effort can now be used together with modern computational, cell biological and molecular methodologies to mine this scientific treasure exhaustively to address a given question. Driven by the dramatic increase of sequence information, we are therefore witnessing the rise of a new generation of scientific methodologies that are centered on the extensive use of these data in order to gain functional understanding of how biological processes are regulated. To characterize this new brand of techniques the term functional genomics has been coined.

Large scale gene expression profiling

Among the most powerful and versatile representatives of this class of new methodologies are high-density arrays of oligonucleotides and complementary cDNAs. Nucleic acid arrays rely on the hybridization of labeled RNA or DNA in solution to DNA molecules immobilized on a surface (probes). When performed in a massively parallel fashion and paired with high signal to noise fluorescent labeling and detection, high precision lithography or printing, miniaturization and massive computational power for data treatment, storage and mining, this approach theoretically allows a quick and fast profiling of RNA abundance and therefore the indirect extrapolation of the expression level of all known genes in the organism of interest. The two different types of arrays mainly in use nowadays are presented in Figure 11. Since in our studies we used oligonucleotide arrays from the company Affymetrix, I will concentrate on the features of these types of arrays.

One of the main differences to cDNA arrays is that oligonucleotide arrays are produced by light directed oligonucleotide synthesis (Fodor *et al.*, 1991). This method combines photolithography, as developed for computer microchip production, and solid-phase DNA synthesis to produces arrays with extremely high information content. For details see Figure 12.

In addition, the way in which the genes of interest are represented on the array is different too. While on cDNA arrays, each gene is normally represented by one spot, on oligonucleotide arrays each gene is represented by a series of 14 to 20 independent non-overlapping single 25-mer oligonucleotides (perfect match [PM] probe). Additionally, each probe is represented by a second, so-called mismatch (MM) probe that is identical to its PM partner except for a single base difference in a central position. The MM probes act as specificity controls, which reduce problems due to both background and cross-hybridization. Expression levels are then determined from the difference of the PM to MM signals across all probes representing a gene (Lockhart *et al.*, 1996 and Figure 13).

Most large-scale gene expression profiling experiments are based on the basic assumption that those genes that change their expression level upon the experimental perturbation most dramatically, are the ones of interest. In studies with multiple experimental perturbations, this paradigm is changed in the following way: genes with similar expression behavior are likely to be functionally related (guilt by association) (Lockhart and Winzeler, 2000).

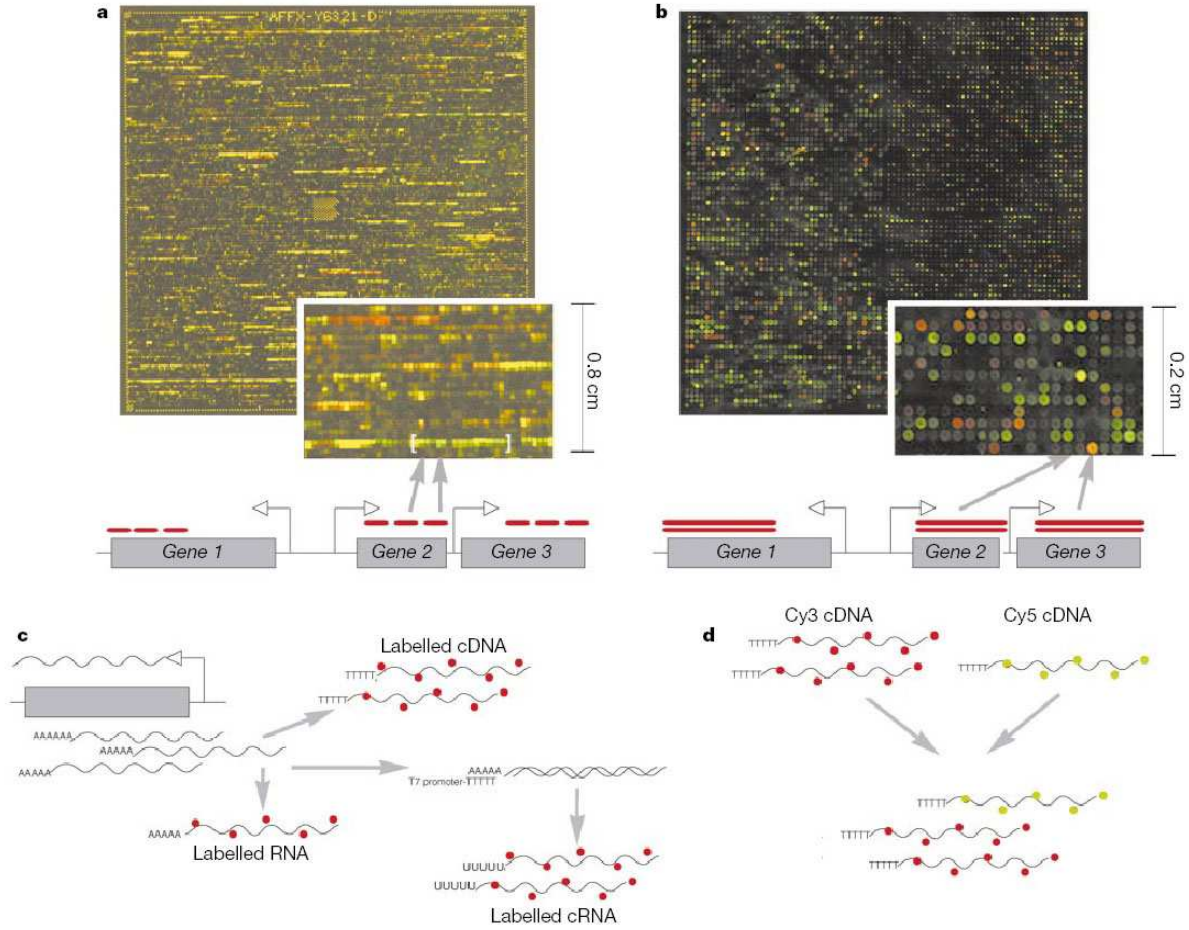

Figure 11 *Principal types of arrays used in gene expression monitoring*. In (a) an oligonucleotide array as produced by the company Affymetrix is depicted. In (b) a cDNA array after hybridization of labeled samples and fluorescence detection. Typically, for oligonucleotide arrays, multiple probes per gene are placed on the array (20 pairs in the example shown here), while in the case of robotic deposition, a single, longer (up to 1,000 bp) double-stranded DNA probe is used for each gene or EST. After hybridization of labeled samples (typically overnight), the arrays are scanned and the quantitative fluorescence image along with the known identity of the probes is used to assess its relative abundance in one or more samples. For technical reasons, the information obtained from spotted cDNA arrays gives the relative concentration (ratio) of a given transcript in two different samples (derived from competitive, two-color hybridizations). (c) Different methods for preparing labeled material for measurements of gene expression. The RNA can be labeled directly, using a psoralen–biotin derivative or by ligation to an RNA molecule carrying biotin26; labeled nucleotides can be incorporated into cDNA during or after reverse transcription of polyadenylated RNA; or cDNA can be generated that carries a T7 promoter at its 5′ end. In the last case, the double-stranded cDNA serves as template for a reverse transcription reaction in which labeled nucleotides are incorporated into cRNA. Commonly used labels include the fluorophores fluorescein, Cy3 (or Cy5), or nonfluorescent biotin, which is subsequently labeled by staining with a fluorescent streptavidin conjugate. (d) Two-color hybridization strategy often used with cDNA microarrays. cDNA from two different conditions is labeled with two different fluorescent dyes (usually Cy3 and Cy5), and the two samples are co-hybridized to an array. After washing, the array is scanned at two different wavelengths to detect the relative transcript abundance for each condition. cDNA array image courtesy of J. DeRisi and P. O. Brown. (From Lockhart and Winzeler, 2000)

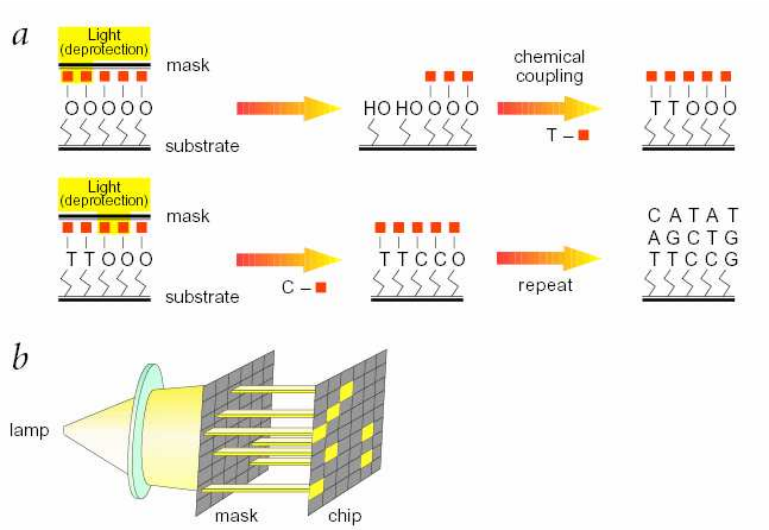

Figure 12 *Light directed oligonucleotide synthesis*. (a) A solid support is derivatized with a covalent linker molecule terminated with a photolabile protecting group. Light is directed through a mask to deprotect and activate selected sites, and protected nucleotides couple to the activated sites. The process is repeated, activating different sets of sites and coupling different bases allowing arbitrary DNA probes to be constructed at each site. (b) Schematic representation of the lamp, mask and array. (From Lipshutz et al., 1999).

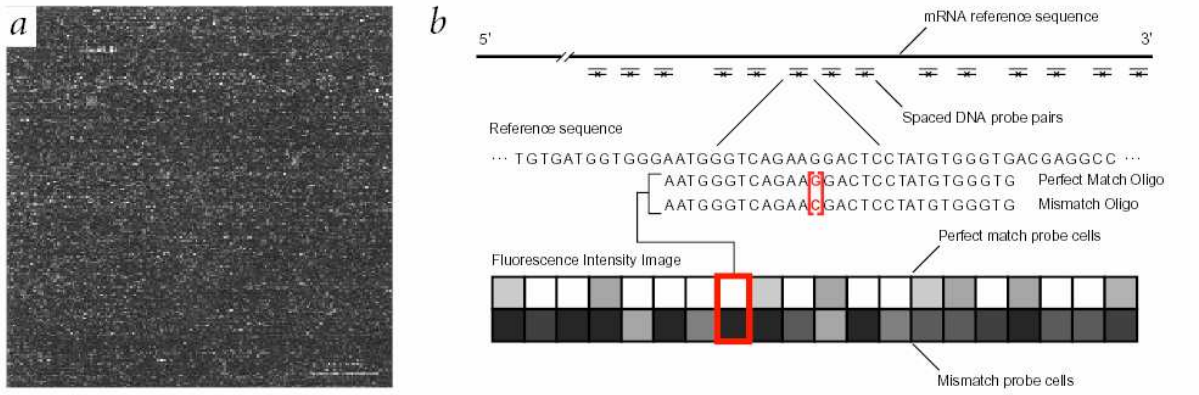

Figure 13 *Gene expression monitoring with oligonucleotide arrays.* (a) A single 1.28x1.28 cm array containing probe sets for approximately 40,000 human genes and ESTs. This array contains features smaller than 22x22 μm and only four probe pairs per gene or EST. (b) Expression probe and array design. Oligonucleotide probes are chosen based on uniqueness criteria and composition design rules. For eukaryotic organisms, probes are chosen typically from the 3´ end of the gene or transcript (nearer to the poly(A) tail) to reduce problems that may arise from the use of partially degraded mRNA. The use of the PM minus MM differences averaged across a set of probes greatly reduces the contribution of background and cross-hybridization and increases the quantitative accuracy and reproducibility of the measurements. (From Lipshutz *et al.*, 1999).

Large scale expression profiling has found multiple uses in modern biology. On the one side, it is widely used to hunt for new genes involved in all possible biological processes. As such, it complements nicely the available genetic, biochemical and molecular tools already available for this purpose.

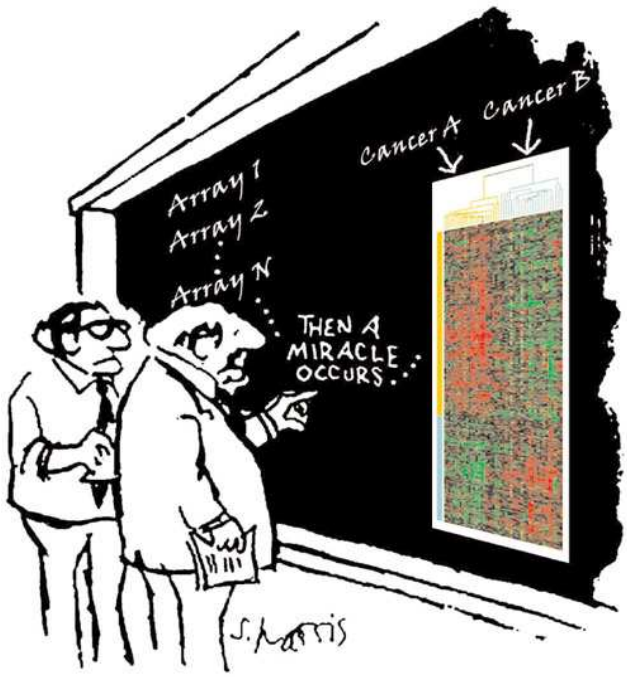

Figure 14 *"I think you should be more explicit here in step two."* Modified with permission from a cartoon by Sidney Harris and from an image provided by Patrick Brown. (From Leung *et al.*, 2001)

Nowadays the true challenge however does not rely in the hybridization experiment *per se* but in the following data mining steps. Faced with such an unprecedented amount of genomic data, new strategies have to be used to analyze them. Candidate genes are therefore mostly selected by predefined statistical criteria. Additionally, as every biological system shows inherent fluctuations in the expression levels of most genes, the use of multiple replicas has proven to be an extremely valuable approach to enhance the statistical relevance of the expression data. Although sophisticated software tools have been developed to mine the expression level data for functional relevance, this step still remains the most difficult and critical step in large-scale expression profiling (Knight, 2001 and Figure 14).

The final aim of large scale gene expression profiling is the identification of the expression profile of all genes in the genome of the organism of interest (global gene expression profiling). In spite of the many claims, one can hear on the subject this goal is not achieved yet. The inherent difficulties in correctly annotating the available genome information together with residual problems in the production, hybridization and detection of the arrays make this a very difficult goal to achieve.

Chapter 3

Signaling systems, guided cell migration and organogenesis: insights from genetic studies in *Drosophila*

Carlos Ribeiro, Valérie Petit and Markus Affolter

Submitted to the journal Developmental Biology

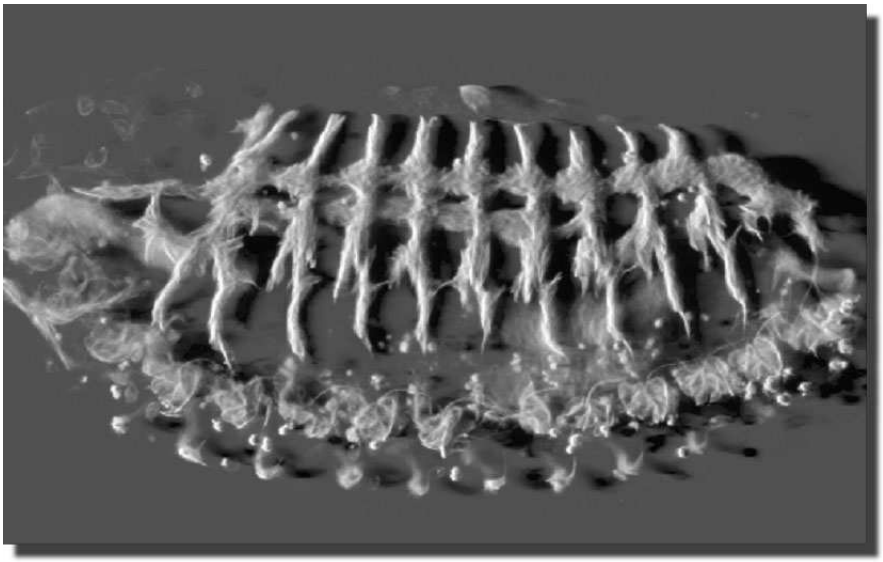

Introduction

During the development of multicellular organisms, cells change their relative position extensively as organs and tissues take up their final location and function. Over many decades, such cell movements have been analyzed in tissue explants or *in vitro* using cultured cells, and these studies have provided a wealth of knowledge regarding the intracellular events that occur as a cell moves over a substratum. Both the actin cytoskeleton and the microtubular network have to be reorganized extensively in a migrating cell, ultimately contributing to the forward movement and to the temporal stability of the cell (Lauffenburger and Horwitz, 1996; Sheetz *et al.*, 1999).

More recently, events which focus the migratory forces into a given direction have been investigated in more detail in the context of single cells. Studies using *Dictyostelium discoideum* and neutrophils have resulted in the description of molecular scenarios that allow a cell to translate a shallow extracellular concentration gradient of a chemoattractant into a migratory response (Chung *et al.*, 2001; Iijima *et al.*, 2002; Sanchez-Madrid and del Pozo, 1999). Upon the activation of a cell surface receptor by binding to its chemoattractive ligand, positive and negative feedback loops along the cell surface enhance the signal intracellularly proximal to the signal and decrease it in more distal regions. These events ultimately lead to a localized signaling centre at the front of the cell, characterized in these systems by increased levels of lipid products of phosphoinositide 3-kinase (PI3K) activity. This signal is then thought to be further translated via members of the small GTPase family into appropriate cytoskeletal responses, eventually allowing the cell to displace its body in a coordinated manner (Ridley and Hall, 1992).

Although chemoattraction plays a crucial role in cell migration during the development of multicellular organisms, migrating cells are faced with a number of additional constrains in such an environment. In many cases, cells first have to acquire the capability to detach from surrounding cells and invade other territories, and migration has to be initiated at precise developmental times. Often, cells do not move individually but in groups, and not all cells in such groups perform the same role in the migratory process. In particular cases, it appears that cell migration sculpts the three dimensional appearance of entire organ systems. Ultimately, migrating cells have to stop their movement as they reach their final destination and differentiate into non-motile cells of distinct functions. The necessity of cells to coordinate their movement with their neighborhood in multicellular systems requires that motility as such is regulated by events that control cell adhesion, either between similar and/or different cells and the cellular matrix. *In vivo*, each cell migration event has its own particularity with regard to the issues just described.

We would like to give a brief overview of the current knowledge gained from the genetic analysis of cell migratory events in *Drosophila melanogaster*. Since studies regarding cell migration

are most advanced in germ cells, border cells, hemocytes and tracheal cells, we limit our comparison to these systems. We describe a number of signaling pathways that have recently been associated with these cases of directional cell migration, and outline the different cellular contexts that allow migration to shape organs and tissues of completely different architecture (see Figure 15 for a schematic representation of the systems described in this review).

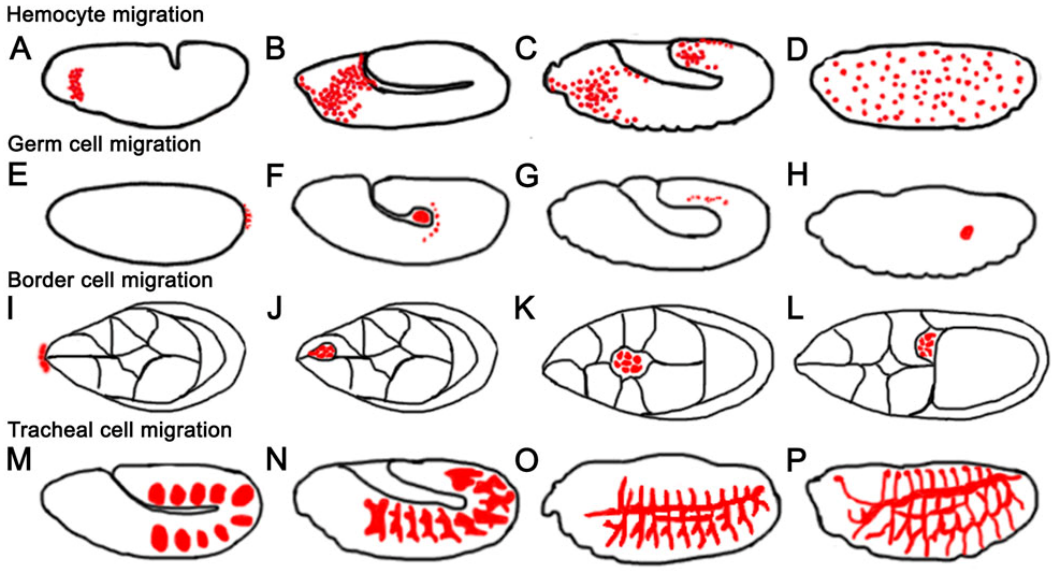

Figure 15 *Schematic representation of the migratory behavior of distinct cell populations in the Drosophila embryo.* Hemocyte migration*:* At embryonic stage 8 hemocytes originate from the head mesoderm (A). This cluster of cells splits up at stage 10 (B) and after one loose group has crossed the amnioserosa at stage 12 (C), the two clusters spread towards the middle of the embryo and disperse evenly throughout the embryo at stage 15 (D). Germ cell migration*:* At embryonic stage 5, germ cells are determined at the posterior pole of the blastoderm embryo (E). They are passively swept into the midgut pocket, where at stage 9, they start to actively cross the endoderm as single cells (F). Once they have reached the overlaying mesoderm, they associate with the gonadal mesoderm at stage 11 (G) where, at stage 14, they coalesce to form the embryonic gonad (H). Border cell migration: After determination (I), the border cells detach from the follicular epithelium and invade the germ cell cluster at the beginning of stage 9 of oogenesis (J). During stage 9 they migrate as a group of cells in between the nurse cells in direction of the oocyte (K). Once they reach the oocyte, they migrate dorsally during stage 10 (L) to come to lie over the oocyte nucleus. Tracheal cell migration: The ten tracheal pits on each side of the embryo are formed by invagination of groups of ectodermal cells at embryonic stage 10 (M). The cavity formed is then expanded at stage 12 by the outgrowth of the primary branches (N). Fusion of adjacent metameres at stage 14 (O) and 16 (P) leads to the formation of an interconnected tubular network. Figure modified from (Cho *et al.*, 2002; Gupta and Schupbach, 2001; Petit *et al.*, 2002; Starz-Gaiano and Lehmann, 2001).

Migratory systems and their signaling mechanisms

Hemocytes

Hemocytes are the *Drosophila* blood cells and play a major role in the innate immune response and in the removal of apoptotic cells. Prior to the initiation of their role as blood cells, they are deployed throughout the embryo by a stereotyped, genetically encoded migratory program. Hemocytes originate as a cluster of cells from the head mesoderm (Fig. 15A). This cluster loosens up and splits into two ill-defined groups of cells (Fig. 15B), one moving to the posterior end of the embryo by crossing the amnioserosa, which at that stage is folded due to germ band extension (Fig. 16C). Both populations then spread towards the middle of the embryo and disperse evenly throughout the embryo as single cells (Fig. 15D, Cho *et al.*, 2002; Tepass *et al.*, 1994).

The characterization of the genes encoding the fly homologue of the PDGF/VEGF receptor (PVR, also named VEGF receptor or Stasis) and its putative ligands (PDGFs/VEGFs; named PVFs in the following) has shown that the PDGF/VEGF signaling pathway controls important aspects of the migratory behavior of the *Drosophila* hemocytes (Cho *et al.*, 2002). Upon specification, hemocytes start to express PVR (Cho *et al.*, 2002; Heino *et al.*, 2001); developing blood cells lacking PVR differentiate and initiate migration correctly but stall before crossing the amnioserosa and do not disperse uniformly. The PVFs are expressed in cell populations along the migratory route of the hemocytes. Due to apparent functional redundancy, mutants for single *Pvf* genes show no effect on blood cell migration; however, inactivation of all three *Pvf* genes by RNAi injection revealed a phenotype similar to the one seen in mutants for the receptor. Strikingly, ectopic expression of a *Pvf* results in the misrouting of hemocytes, supporting a role of the PDGFR/VEGFR pathway in guided migration of developing blood cells (Cho *et al.*, 2002).

Germ cells

Similar to hemocytes, germ cells migrate without being firmly attached to each other. However, instead of dispersing throughout the embryo, they converge into the future somatic gonad tissue. The *Drosophila* pole cells are formed at the posterior pole of the blastoderm embryo (Fig. 15E). As a result of their adhesiveness to the underlying tissue they are passively carried into the midgut pocket by the subsequent movements of germband extension and midgut invagination. Subsequently, the germ cells actively invade and cross the endodermal epithelium to reach the overlaying mesoderm (Fig. 15F). Germ cells

then migrate towards the gonadal mesoderm where they coalesce, giving rise to the compact embryonic gonad (Fig. 15G, 15H, Starz-Gaiano and Lehmann, 2001).

Despite the fact that extensive loss of function genetic screens have been undertaken to elucidate the molecular mechanisms underlying germ cell migration in *Drosophila,* only a limited number of key components have thus far been identified. These components reveal the existence of attractant and repellant factors that are produced by somatic cells and guide migrating germ cells (Starz-Gaiano and Lehmann, 2001).

In mutants of the genes encoding the *Drosophila* homologues of the mammalian lipid phosphate phosphatase-1 (*wunen* and the neighboring *wunen-2*), germ cells fail to reach the somatic mesoderm; ectopic expression of *wunen or wunen-2* throughout the mesoderm has a repellant effect on germ cells. *wunen* RNA is expressed at the bottom of the posterior midgut and the corresponding protein thus appears to repel germ cells from this part of the midgut pocket. In analogy to the mammalian lipid phosphate phosphatase-1 protein, the *Drosophila* Wunen proteins might expose their catalytic site extracellularly and either produce a repellant or destroy a phospholipid acting as an attractant (Starz-Gaiano and Lehmann, 2001; Zhang *et al.*, 1996; Zhang *et al.*, 1997).

A separate attractive signal is produced by the *columbus* gene, which encodes the enzyme HMGCoA reductase (HMGCoAR) (Van Doren *et al.*, 1998). HMGCoAR is expressed at high levels in the somatic gonadal precursors. In mutants for *columbus*, germ cells fail to associate with the somatic mesoderm; ectopic expression of HMGCoAR attracts germ cells to the newly expressing tissue. The cell surface molecules which represent the actual signal produced in the somatic gonad in response to the activity of HMGCoAR, as well as their presumptive receptors on germ cells, remain elusive.

Border cells

Border cells represent one of the best studied systems with regard to cell migration in the fruitfly. Border cells are a group of about eight cells, which originate from the most anterior part of the egg chamber (Fig. 15I) and which after detaching from the monolayered follicular epithelium invade the germ cell cluster (Fig. 15J) and migrate, still as a group, on and in-between the nurse cells in the direction of the oocyte (Fig. 15K). When they reach the oocyte, they migrate dorsally where they come to stop over the oocyte nucleus (Fig. 15L). The border cell cluster ultimately contributes to the formation of the micropyle, the structure on the eggshell that allows the entry of the sperm and therefore fertilization (Montell, 2001; Rorth, 2002).

A number of elegant studies have contributed to our current understanding of border cell specification and the subsequent events culminating in guided migration. Border cells are thought to

be specified within the follicular epithelium by the JAK-STAT pathway leading to the expression of the transcription factor Slow border cells (Slbo) which controls the expression of most genes required for migration (Beccari *et al.*, 2002; Montell *et al.*, 1992; Silver and Montell, 2001). Specification is followed by the detachment of the border cell cluster from the follicular epithelium and the invasion of the space in between the nurse cells. Border cells delaminate from the follicle cell epithelium in a process reminiscent of an epithelium-to-mesenchyme transition. This is of special interest as this process is reminiscent of the situation encountered in many human metastatic tumors (Thiery, 2002). Somewhat surprisingly, the classical DE-cadherin is required both in the migrating border cells and in their substratum for the migration to occur. This observation suggests that homophilic interaction between DE-cadherin in the two cell types provide the adhesion and/or traction required for migration (Niewiadomska *et al.*, 1999).

Migration in between the nurse cells towards the oocyte is controlled by two receptor tyrosine kinase (RTK) signaling pathways, centered around the PVR (Duchek *et al.*, 2001) and the epidermal growth factor receptor (EGFR) (Duchek and Rorth, 2001). Migration of the border cell cluster is primarily guided towards the oocyte by the PVR ligand PVF1. The *Drosophila* EGFR has a largely redundant role in this migration process so that cells can find their way using either PVR or EGFR. When border cells meet the oocyte, EGFR has also a second guidance function; it is required for dorsally directed migration in response to the ligand Gurken, which is concentrated in the dorsal aspect of the oocyte membrane.

Still little is known about the cellular events induced by the guidance receptors and the intracellular signal relay. Chemotaxis in *Dictyostelium* and neutrophils suggests that PI3K provides the localized intracellular signal. Experiments in which PIP3 levels were manipulated using overexpression of an activated form of PI3K suggest that PIP3 does not accumulate preferentially at the leading edge of the border cell cluster (Fulga and Rorth, 2002), but further investigations are necessary to clarify this important issue.

It has recently been shown that an early consequence of signaling via the guidance receptors at the cellular level is the formation of a single long cellular extension (LCE) by one cell of the border cell cluster (Fig. 16A). Formation of these LCEs requires a functional *DE-cadherin* gene, but again PI3K signaling does not appear to control LCE formation. Interestingly the interaction between DE-Cadherin and Myosin VI seems to be required for proper border cell migration by linking this adhesive complex to the cytoskeleton. It has been suggested that Myosin VI promotes LCE formation and the LCE itself may function as a “pathfinder” and grapple, helping the border cell cluster to be pulled forward towards the oocyte by Myosin II mediated contraction of the LCE (Fulga and Rorth, 2002; Geisbrecht and Montell, 2002; Schober and Perrimon, 2002).

Tracheal cells

Tracheal development represents a very interesting case in which cell migration not only leads to the repositioning of cells within the organism but sculpts the three-dimensional appearance of the entire organ. Again, only a limited number of cells display a migratory behavior. The exceptional features of the developing tracheal system with regard to cell movement relies in the fact that cells migrating in different directions remain firmly connected with each other throughout the migratory process, ultimately giving rise to a branched tubular network.

The respiratory system of *Drosophila* develops from ten clusters of ectodermal cells, the tracheal placodes that invaginate to form the tracheal pits on both sides of the embryo, each containing approximately 80 cells (Fig. 15M). Each sac is expanded without further cell division in six directions by stereotypical, directed migration and cell shape changes (Fig. 15N). Subsequent fusion events lead to the interconnection of the individual metameres (Fig. 15O, 15P, reviewed in Affolter and Shilo, 2000; Metzger and Krasnow, 1999; Petit *et al.*, 2002; Samakovlis *et al.*, 1996).

Similar to border cells, the JAK/STAT pathway is crucial in specifying the tracheal cell fate. In this particular case, JAK/STAT signaling induces the expression of the transcription factor Trachealess (Trh) in the tracheal placodes(Brown *et al.*, 2001; Chen *et al.*, 2002). Trh is essential for making the cells competent for further migration events by inducing the expression of the FGF receptor (FGFR) Breathless (Btl) and the intracellular FGF signaling component Downstream of FGFR (Dof)/Stumps (Boube *et al.*, 2000; Isaac and Andrew, 1996; Wilk *et al.*, 1996). This confers tracheal cells with the ability to respond to the only known chemoattractant in the tracheal system, the *Drosophila* FGF-like protein Branchless (Bnl). *bnl* is expressed dynamically in cells surrounding the invaginated tracheal placodes, prefiguring the direction of outgrowth of the six primary branches (Sutherland *et al.*, 1996). In the absence of either Bnl/FGF, Btl/FGFR (Glazer and Shilo, 1991; Klambt *et al.*, 1992; Reichman-Fried and Shilo, 1995), or Dof/Stumps (Imam *et al.*, 1999; Michelson *et al.*, 1998; Vincent *et al.*, 1998) cell migration and subsequent events in tracheal development fail to occur .

The existence of an overlap in the molecular mechanisms used in axonal pathfinding in the central nervous system and those used in guided tracheal migration has also been suggested (Englund *et al.*, 2002). The authors of the study propose that certain tracheal branches respond in an attractive and repulsive manner to Slit signaling and that these effects are mediated by different combinations of the Slit receptors Roundabout (Robo) and Roundabout2 (Robo2). The effects seen in mutants for Slit signaling are less penetrant than the ones seen in mutants for FGFR signaling and the exact role of these molecules in tracheal morphogenesis awaits further clarification.

Recently, *in vivo* confocal microscopy has provided compelling evidences that the FGFR pathway controls

motility by inducing dynamic filopodia exclusively in the cells at the tip of the embryonic tracheal branches (Ribeiro *et al.*, 2002; Sato and Kornberg, 2002) (Fig. 16B). The motile force produced by the cells at the tip of the branches seems to be used to drag along the passive distal cells eventually leading to the formation of an elongated, branch-like structure. A structure comparable to the LCE in border cells though has not been observed emanating from the tracheal cells indicating different strategies in generating the tractive force.

Strikingly FGFR signaling mediated chemoattraction is not sufficient for successful outgrowth of tracheal branches. As shown in detail for the embryonic dorsal branch, further signaling systems (in this case the BMP-like Decapentaplegic [DPP] signaling cascade) are needed to integrate the motility program into the branching morphogenesis program thereby allowing the productive and correct morphogenesis of individual branches (Ribeiro *et al.*, 2002; Vincent *et al.*, 1997). DPP is thought to control cell rearrangements (*e.g.* intercalation), cell shape changes or adhesive properties of the cells specific to the dorsal branch. The molecular mechanisms, which mediate the signaling information of the FGFR to the cytoskeletal motility machinery and integrate the effects of the additional signaling systems acting in trachea, remain to be elucidated.

Progress has recently been made in understanding the molecular interactions between tracheal cells and their surrounding substrata. Surface receptors of the integrin family have been implicated in promoting the spreading of the visceral branch over the visceral mesoderm (Boube *et al.*, 2001). The αPS1 and the αPS2 integrins of *Drosophila* are specifically expressed on the surface of the cells of the tracheal visceral branch and the visceral mesoderm, respectively. Specific interactions of both integrin receptors with the extracellular matrix allow the visceral branch to move over the visceral mesoderm; in mutants for the αPS1 integrin, the visceral branch stalls after the first contact with its future substratum. A similar, although molecularly less well understood, mechanism is used by the cells of the dorsal trunk. These cells use a specific mesodermal cell, the so-called bridge cell, as a substratum to cross the gap separating adjacent metameres (Wolf and Schuh, 2000).

Comparison between the different systems

Genetic analysis of cell migration in *Drosophila* has recently led to the identification of a number of chemoattractants and their receptor systems. Somewhat strikingly, all of the identified receptors are transmembrane tyrosine kinases (PVR, EGFR, and FGFR). The same receptors might also be required for cell migrations at other developmental stages. For example, FGF signaling was shown to be required in the pupa for the formation of the air sac by promoting filopodia

based cell motility and cell proliferation (Sato and Kornberg, 2002), for the recruitment of mesodermal cells to the male genital imaginal disc (Ahmad and Baker, 2002), for the migration of midline glia cells (Klambt *et al.*, 1992) and for the spreading of mesodermal cells along the dorsoventral axis of the early *Drosophila* embryo (Beiman *et al.*, 1996; Gisselbrecht *et al.*, 1996; Michelson *et al.*, 1998). Clearly, long range cell movements during *Drosophila* development appear to be controlled to a large extent by RTKs.

What are the cellular targets of these RTK signaling systems? Although some of these pathways, in particular the EGFR pathway, have been extensively studied at the genetic level with regard to their gene regulatory effects, little is known about the requirements of downstream signaling components concerning the regulation of migration. Cellular analysis has established that in many cases these signaling systems regulate the formation of cellular extensions linked to cell migration (e.g. LCE in border cells and filopodia in trachea [Fig. 16], Fulga and Rorth, 2002; Jaglarz and Howard, 1995; Ribeiro *et al.*, 2002; Tepass *et al.*, 1994) and it is thought that these receptor systems directly regulate cytoskeletal dynamics rather than transcription. It is likely that actin polymerization is one of the intracellular events regulated by these receptors, but whether the information is transmitted via the local accumulation of specific lipid products (in analogy to the accumulation of PIP3 in neutrophils and *Dictyostelium*) has been questioned.

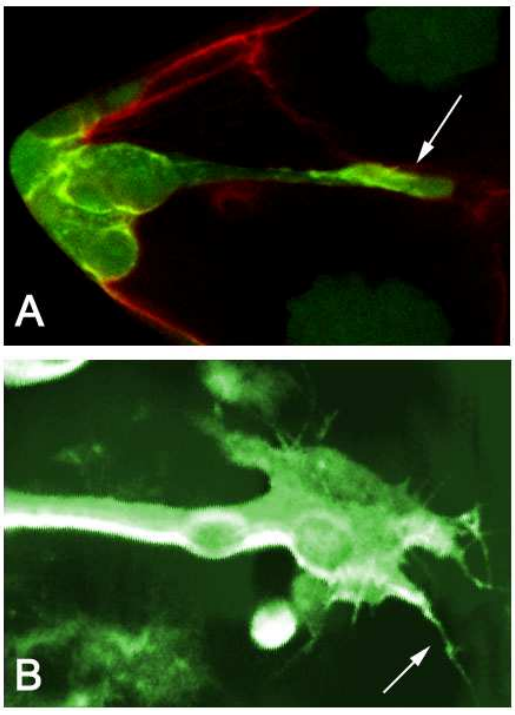

Figure 16 *Examples of cellular extensions made by migrating cells.* (A) Fixed egg chamber expressing a GFP actin fusion construct in border cells (green) show a very prominent long cellular extension (LCE; arrow) extending from one border cell and invading the space between the nurse cells (membranes are visualized in red with a lipophilic dye); (Image kindly provided by Tudor Fulga and Pernille Rorth). (B) In the developing tracheal system, numerous dynamic filopodia (arrow) are observed protruding from the tip cells of the dorsal branches. Depicted here is a 3D reconstruction of a dorsal branch expressing the same GFP actin fusion construct and visualized in a living embryo.

Quite obviously, migration is crucial for the development of organs and tissues of rather different final shape and structure (Fig. 17 bottom and Fig. 15D, H, L and P). The different migratory strategies of the systems discussed here closely reflect the different purposes for which migration is used and the final role the migrating cells will perform at their site of arrival. In one extreme case, hemocytes are dispersed as uniformly as possible throughout the embryo (Fig. 15D); quite in contrast, tracheal cells remain tightly attached to each other in an epithelial tubular structure while subpopulations of cells migrate in different directions, thereby sculpting the three-dimensional appearance of the entire organ system (Fig. 15P).

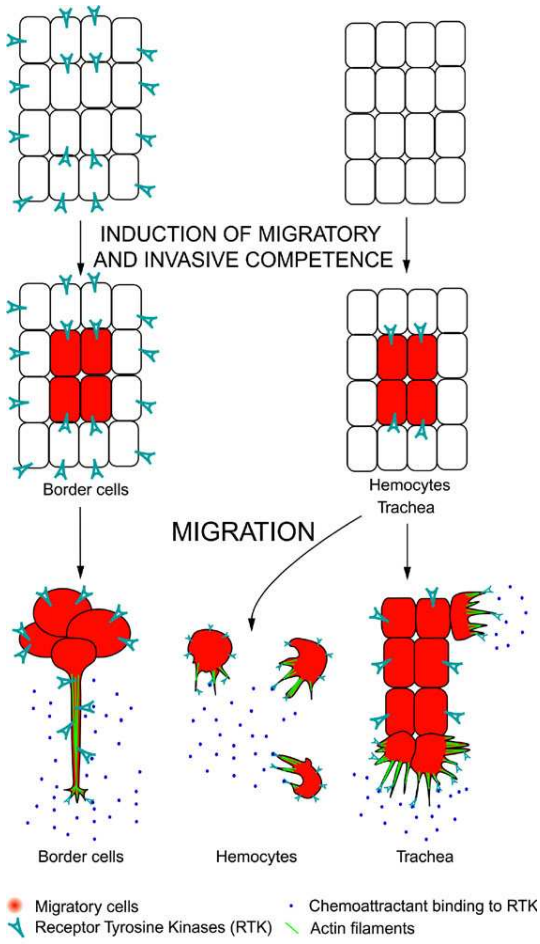

Figure 17 *Determination and induction of migratory fates in* Drosophila*.* Migratory cells are determined out of a field of cells by different signaling events (*e.g.* JAK/STAT). This leads to the expression of specific transcription factors (*e.g.* Slbo for border cells, Trh for tracheal cells), which, together with additional inductive events, activate a transcriptional program that renders the cells competent for invasion and migration (*e.g.* in trachea and hemocytes by the induction of the corresponding receptors and other intracellular signaling mediators). Subsequently chemoattractants activate tyrosine kinase guidance receptors which transduce the signal to the actin cytoskeleton resulting in the induction of cellular extensions, invasiveness and ultimately guided migration. Migration is integrated into the cellular context of each system and leads to strikingly different outcomes: in the case of the border cells, cells migrate as a group, in the case of hemocytes, cells migrate as single cells and in the case of tracheal cells, motility of a subgroup of cells leads to the three dimensional sculpting of an interconnected tubular system.

These examples illustrate the requirement for a complex interplay between the cell motility machinery and organ-specific programs that specify functional requirement. It is questionable, for example, whether tracheal cells have to retract their rear end actively, or whether this step is unnecessary due to their migration as an epithelial sheet. Migrating cells also do interact quite differently with cells in their immediate environment, and little is known at what level such interactions (via cadherins and integrins) intersect with the motility machinery.

A very interesting question to address in the future is how a cell achieves the competence to migrate as a result of the activation of a particular signaling system during development. In several cases transcription of the gene encoding the chemoattractant receptor is specifically activated in cells prior to migration (PVR in hemocytes, FGFR in tracheal, glial and muscle cells; Fig. 17 top right). Although this might suggest that particular receptors are migration-inducers, the same receptors induce migration only in a specific time window and regulate other events in the same cells. This is very striking in the case of the EGFR, a receptor which is widely distributed (most or all cells in *Drosophila* express it), and yet only subgroups of cells respond in a particular time windows with guided migration to receptor activation as in the case of border cells. Much has been learned in the last few years about the specific interpretation of widely used signaling systems with regard to nuclear gene-regulatory events, implying an integration of nuclear selector proteins and signaling mediators on specific enhancer elements (Affolter and Mann, 2001; Curtiss *et al.*, 2002). Little or close to nothing is known about the molecular mechanisms involved in the generation of specific cytoplasmatic responses of different cells to widely used signaling systems.

The recent development of *in vivo* live visualization methods and their combination with the powerful genetic and reverse genetic approaches available in several animal model systems will be a great help in integrating cell movement into tissue and organ development in the near future (Lichtman and Fraser, 2001). These studies should reveal to what extent common themes prevail and to what extent migrating cells use different molecular routes to help them find their way.

Chapter 4

Regulation of cell migration during tracheal development in *Drosophila melanogaster*

Valérie Petit, Carlos Ribeiro, Andreas Ebner and Markus Affolter[1]

Published in 2002 in the International Journal of Developmental Biology, volume 46, pages 125-132

Cell migration plays a fundamental role in numerous normal and pathological processes, including embryonic development, wound healing, inflammation and metastasis of tumor cells. Much of the current understanding of the mechanisms controlling cell migration comes from *in vitro* studies of cells in culture. Notably, the nature of the molecular machinery producing the force to drive cell locomotion has been elucidated starting from *in vitro* systems. Recent studies have identified many genes involved in the regulation of guided cell migration *in vivo*. We will try to compare the results of these two fields, using tracheal cell migration in *Drosophila melanogaster* as an *in vivo* model system, and discuss some of the directions and questions of future studies.

Current view of cell migration of individual cells over a two dimensional substrate

Cell locomotion involves a succession of adhesions (formation of cell-substratum contact sites) and de-adhesions (disassembly of contacts) of the cell to the underlying substrate, accompanied by a net forward movement of the cell (for reviews see Lauffenburger and Horwitz, 1996; Sheetz *et al.*, 1999). At the macroscopic level, a succession of several steps leading to cell locomotion can be distinguished: formation of membrane protrusions, establishment of stable contacts between the cell and the substratum, cytoskeletal contraction to move the cell body forward, release of adhesions at the rear of the cell and recycling of membrane components from the back to the front of the cell (see Fig. 18).

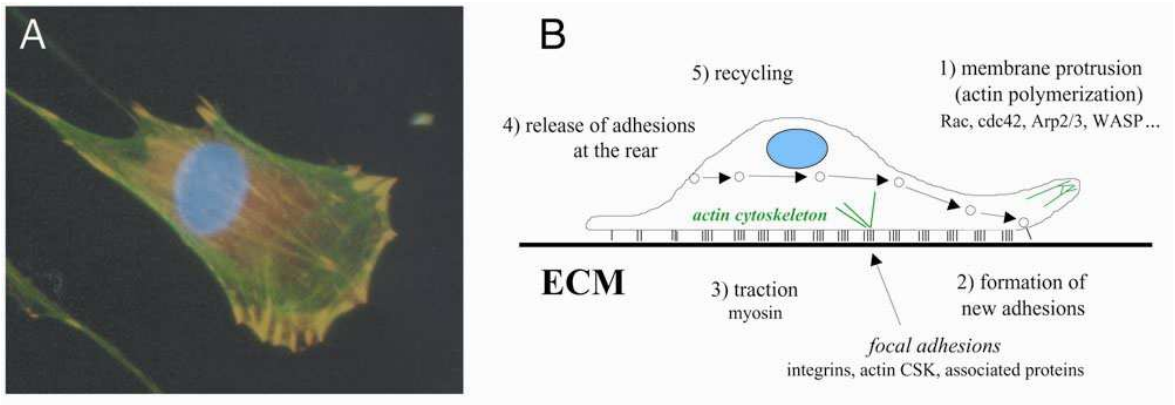

Figure 18 *Cell migration over a two dimensional substrate.* A, Indirect immunoflurescence of focal adhesions and stress fibers in human foreskin fibroblasts as revealed by vinculin staining in red and F-actin staining in green. The nucleus is revealed by DAPI staining. (Courtesy of S. Dufour). B, Illustration of a migrating cell and the five steps involved in the locomotion process. ECM, extracellular matrix; CSK, cytoskeleton. (adapted from Lauffenburger and Horwitz, 1996).

A number of molecular components have been identified that play important roles in the steps mentioned above. The motile cell first extends membrane processes, such as filopodia or lamellipodia, from the leading edge in the direction of movement. These protrusive extensions are produced by local actin polymerization. Actin filaments grow at their barbed end toward the leading edge of the cell, which provides the force for membrane protrusion (for a review see Machesky and Insall, 1999). New barbed end originate either from nucleation of new filaments from G-actin pools, or from uncapping, severing or branching of existing filaments. Numerous reports have now identified the Arp2/3 complex and members of the WASP (Wiskott-Aldrich Syndrome protein) family as important initiators of actin filament nucleation and branching at the leading edge of motile cells (Machesky *et al.*, 1994; Machesky and Gould, 1999; Machesky and May, 2001; Pantaloni *et al.*, 2000; Zigmond, 2000). Additional proteins play important roles in the dynamics of actin filaments by capping their ends (capping protein, gelsolin), severing them (gelsolin, ADF/cofilin), crosslinking them (α-actinin, fascin, filamin), sequestering G-actin subunits (β-thymosins, profilin), recruiting actin filaments to the surface (Ena/Mena/VASP family) and promoting pointed end depolymerization to provide G-actin monomers for addition at the barbed ends (ADF/cofilin) (for reviews see Cooper and Schafer, 2000; Pantaloni *et al.*, 2001). Numerous reports indicate that quantitative alteration of some of these proteins affects the speed of cell migration. In addition, the function of most of these proteins is affected by the presence of PIP2 (phosphatidylinositol-4,5-biphosphate) (Toker, 1998).

Membrane extension at the front of the cell eventually lead to the formation of new attachments to the substratum. Specialized structures are formed at this contact point, termed focal adhesions, where transmembrane adhesion receptors, mainly of the integrin family, provide a structural link between the actin cytoskeleton and extracellular matrix (ECM) components (for reviews see Critchley, 2000; Jockusch *et al.*, 1995; Petit and Thiery, 2000). Various cytoskeletal and signaling proteins assemble at the cytoplasmic face of focal adhesions and serve as signal transducers between the ECM and the actin cytoskeleton (Schoenwaelder and Burridge, 1999; Yamada and Geiger, 1997). Quantitative changes of focal adhesion components, such as the adhesive receptors (integrins), cytoskeletal components (*i.e*. Focal adhesion kinase (FAK), Src kinase, paxillin, vinculin or talin) or changes in integrin/ECM ligand affinity can alter the adhesive strength of the cell to the substratum and hence the speed of cell migration. Maximal cell migration occurs at intermediate adhesive strength when cytoskeletal forces are in balance with adhesion (Huttenlocher *et al.*, 1996; Palecek *et al.*, 1997).

To move the cell body forward, intracellular contractile forces depending on myosin motor activity are generated at these cell-substratum contacts. Under conditions in which the adhesive strength is too low, cells are unable to

generate enough traction to move, whereas under conditions of high adhesiveness, cells are unable to break cell-substratum attachments. Mechanisms that allow the release of cytoskeletal connections at the rear of the cell involve the coordinated regulation of physical and biochemical processes (Palecek *et al.*, 1998; Palecek *et al.*, 1996). As a last step, the motile cell has to recycle membrane and associated adhesion receptors to the front of the cell in order to recruit them to the extension process. Membrane is internalized at the rear of the cell and delivered through the endocytic pathway to the sites of protrusion in migratory cells (Bretscher and Aguado-Velasco, 1998; de Curtis, 2001).

Regulation of motility of cells in culture

Various factors in the cellular microenvironment participate in the regulation of local actin polymerization and cell migration. These include a number of soluble growth factors, chemotactic factors and ECM proteins, the pivotal role of which has been clearly established using *in vivo* and *in vitro* model systems. These different ligands bind to their appropriate receptors on the cell surface and trigger signaling pathways that impinge on the reorganization of the cytoskeleton, thereby regulating actin polymerization/depolymerization and the state of adhesion site assembly and disassembly, ultimately allowing the cell to migrate. In the following, we will briefly outline how a signal from outside of the cell can be converted into a migratory response and what is known at present about the regulation of this complex process.

An important role for small Rho GTPases in cytoskeletal reorganization required for cell migration

Members of the Rho (Ras homologous) family of GTPases are major elements regulating changes in cell morphology and reorganization of the cell cytoskeleton in response to external stimuli. Similar to Ras, Rho family GTPases cycle between inactive GDP-bound and active GTP-bound forms. This cycling is regulated by guanine nucleotide exchange factors (GEFs) which exchange GDP for GTP, and GTPase-activating proteins (GAPs) which induce the hydrolysis of bound GTP to GDP. The balance of GEF and GAP activity toward Rho proteins determines their level of activity in the cell. Members of the Rho family have been identified in organisms ranging from yeast to humans, including for example RhoA-E, G, H, Rac1-3, Cdc42, G25K, TC10 and Rnd1-3 in mammals (for a review see Hall, 1994). In fibroblasts, RhoA is implicated in the formation of actin stress fibers and focal adhesions (Hotchin and Hall, 1995; Ridley and Hall, 1992), whereas Rac1 and Cdc42 participate in the formation of lamellipodia and filopodia, respectively, as well as in the

regulation of associated focal complexes (Ridley and Hall, 1992). Although the role of Rho family GTPases is not fully understood, numerous studies using mutants as well as dominant negative and constitutively activated forms of these GTPases support their importance in cell migration *in vitro* and *in vivo* (Keely *et al.*, 1997; Murphy and Montell, 1996; Nobes and Hall, 1999; Shaw *et al.*, 1997).

Downstream effectors of small G proteins in cell migration

In the GTP-bound form, Rho GTPases interact with effector proteins in order to elicit a downstream response. Identification of specific targets has lead to a better understanding of how Rho proteins regulate different cellular processes (for reviews see Bishop and Hall, 2000; Van Aelst and D'Souza-Schorey, 1997). We will focus on the targets that control the reorganization of the cytoskeleton required for cell migration.

Some effectors act rather directly on the actin polymerization process. This is the case for phosphatidylinositol-4-phosphate 5-kinase (PIP 5-kinase), a target of Rac. Through the increase of PIP2 levels, PIP5-kinase regulates the function of many actin-associated proteins (for example gelsolin, profilin and vinculin). This is also the case for WASP, an exclusive target of Cdc42 (Rohatgi *et al.*, 1999). WASP contains multiple domains that interact with different signaling molecules, phosphoinositides and components of the machinery required for actin polymerization, such as actin monomers and the Arp2/3 complex (for a review see Zigmond, 2000). In its inactive state, WASP adopts an auto-inhibitory conformation, in which the C-terminus interacts with the central part of the molecule. Upon activation by GTP-Cdc42, which competes with the C-terminus for the same binding site, this intramolecular inhibition is released and permits the binding of WASP to the Arp2/3 complex (Kim *et al.*, 2000). Binding of WASP to the Arp2/3 complex activates the actin-nucleating function of the latter and thereby locally increases actin polymerization.

As already mentioned, cell migration involves a succession of adhesion and de-adhesion of the cell to the substrate, which implies a tight regulation of the assembly and disassembly of focal adhesions and their associated stress fibers. Phosphorylation of myosin light chain (MLC) is required for its association with actin, which leads to contraction and stabilization of stress fibers. MLC phosphorylation is regulated by the opposing effect of MLC-kinase (MLCK) and MLC-phosphatase. Some targets of Rho proteins exert their effects by regulating the phosphorylation state of MLC, and in this manner affect the adhesive state of the cell. This is the case for the serine/threonine kinase Pak (p21-activated kinase) , a target of Cdc42 and Rac. Paks are serine/threonine kinases that contain a Cdc42/Rac interaction motif called the CRIB (Cdc42/Rac-interactive binding) site (for a review see Bagrodia and Cerione, 1999). Expression of different mutant forms of Pak1 showed that it induces two types of

effects on cell morphology, one related to its protein kinase activity, which is essential for the disassembly of focal adhesions, and one that is kinase-independent and promotes lamellipodia formation and membrane ruffling (Manser *et al.*, 1997; Obermeier *et al.*, 1998; Sells *et al.*, 1997; Zhao *et al.*, 1998). Moreover, Pak activation leads to a decrease in MLC phosphorylation through phosphorylation of MLCK, thus destabilizing actin stress fibers (Sanders *et al.*, 1999).

In contrast to Pak, the Rho-associated serine/threonine kinases ROKα/β, which are targets of the Rho GTPase, phosphorylate MLC and inactivate the MLC-phosphatase thus increasing actomyosin assembly (Amano *et al.*, 1996; Kimura *et al.*, 1996). Therefore, activation of these effectors by Cdc42/Rac or Rho provides a molecular control of the level of MLC phosphorylation and hence the adhesive strength of a cell to the substrate.

Regulation of G protein activity by extracellular ligands

A number of soluble growth factors and ECM proteins have been reported to induce cell migration by interacting with their appropriate receptors, ultimately regulating GTPase activity. For many of these ligands, the molecules linking the activated receptors to the Rho-family GTPases have not been identified yet. A nice example describing the isolation of molecules regulating Rac GTPase *in vivo* has recently been reported in studies aimed at a better understanding of axon guidance in the visual system of *Drosophila* (for a review see Lin and Greenberg, 2000). In that particular case, the activated guidance receptor(s) appears to directly recruit the SH2-SH3 adaptor Dreadlocks (Dock)/Nck, which in turn binds to the Pak kinase mentioned above (Hing *et al.*, 1999). In parallel, Trio, a GEF for Rac, is also activated by the guidance signal, pushing the equilibrium of Rac to GTP-Rac, which in turn promotes Pak kinase activation (Newsome *et al.*, 2000). These studies thus propose that distinct signals transduced via Trio and Dock act combinatorially to activate Pak in spatially restricted domains within the growth cone, thereby controlling the direction of axon extension.

Since directed cell migration and axon guidance both occur through regulated actin polymerization/depolymerization, the genetic isolation of genes involved in axon guidance might identify components more generally implicated in actin metabolism, which might therefore also play a role in cell migration.

Regulation of migration *in vivo*

Most of the knowledge summarized above concerning the basic steps involved in cell migration has been derived from studying cells in culture. Many of the concepts derived from these studies have been partially confirmed in *in vivo* systems but numerous questions regarding the developmental control of cell motility remain. Tracheal morphogenesis in the embryo of *Drosophila melanogaster* has been used as a model system to study the genetic control of cell migration in a shaping organism. We will first describe what is known about tracheal development and present a conceptual framework for the regulation of tracheal cell migration as derived from these studies. We then try to span links between these *in vivo* studies and the movement of cells over two dimensional substrates and elaborate on important questions that remain to be addressed in the future.

The tracheal system of Drosophila melanogaster

The tracheal system of *Drosophila* consists of a branched network of epithelial tubes that provides oxygen from the environment to all tissues of the body. The interconnected network develops from individual clusters of ectodermal cells that invaginate into the underlying mesoderm and form 10 sacs on each side of the embryo, each containing about 80 cells (for reviews see Affolter and Shilo, 2000; Manning and Krasnow, 1993; Metzger and Krasnow, 1999; Shilo *et al.*, 1997). Without further cell divisions, each sac forms five to six primary branches (dorsal branch, dorsal trunk anterior and posterior, lateral branch anterior and posterior, and visceral branch) by stereotypical, directed cell migration (see Fig. 19). Each of these branches has a defined identity that specifies tube size and the subsequent determination of specialized cell fates at precise positions and in the appropriate number. Most branches differentiate a number of terminal cells, which form fine cytoplasmic extensions through which gas is exchanged with the target tissues. In addition, fusion cells at the extremity of dorsal and lateral branches and the dorsal trunk allow the interconnection of adjacent tracheal metameres, leading to the formation of a continuous luminal network.

Tracheal cell fate determination

The determination of tracheal identity in clusters of cells, the tracheal placode, is achieved in part by the local expression of the Trachealess (trh) and the Drifter/Ventral veinless (Drf/Vvl) transcription factors (Anderson *et al.*, 1995; de Celis *et al.*, 1995; Isaac and Andrew, 1996; Wilk *et al.*, 1996; Zelzer and Shilo, 2000b). *Trh* encodes a basic helix-loop-helix (bHLH)-PAS-domain protein which forms a complex with Tango (Tgo), a broadly expressed bHLH-PAS protein, whereas *drf/vvl* encodes a

POU-domain DNA binding protein. The expression of numerous genes crucial for tracheal development is dependent on *trh*, *vvl* or the cooperation of both; these genes encode, for example, the FGF receptor Breathless (Btl), the FGF signal transduction component Downstream of FGF-R (Dof), the Dpp type I receptor Thick veins (Tkv) and the EGF signaling component Rhomboid (Rho) (Boube *et al.*, 2000).

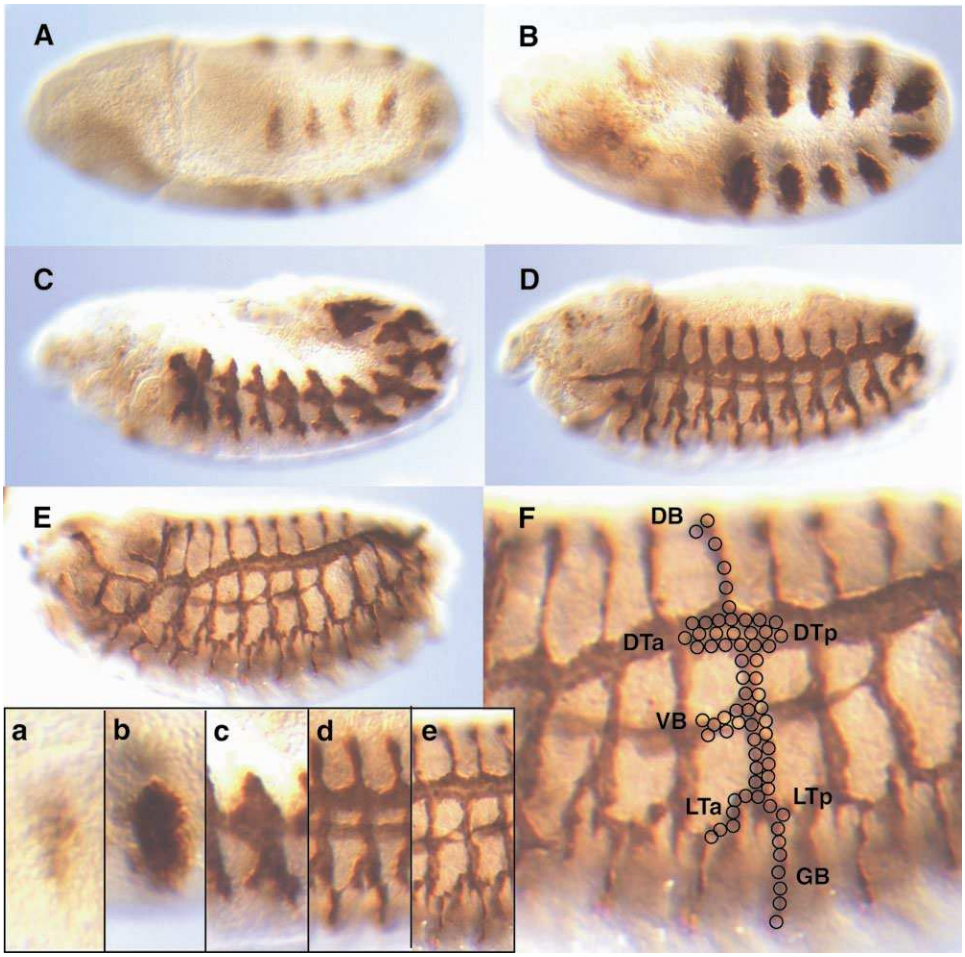

Figure 19 *Embryonic development of the tracheal system*. (A-E) Tracheal cells are visualized by anti-β-Gal staining of the 1-eve-1 enhancer trap line. This line has a P-element inserted in the 5 prime region of the *trh* gene (Perrimon *et al.*, 1991; Wilk *et al.*, 1996). Expression is first detected at late stage 10 (A) in the ectoderm and outlines the tracheal pits at stage 11 (B). Outgrowth of primary branches at stage 12 (C) and stage 14 (D). At stage 16 (E), dorsal and lateral trunks are fused. Nomenclature of the tracheal branches (F): dorsal branch (DB, 5-7 cells), dorsal trunk anterior and posterior (DTa/p, 19-21 cells), visceral branch (18-20, not all cells are shown), lateral trunk anterior (LTa, 7-10) and lateral trunk posterior (LTp, 4) and ganglionic branch (GB, 6-8). Cell numbering is according to (Samakovlis *et al.*, 1996). (a-e) Enlargements of the corresponding stages in A to E.

After their determination, the placodes invaginate in a concerted manner and form a tracheal sac. This process generates a lumen, from which tubular branches subsequently bud off in five to six directions. Recent studies suggest that EGF receptor and Hedgehog transduction pathways might contribute to the process of tracheal invagination (Glazer and Shilo, 2001; Llimargas and Casanova, 1999).

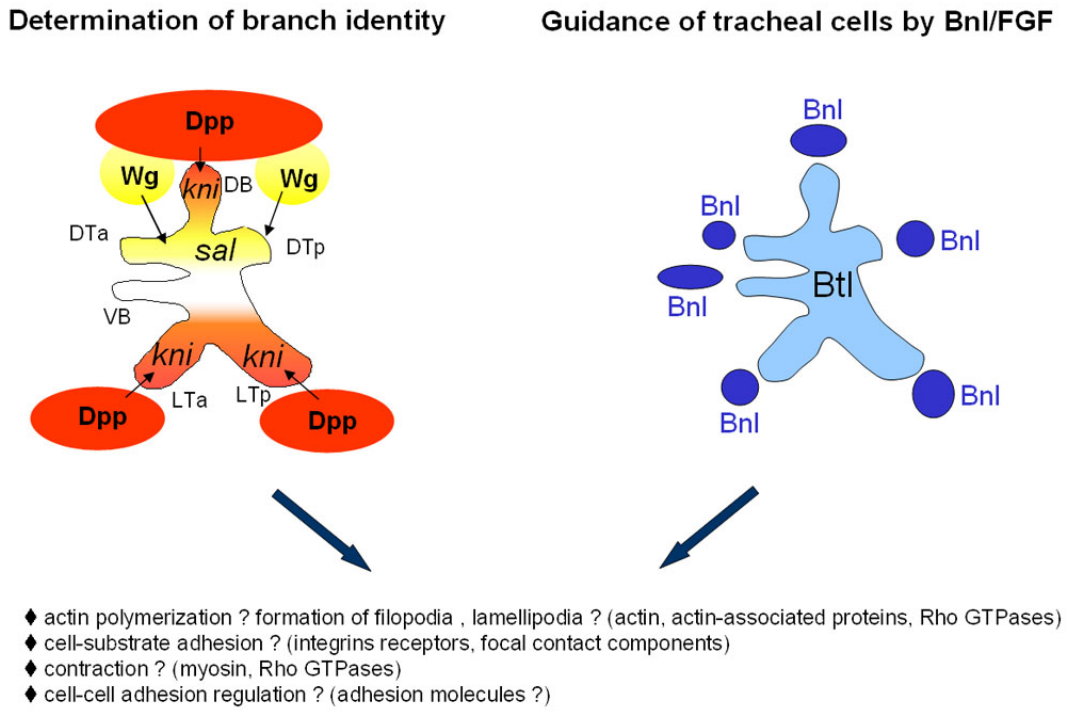

Figure 20 *Illustration of a tracheal placode and the signaling pathways involved in branch fate determination and guidance of tracheal cells.* The six primary branches are represented: DB, dorsal branch; DTa and DTp, dorsal trunk anterior and posterior; LTa and LTp, lateral trunk anterior and posterior; VB, visceral branch. The sal expression domain is outlined in yellow, whereas the kni expression domain that depends on Dpp signaling is represented in orange. Tracheal integration of these signaling pathways eventually leads to cell migration in the proper direction by mechanisms that remain to be determined. Bnl, Branchless; Btl, Breathless; Dpp, Decapentaplegic; kni, knirps; sal, spalt; Wg, Wingless. A comprehensive list of genes involved in tracheal cell migration can be found at http://www.bioz.unibas.ch/affolter/trachea

Subdivision of the tracheal placode

In the early tracheal placode, the fate of cells with respect to their future position in the tracheal tree is not specified (Samakovlis *et al.*, 1996). Positional cues are provided by nearby cells, which induce specific tracheal subfates within the tracheal fields and thereby assign cells to the future branches prior to the initiation of migration. The Decapentaplegic (Dpp) signaling pathway specifies the fate of the tracheal branches that will bud from the dorsal and ventral part of the tracheal placode. The Dpp ligand, a member of the TGFβ family, is expressed in ectodermal cells positioned dorsally and ventrally to the invaginated placodes (Vincent *et al.*, 1997; Wappner *et al.*, 1997). In the absence of Dpp signaling, the dorsal branches do not form and the lateral trunk and ganglionic branches show severe defects. When Dpp signaling is activated in all tracheal cells, prospective dorsal trunk cells migrate in dorsal direction instead of migrating along the anteroposterior axis. Dpp signaling activates the expression of the zinc finger proteins Knirps (Kni) and Knirps-related (Knrl)

in responding tracheal cells (Chen *et al.*, 1998). Activation of Kni/Knrl is not only essential to determine the correct number of cells in dorsal and ventral branches, but is also critical in allowing cells to respond to the chemoattractant Bnl (see below), to control subsequent branch patterning events, and to determine the size of the tube to be formed during morphogenesis (Beitel and Krasnow, 2000; Chen *et al.*, 1998).

Two other signaling pathways have recently been described that play similar roles in subdividing the tracheal placode. The wingless/WNT pathway is required for the formation of the dorsal trunk by activating the expression of the transcription factor *spalt* (*sal*) (Chihara and Hayashi, 2000; Llimargas, 2000). When Wg signaling is activated in all tracheal cells, visceral branch cells turn on *sal* expression and migrate as dorsal trunk cells. On the other hand, the dorsal trunk is missing in mutants affecting the function of proteins of the Wg/WNT pathway (*armadillo, porpucine, dishevelled, pangolin/dTCF*). Wg protein is expressed by ectodermal cells on the anterior and posterior side of each tracheal placode, but it appears that other DWnt ligands also act on tracheal development. A recent study describes a role for the Hedgehog (Hh) signaling pathway in tracheal branch patterning (Glazer and Shilo, 2001). Hh protein is expressed in ectodermal segmental stripes abutting the anterior border of the tracheal placodes, and induces expression of target genes such as *patched* in anterior tracheal cells. In addition to defects observed in invagination of the placode, cells in many tracheal branches fail to migrate properly in *hh* mutants.

Although target genes for the above pathways have been identified in tracheal cells, how these signaling pathways are interpreted and specify cell migration remains elusive. An attractive hypothesis is that these pathways activate the expression of distinct cell adhesion molecules in each branch leading to the cell sorting of the different tracheal cells.

Guided migration of primary tracheal cells

Although Dpp, Wnt and Hh signaling defects result in the absence of cell migration in distinct directions and despite the fact that the corresponding ligands are expressed in non-tracheal cells around the placode, none of these signaling molecules appears to act as a chemoattractant. Until now, the only known chemoattractant for tracheal cells is the Fibroblast Growth Factor (FGF)–like protein encoded by the *branchless* (*bnl*) gene (Sutherland *et al.*, 1996). *bnl* is expressed dynamically in groups of non-tracheal cells around the invaginated placode and prefigures the direction in which the six primary branches will grow out. The *breathless* (*btl*) FGF-R gene is expressed on the surface of all tracheal cells and mediates the effect of Bnl in the tracheal system (Glazer and Shilo, 1991; Klambt *et al.*, 1992; Reichman-Fried *et al.*, 1994). In *bnl* and *btl* mutants, the specification of tracheal cells is normal and the placode invaginate but primary branches fail to migrate. In contrast,

ectopic Bnl can redirect tracheal cell migration to new sites of expression, thus demonstrating its role as a chemoattractant (Sutherland *et al.*, 1996).

Signal transduction through the vertebrate FGF-R requires association of the FGF-ligand with its receptor as well as with heparan sulfate proteoglycans (HSPGs) in order to form an active signaling complex (Schlessinger *et al.*, 2000). Recent studies have identified enzymes required for the biosynthesis and modification of HSPGs which are essential for signaling by Btl during *Drosophila* tracheal morphogenesis. Indeed, mutations in *sugarless* and *sulfateless*, which encode the homologues of UDP-D-glucose dehydrogenase and heparan sulfate N-deacetylase/N-sulfotransferase, respectively, result in defects in the migration of tracheal cells similar to those observed in the absence of the Bnl/FGF ligand or receptor (Lin *et al.*, 1999).

Once activated, the FGF receptor signaling complex signals through the mitogen activated protein kinase (MAPK) cascade, which is a signal transduction pathway common to many receptor tyrosine kinases (RTKs). A novel component of the FGF-R signaling cascade in *Drosophila*, which acts specifically in the FGF-R and not in other RTK signaling pathways, has been identified. This gene, named *downstream of FGF-R* (*dof*), is essential for the FGF-mediated activation of the MAPK cascade and for tracheal cell migration as well as for mesoderm development (Vincent *et al.*, 1998); mutations allelic to *dof* have been described and the corresponding genes called *heartbroken* or *stumps* (Imam *et al.*, 1999; Michelson *et al.*, 1998). Dof is present exclusively in cells that express FGF receptors and represents a novel cytoplasmic protein containing putative ankyrin-repeats and a coiled-coil domain. *dof* mutant embryos show the same defects in tracheal migration as *bnl* and *btl* mutant embryos, as well as defects in mesodermal migration similar to those seen in embryos carrying mutation in the gene *heartless (htl)*, which encodes the second *Drosophila* FGF-R. Dof has been shown to act downstream of both FGF-Rs and upstream of Ras in the activation of the MAPK cascade, but its precise role in conveying the chemotactic response in tracheal cells remain to be elucidated. No Dof homologs have been identified so far in other organisms.

Although localized *bnl* expression directs the budding of all primary branches, tight spatial control of *bnl* does not appear to be essential for the formation of dorsal trunk branches (Sutherland *et al.*, 1996). Dorsal trunk formation thus appears to rely on additional guidance cues. Wolf and Schuh recently identified a mesodermal cell, named bridge cell, located at the posterior edge of each dorsal trunk bud and expressing the transcription factor *hunchback* (*hb*) (Wolf and Schuh, 2000). In *hb* mutants, dorsal trunk branches fail to complete migration and subsequently fail to fuse; all the other branches seem to migrate properly, suggesting that the *hb*-expressing bridge cell is essential for dorsal trunk formation (Wolf and Schuh, 2000). The precise function of the bridge cell and molecular targets of *hb* remain to be elucidated.

Additional substrates for migration

Little is known about the substrates supporting tracheal cells during the locomotion process. A recent study identified and described the different cellular contexts encountered by each branch of the tracheal system during its formation (Franch-Marro and Casanova, 2000). Tracheal cells that form the dorsal branches migrate in preexisting grooves between muscle precursors of adjacent metameres, whereas cells that form the dorsal trunk and ventral branches migrate across or along mesodermal cells. Visceral branch migration has been studied in more detail and cell surface receptors of the integrin family have been implicated in the migration process (Boube *et al.*, 2001). The αPS1 integrin encoded by the *multiple edematous wings (mew)* gene is specifically express in the visceral branch cells under the control of the transcription factors *kni/knrl* (Boube *et al.*, 2001). In *mew* mutants visceral branches migrate normally out from the placode and toward the visceral mesoderm but fail to migrate along this substrate upon contact (Boube *et al.*, 2001). These results indicate that the αPS1 subunit is required for migration over the mesoderm, stimulating motility rather than guiding it. Additional cues, possibly Bnl itself, regulate the initial guided migration from the placode to the visceral mesoderm and presumably support integrin-mediated migration over the mesoderm. This report is the first identification of an adhesion molecule whose expression is restricted to a subset of tracheal cells under the dependence of the transcription factors that initially subdivide the tracheal placode (see above). It will be interesting to find out whether other branches also express distinct adhesion molecules to allow for their migration along distinct pathways.

Although the development of the tracheal system and genes controlling this process have been investigated for a number of years in several laboratories, many questions concerning the migration of tracheal cells remain unanswered. How is the motile state specifically induced in tracheal cells at the appropriate time? How is cell movement directed by the Bnl/FGF chemoattractant? How are the additional, branch-specific signaling systems interpreted? What are the molecular links between the guidance cues and the cellular machinery of migration? And how is migration arrested at the correct destination? In the last chapter, we will compare the *in vivo* and the cell culture experiments and briefly comment on how some of these questions might be addressed.

Cell migration in vivo: which processes are controlled by extracellular signals?

As outlined in the first sections, cell locomotion involves a highly regulated succession of filopodia/lamellipodia formation, adhesion and de-adhesion. Numerous molecules have been identified that are either involved as effectors (actin polymers, adhesion complexes, etc.) or as regulators (WASP, small G proteins, cell surface receptors) of the migration process. Less is known about guided cell migration events *in vivo* but genetic studies start to provide insight into the molecular control of guidance. Numerous genes have been identified that are required for tracheal development and a first picture of the branching process can be drawn. Most of the identified gene products (which are either implicated in cell signaling and/or in transcriptional regulation; see Fig. 20 and http://www.bioz.unibas.ch/affolter/trachea) are regulating the migration process, and are not part of the migration machinery as such. Why did these genetic studies only lead to the isolation of regulatory components?

Many of the proteins that play essential roles in the locomotion process as defined in cell culture studies (*i.e*. actin and actin regulatory proteins) are also required for other essential processes (*i.e*. cell polarity and cell division); therefore it might be difficult to associate these factors directly with tracheal cell migration in straightforward genetic screens. In addition, genes encoding such factors might have a strong maternal contribution, allowing a homozygous mutant embryo to use the maternally provided wild type gene product for zygotic tracheal development. The generation of homozygous mutant germ line clones will help in the identification of such factors this question. However, more than 40% of lethal mutations do not complete oogenesis in homozygous germ line clones, thus prohibiting the analysis of later developmental stages. Conditional mutations and reverse genetics using constructs expressing dominant active and dominant negative gene products will have to help to define the role of these generally required components.

Despite these limitations, the genetic studies on tracheal development have given insight into a directed migratory process *in vivo* and how this process might be regulated. Clearly, FGF signaling acts as a major guidance system and the local production of the Bnl/FGF ligand prefigures subsequent migration directions. The expression pattern of Bnl is extremely dynamic and presumably controlled by separate transcriptional enhancers under the control of the earlier-acting genes that specify positional cues along the anterior-posterior and dorsal-ventral body axes (Metzger and Krasnow, 1999). It will be crucial to find out how the FGF signaling pathway is connected to cytoskeletal regulation and how Dof, a novel protein, fits into this scheme. Studies at the cellular level have to address the question of whether FGF signaling induces the formation of filopodia/lamellipodia and/or regulates cell adhesion. Using GFP-tagged proteins and four-dimensional confocal microscopy in living embryos, the dynamics of the migration process will have to be addressed, both in wild type and mutant situations. It is likely that Ras, Cdc42, Rac and Rho are major targets of FGF signaling with regard to guidance but this remains to be

demonstrated. Mutations in some of the small GTPases have been isolated (Fehon *et al.*, 1997; Strutt *et al.*, 1997) and dominant negative and constitutively active forms have been engineered; their effects on tracheal development will have to be analyzed in detail. It will also be crucial to find out in which cells of a migrating branch FGF signaling is initiated or is strongest and whether FGF signaling polarizes the responding cells.

Interestingly, and in addition to Bnl/FGF signaling, several other signaling systems (Dpp, Wnt, Hh) are crucial for the formation of distinct tracheal branches. The involved signaling molecules do not act as chemoattractants, but instruct tracheal cells at the onset of the migration process with regard to their migration directionality; for example, all tracheal cells that respond to Dpp signaling migrate along the dorsoventral axis, irrespective of where the Dpp signal comes from. Consistent with this observation, Dpp does not appear to polarize the responding cells but results in specific changes in nuclear gene expression. But what are the cellular events targeted by these signaling pathways, or in other words, what genes are transcriptionally controlled by Kni/Knrl? Is the actin polymerization machinery modified, or is cell adhesion differentially regulated by Dpp (and Wnt) signaling? If cell adhesion is regulated, is adhesion in-between tracheal cells or adhesion of tracheal cells to the migration substrate regulated? Clearly, without the information of Dpp and Wnt signaling, tracheal cells do not respond to the Bnl chemoattractant with directed outgrowth, and signaling from these two pathways has to be integrated somewhere in the locomotion process. These examples illustrate the complexity of information that needs to be processed by migratory cells *in vivo* in order to navigate properly through a developing organism.

An interesting question to be addressed in the future concerns the genetic regulatory network governing the formation of tracheal cells as such, a process which initiates tracheogenesis. Tracheal cells respond in a certain time window to the Bnl/FGF signaling system or to other RTKs by directed migration (Dossenbach *et al.*, 2001); most cells in the organism respond to receptor tyrosine kinase signaling with altered nuclear gene expression. What primes tracheal cells to respond in this specific fashion? Some of the selector genes under whose control epidermal cells are determined to become tracheal cells have been identified (*trh*, *tgo*, *dfr/vvl*). It is likely that some of the targets regulated by these transcription factors set the stage for the subsequent migration process, and the identification of these target genes would provide information regarding to the establishment of the “migratory-competent” state of the cell. Of course it is equally possible that the tracheal determinants repress the expression of inhibitors of cell migration. Careful comparison of the transcriptome of tracheal cells with adjacent epidermal cells using DNA chip technology and other novel, more sensitive techniques should provide insight into this question.

Chapter 5

Introduction to cellular junctions in *Drosophila* epithelial cells

Epithelial tissue has developed two particular features, which enables it to fulfill its function as tight compartment delimiter while permitting it to participate in the controlled exchange of molecules. First of all, the cells exhibit a polarize phenotype that is visible in the asymmetric distribution of cell components and a polarization of the membrane itself. This organization is mainly established and maintained by the formation of highly elaborate cell-cell junctions, which guarantee close adhesion between the cells and provide the barrier function characteristic of epithelia (Bilder, 2001; Knust and Bossinger, 2002; Tepass *et al.*, 2001).

Cell-cell junctions however have to not only function as a tight barrier to the external world and provide structural stability to the organism, they also have to allow the developing embryo to undergo the essential morphogenetic movements responsible for shaping the nascent organism. This requires a high degree of flexibility and stability as during those processes extra forces act on the junctional complexes while complex rearrangements take place.

Research on cell-cell junctions has mainly concentrated on studying the establishment and the molecular architecture of the different complexes involved in this cellular function. The mechanisms underlying junctional dynamics and remodeling have however been more difficult to understand. This could be due to the fact that most of our knowledge on junctional complexes comes from studies in cell culture. In the last years, however *Drosophila* research has been contributing strongly to this field opening the possibility to understand the role of cellular junctions in controlling the morphogenetic processes taking place during development.

The cells of all epithelia analyzed so far show a very similar structural and molecular organization while retaining some remarkable differences. All epithelia have an adhesive belt termed zonula adherens (ZA) that encircles the cells just below the apical surface. One of the main features of the ZA is its tight association with cytoplasmic actin fibers, which are thought to play a major role in ensuring the stability of the tissue while serving as driving force for changes in cell morphology. While vertebrates develop a tight junction (TJ), a specialized plasma microdomain apical to the ZA, *Drosophila* develops a different structure just basal to the ZA. This structure, the septate junction (SJ), forms a region of close membrane contacts that extend over large parts of the lateral membrane domain. Even if *Drosophila* does not have *bona fide* TJs a distinct region apical to the ZA, the subapical region (SAR) harbors protein complexes that are present in vertebrate TJs (Fig. 21). It is however very important to stress that these different microdomains are not completely isolated and independent. Only the complex interplay of the different junctional domains leads to the establishment and maintenance of the cellular polarization.

While early *Drosophila* cellularization has established itself as an excellent system to study the establishment and *de novo* formation of the

junctional complexes we will not further discuss this very interesting and essential question of junctional biology and concentrate in describing the molecular architecture and composition of the ZA .

The components of the SAR are thought to be the main players in apical polarization. As such especially Crumbs an apical transmembrane protein plays a major role in defining and maintaining the apical surface. When overexpressed the apical surface expands leading to polarization phenotypes.

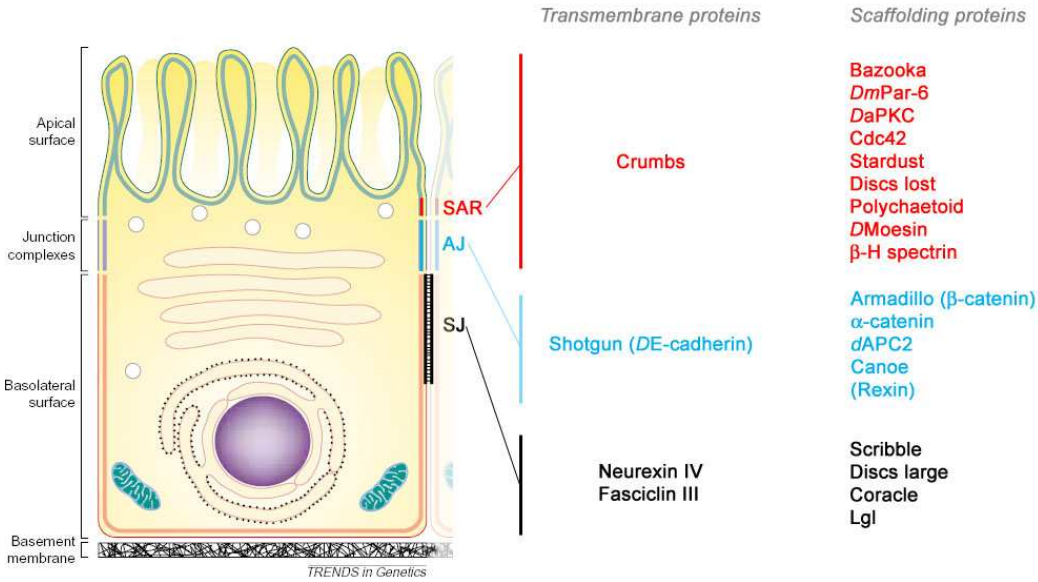

Figure 21 *Schematic representation of the cell structure in an ectodermal epithelial cell.* Subdomains of the plasma membrane are indicated on the left while cellular junctions and the distribution of their proteins are listed to the right. In red, the components of the sub apical region (SAR), in blue, the components of the adherens junctions (AJ) and in black, the components o the septate junctions (SJ). All these components are present and mostly even transcriptionally upregulated in tracheal cells. (adapted from Bilder, 2001; Knust and Bossinger, 2002)

Most of the scaffolding proteins are characterized by PDZ domains that serve as interaction domains with other proteins of the complexes. They also bind to C-terminal regions of transmembrane domains and are therefore thought to serve as organizers for many signaling receptors. As such, the junctions are more and more seen as autonomous organizing centers in epithelial cells, which additionally to their structural role also serve as modulators and coordinators of signaling events and other complex cellular processes (Lecuit and Wieschaus, 2002).

The best-characterized complex of the AJs is the *D*E-Cadherin/α-Catenin/β-Catenin complex. *D*E-Cadherin is a classic Cadherin and as a transmembrane protein, it is thought to be responsible for connecting AJs from adjacent cells. From multiple protein structure studies different Cadherin-Cadherin interaction models have been proposed (Fig. 22 and Tepass *et al.*, 2000). Especially the role of Calcium ions as a known major regulator of cis- and trans-dimerization has been given major attention in these studies.

The extent of overlap of the trans-interactions is however still very controversial. A short overlap at the N-terminal region (termed zipper model) would offer an easy model to explain the plasticity required for morphogenetic events. However, it is possible that the extent of overlap is regulated (maybe by the availability of Ca^{2+}) reconciling both interaction models and explaining the structural basis of junctional plasticity (for an excellent review on Cadherins see Tepass *et al.*, 2000).

The cytoplasmic tail of *D*E-Cadherin interacts with β-Catenin (Armadillo) which in turn interacts with α-Catenin. α-Catenin is then thought to play a key role in AJ formation through its interaction with various other AJ complex components (Nagafuchi, 2001). Especially the connection to the actin belt is mediated by α-Catenin serving as scaffold for the interplay of the cellular cytoskeleton and the junctions.

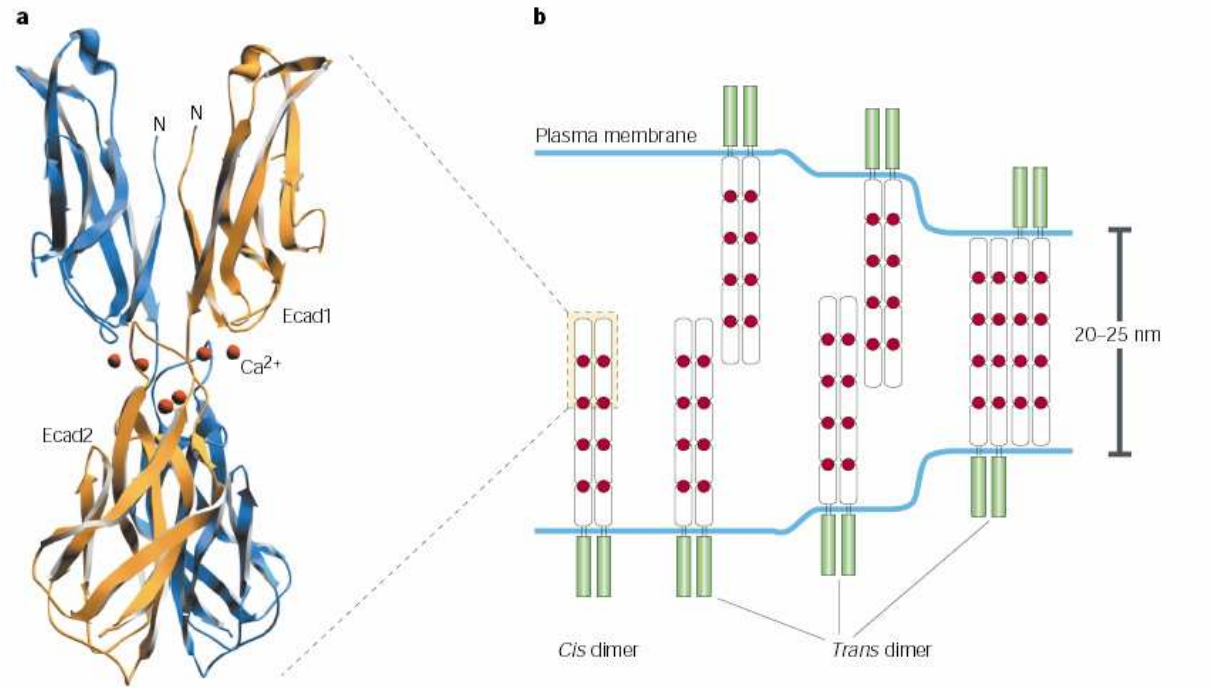

Figure 22 *Ca^{2+}-mediated cis- and trans-dimer formation of vertebrate classic cadherins.* (a) Dimer interface between two N-terminal repeats of E-cadherin domains 1 (Ecad1) and 2 (Ecad2). Each cadherin molecule binds three calcium ions that are important in the rigidification and *cis*-dimer association of cadherins. (b) A *cis* dimer consists of two cadherin molecules within the same plasma membrane that are associated laterally. The pairs of cadherin molecules from opposing cells that associate with one another are referred to as *trans* dimers. Different models for *trans*-dimer formation have been proposed that suggest different extents of lateral overlap between the extracellular regions. Red dots indicate the location of Ca^{2+} ions between adjacent CDs. (From Tepass *et al.*, 2000)

Chapter 6

In vivo imaging reveals different cellular functions for FGF and Dpp signaling in tracheal branching morphogenesis

Carlos Ribeiro, Andreas Ebner and Markus Affolter

Published in 2002 in the journal Developmental Cell, volume 2, pages 677-683.

Introduction

Cell migration is an essential process during development and pathology. Numerous cells arise at a distance from the place at which they fulfill their function. These cells have to be endowed with migratory capacities and with navigation systems allowing them to move directionally, often as cell-groups, in the living organism. Migration and navigation have to be regulated in time and space in order to avoid premature displacement or retarded migration arrest. The control of actin polymerization plays an important role in migration and in other processes in which cells explore their environment (Cooper and Schafer, 2000; Machesky and Insall, 1999; Pantaloni *et al.*, 2001). Structures known as filopodia and lamellipodia extend forward from the leading edge of motile cells and explore the environment. The formation of these actin-containing extensions is essential for cell motility. Interactions of cells or cellular extensions with molecules displayed on neighboring cells or deposited in the extracellular matrix help to coordinate movement in space (Lauffenburger and Horwitz, 1996; Sheetz *et al.*, 1999). Although much has been learned about the molecular control of motility from cell culture experiments (see also discussion), less is known about how all the relevant cues are integrated *in vivo* as a cell moves from one place to another in a developing organism. Certainly, *in vivo* analyses are required to fully appreciate the complexity of events underlying guided cell movements.

The genetic mechanisms regulating concerted cell migration have been analyzed *in vivo* in a number of systems (Montell, 1999; Nieto, 2001; Starz-Gaiano and Lehmann, 2001). Tracheal development in *Drosophila melanogaster* has been extensively used to study the control of cell movement in branching morphogenesis. The highly branched and tubular network, which extends throughout the entire organism and provides oxygen to all organs and tissues after larval hatching, is established during embryogenesis from individual groups of cells (placodes) by genetically programmed, stereotyped cell migrations and cell shape changes (Manning and Krasnow, 1993; Samakovlis *et al.*, 1996). A large number of genes that are involved in the migration process have been identified and a coherent picture of how this branched network is established is emerging (Affolter and Shilo, 2000; Metzger and Krasnow, 1999; Petit *et al.*, 2002; Zelzer and Shilo, 2000a).

One of the key signaling systems responsible for the correct spatial migration of tracheal cells is the Fibroblast Growth Factor (FGF) signal transduction cascade. An FGF-like ligand encoded by the *branchless* (*bnl*) gene is expressed prior to the migration process in non-tracheal cells surrounding the invaginating tracheal placode in a pattern which prefigures the subsequent migration events (Sutherland *et al.*, 1996). The Bnl/FGF receptor, encoded by the *breathless* (*btl*) gene (Klambt *et al.*, 1992), as well as an FGFR-specific signaling component encoded by the *downstream of FGFR* (*dof*) locus

(Vincent *et al.*, 1998), are expressed in the responding tracheal cells and mediate the cellular effects of Bnl/FGF signaling. In *bnl*, *btl* and *dof* mutants, the specification of tracheal cells is normal and the placodes invaginate but primary branches fail to migrate out. In contrast, ectopic Bnl/FGF can redirect tracheal cell migration to new sites of expression, demonstrating its role as a chemoattractant, the first one to be identified in *Drosophila* (Sutherland *et al.*, 1996). Somewhat surprisingly, the formation of individual tracheal branches via cell migration requires, in addition to Bnl/FGF signaling, other distinct signaling inputs. For the proper formation of dorsal, ganglionic and lateral trunk branches, Dpp signaling is required (Affolter *et al.*, 1994a; Llimargas and Casanova, 1997; Ruberte *et al.*, 1995; Vincent *et al.*, 1997; Wappner *et al.*, 1997). Dpp signaling induces the expression of the zinc finger proteins Knirps (Kni) and Knirps-related (Knrl) in responding tracheal cells (Chen *et al.*, 1998). Activation of *kni/knrl* is not only essential for dorsal and ventral tracheal cells to properly respond to the chemoattractant Bnl/FGF, but also to specify the size of the tracheal tubes to be formed during morphogenesis (Beitel and Krasnow, 2000; Chen *et al.*, 1998). In addition, ectopic Dpp signaling is capable to direct cells from migration along the anterior-posterior axis towards migration along the dorsal-ventral axis, indicating that Dpp signaling also affects in a more direct fashion the migration behavior of tracheal cells.

Two other signaling pathways, namely those triggered by the Wingless (Wg) and the Hedgehog (Hh) ligands, have recently been found to play similar roles in subdividing the tracheal placode and in specifying the formation of distinct tracheal branches. The formation of the dorsal trunk, which results from cell migration along the anterior-posterior body axis, requires the activation of the Wg signaling cascade; as a result of this signaling input, transcription of the *spalt* (*sal*) gene, which encodes a zinc-finger transcription factor, is kept at high levels in dorsal trunk cells, allowing them to respond to Bnl/FGF by directed anterior-posterior migration (Chihara and Hayashi, 2000; Kuhnlein and Schuh, 1996; Llimargas, 2000). Hh signaling is more widely implicated since in *hh* mutants, migration of all tracheal branches is absent or stalled (Glazer and Shilo, 2001); further studies are required to learn more about the requirement for Hh.

The requirement of different signaling systems for the directed outgrowth of primary tracheal branches leads to a number of questions (Metzger and Krasnow, 1999). How are these signaling pathways integrated with the Bnl/FGF pathway? What is the role of the chemoattractant Bnl/FGF? Are tracheal cells intrinsically motile or is motility induced by Bnl/FGF? And how are the patterning signals interpreted in order to achieve epithelial cell migration and tube-assembly events?

In order to start to address these issues we have studied the behavior of tracheal cells *in vivo* at high resolution in time and space using GFP-tagged proteins expressed in tracheal cells, both in wild type and in mutant living embryos.

We find that tracheal cells located at the tip of growing branches make numerous filopodia in a dynamic fashion in wild type embryos. These filopodia are absent in mutants affecting the function of the FGFR

signaling pathway, and are found at highly increased frequency in all tracheal cells upon ubiquitous expression of *bnl*. These results clearly demonstrate that the chemoattractant Bnl/FGF regulates filopodia extension and dynamics in the tracheal target cells. In mutants in which Dpp signaling is compromised, cellular extensions are still formed and cells initially migrate dorsally; however, cells later reintegrate into the dorsal trunk leading to the absence of dorsal branches. From this *in vivo* analysis, we conclude that the two signaling systems affect different cellular functions. The Bnl/FGF chemoattractant controls the formation of cellular extensions through cytoskeletal rearrangements and thus appears to control migration. Dpp signaling is required, in conjunction with Bnl/FGF, for a coordinated morphogenetic movement, allowing tracheal cells to form a stable tracheal branch. Several molecular scenarios that could account for the distinct roles of Bnl/FGF and Dpp in tracheal development are discussed.

Results

Formation of actin-containing cellular extensions during tracheal cell migration

In order to investigate possible dynamic cell shape changes accompanying tracheal cell movement *in vivo* and link them to the different signaling systems, we used 3D-reconstructions of confocal images of living embryos expressing different GFP-tagged proteins in the developing tracheal system (for details see materials and methods). Expression of *GFP-actin* (Verkhusha *et al.*, 1999), driven in tracheal cells by the *btl-Gal4* driver line (Shiga *et al.*, 1996), revealed fine cellular protrusions from cells at the tip of growing branches after initiation of germ band retraction when migration starts (Fig. 23A-C). Such cell extensions were most prominently observed in the developing dorsal and ganglionic branches as well as in the dorsal trunk anterior and posterior (Fig. 23C). During the early stages of branch outgrowth, these cellular extensions were generally short and relatively few in number.

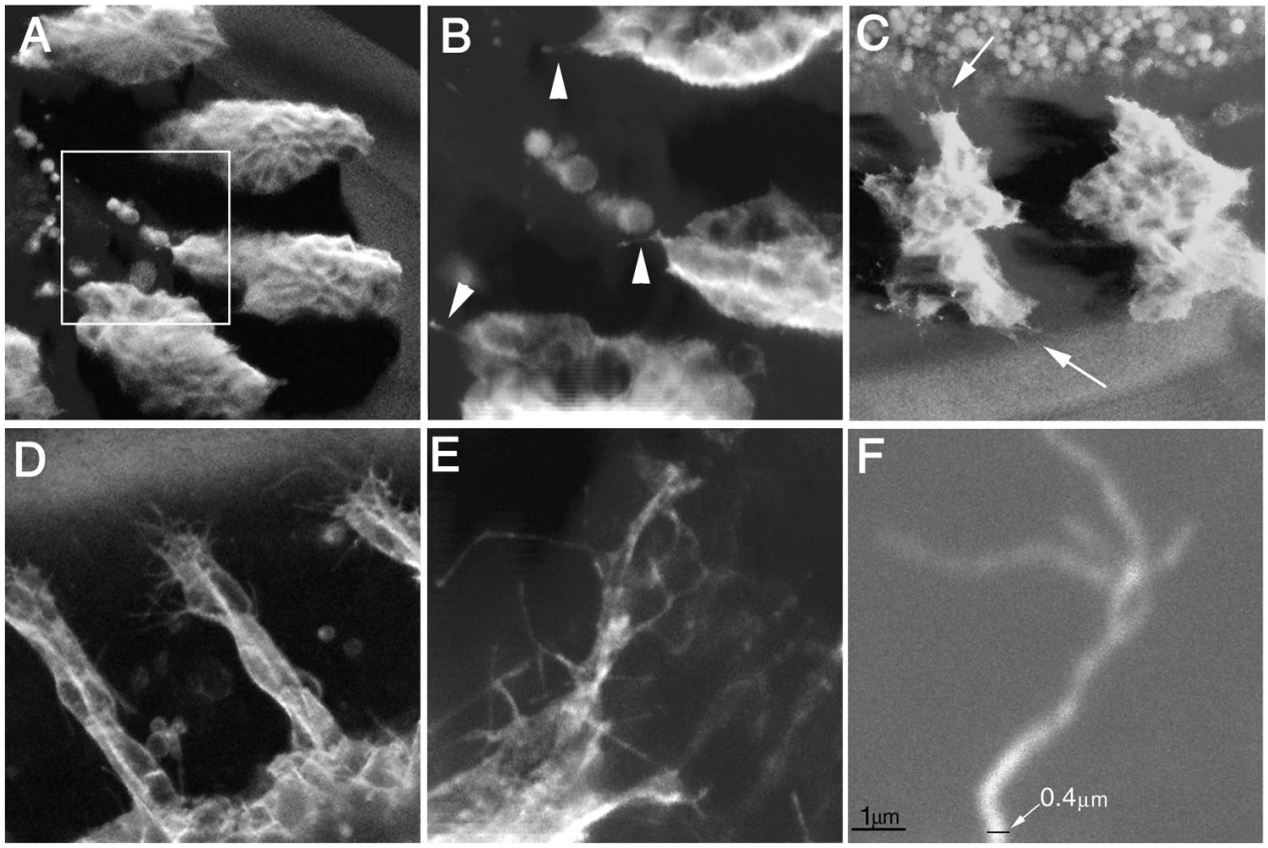

Figure 23 *Filopodia formation in tracheal cells.* 3D reconstructions of living embryos expressing GFP-actin, highlighting the actin cytoskeleton (A, B, C, E, F) or Src-GFP highlighting the membrane (D) under the control of the trachea specific btl-Gal4 driver. B is a higher magnification scan of the region boxed in panel A. (A, B) Short actin extensions (arrowheads) are first visible from the dorsal part of the placode right after onset of germ band retraction (between stages 11 and 12). (C) Later, between stages 12 and 13, short actin extensions are visible from the tip of all growing branches (arrows). (D) Highlighting the membrane of tracheal cells at a later stage (stage 14) reveals cellular extensions from the tip cells of the dorsal branches. These cellular protrusions extend in all directions and can reach considerable lengths (up to 20 μm). Rarely, short cellular extensions are visible in the proximal part of the dorsal branch and the dorsal trunk. (E) High magnification of tip cells from a dorsal branch reveals a complex network of long actin filaments (filopodia) extending in all directions, reminiscent of the cellular extensions seen in D. (F) High resolution scanning of a filopodia protruding from a tip cell of a dorsal branch. The extension has a diameter of 0.4 μm and branches at its distal part. All images are anterior to the left and dorsal to the top.

In order to visualize possible cell shape changes during later migratory phases, we expressed a GFP protein fused to the myristilation site of the Src protein (Kaltschmidt *et al.*, 2000) under the indirect control of the *btl* enhancer. This GFP fusion protein allows to visualize cellular membranes and thus traces the outline of tracheal cells. 3D reconstruction of dorsal branches using a stack of optical sections through a living embryo expressing this construct revealed that the two leading cells formed numerous membranous extensions in all directions (Fig. 23D); only very rarely, extensions from more proximal cells of the dorsal branch or from cells of the dorsal trunk were seen. To ascertain that these membranous extensions contain actin, we also analyzed embryos of the same developmental stage expressing the *GFP-actin* construct. Clearly, a similar network of cell extensions was also

discernable with actin-coupled GFP (Fig. 23E). Reconstruction of such a cellular extension at high resolution demonstrated that the diameter of these extensions was in the range of 0.3 to 0.4 μm (Fig. 23F).

The formation of cell extensions is a dynamic process

To investigate the dynamics of the formation of these cellular extensions we performed a time-lapse confocal analysis of actin cytoskeletal activity in tracheal cells during the migration process, with special emphasis on dorsal and ganglionic branches. For the dorsal branch, serial reconstructions were performed every 2 minutes but only every second reconstruction is shown (Fig. 24A; for a full movie see Movie 1 in supplementary material), while for the ganglionic branches, confocal reconstructions were done every two minutes and all are shown (Fig. 24B; see Movie 2 in supplementary material). In both cases, actin-containing extensions were seen most prominently in the cells at the tip of the branches. Each of the two leading cells in the dorsal branches formed numerous dynamic cellular outgrowths (Fig. 24A). In the ganglionic branches, cell extensions were most prominently seen in the single leading cell (Fig. 24B). The formation of cell extensions was extremely dynamic and their topology changed dramatically with time. Some extensions were found to be short-lived; others were more stable and rather long (up to 20 μm).

We conclude from these data that tracheal cell migration is accompanied by the formation of thin, dynamic actin-containing cell extensions, referred to as filopodia in the following. Filopodia are seen most prominently at the tip of migrating branches, suggesting that cells located at the tip react either differently to migratory (chemotactic) cues compared to neighboring cells, or that the effects of the chemoattractant is limited to those tip cells, possibly by acting at a short range. Consistent with these observations, Bnl/FGF is secreted from cells located in proximity to the cells at the tip of the migrating branches (Sutherland *et al.*, 1996, see also below).

We also wanted to investigate whether Bnl/FGF signaling was sufficient for the formation of filopodia in tracheal cells, and asked whether ectopic expression of bnl in all tracheal cells would lead to the formation of ectopic filopodia. Indeed, numerous actin-containing extensions were seen in a large number of tracheal cells upon the expression of a bnl-transgene under the indirect control of the btl enhancer; all cells, even those of the dorsal trunk, responded to Bnl/FGF with the formation of filopodia (Fig. 25C). These experiments provide clear evidence that tracheal cells react to the Bnl chemoattractant with the formation of dynamic actin-containing filopodial extensions.

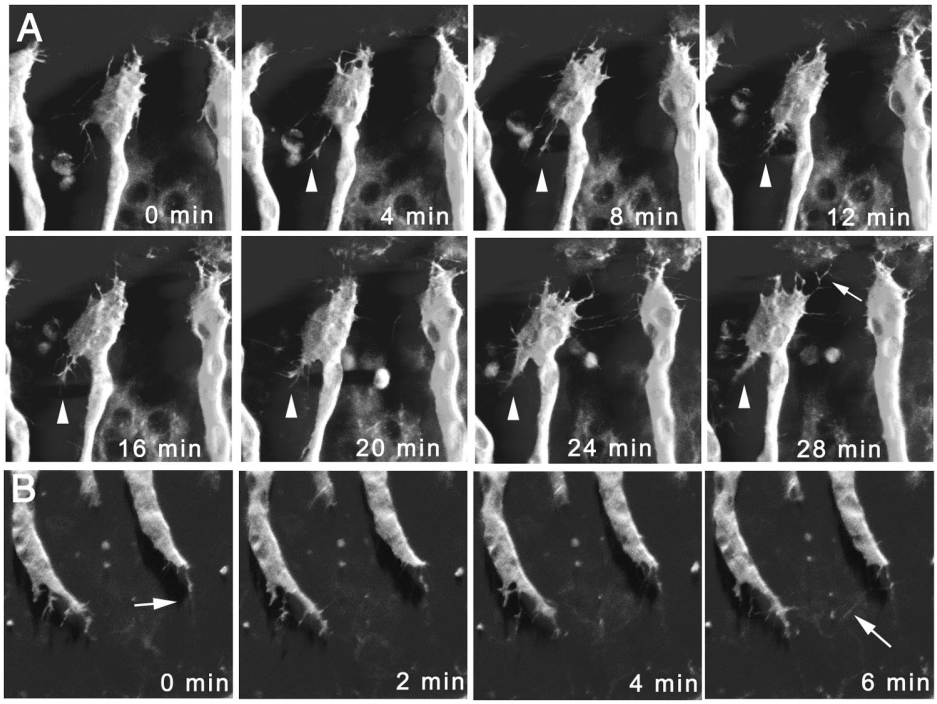

Figure 24 *Tracheal filopodia are highly dynamic.* Time-lapsed 3D reconstructions of living embryos expressing GFP-actin. (A) Dorsal branches were scanned at 2 minutes intervals. Only every second frame is displayed. For a full movie, see Movie 1 in supplementary material. Long filopodia protruding from the two tip cells form a complex, very dynamic network extending in all directions. Filopodia form and retract rapidly. The arrowhead highlights an example of a filopodia that extends, becomes stabilized and thickens. This process is followed by the expansion of the cell body in that direction. Some filopodia form branched structures, as highlighted by the arrow and described previously in Figure 23, panel F. Almost no activity is seen in the proximal parts of the dorsal branch. (B) Ganglionic branches were scanned at 2 minutes intervals. Ganglionic branches behave in the same way as seen and described for the dorsal branch. For a full movie, see Movie 2 in supplementary material. Only the tip cells of the ganglionic branches form long filopodia extending in all directions (arrows). These filopodia are extremely dynamic and rapidly extend and retract. Filopodia in the direction of migration often stabilize and thicken. All images are anterior to the left and dorsal to the top.

Bnl/FGF and Btl are not only required for tracheal cells migration via the formation of primary branches, but also for the gene expression programs that underlie the formation of the secondary and terminal branches. Bnl induces secondary branching via the activation of the *pointed* (*pnt*) gene, and later the expression of *blistered/Dsrf* (*bs/Dsrf*) and *escargot* (*esg*), which are required for terminal branching and for tracheal fusion, respectively (Affolter *et al.*, 1994a; Guillemin *et al.*, 1996; Samakovlis *et al.*, 1996; Tanaka-Matakatsu *et al.*, 1996). Although we have observed dynamic filopodia throughout the migration phase, it is possible that the filopodia shown in Fig. 25 develop under the control of Bnl/FGF signaling via the transcriptional control of secondary or terminal branch genes. In order to investigate whether Bnl induces filopodia formation via the activation of known secondary or terminal genes (*pnt*, *bs/Dsrf*, *esg*), we analyzed filopodia formation in *pnt* mutants *in vivo*; in these mutants, only primary branches form (Samakovlis *et al.*, 1996). Clearly, numerous filopodia were also observed on the tip cells of the migrating branches in pnt mutants,

both in the dorsal branches (Fig. 25D) as well as in the ganglionic branches (data not shown). These results demonstrate that Bnl/FGF signaling induces cytoskeletal dynamics in the absence of transcriptional induction of any known gene, and it is likely that the signaling input directly influences cytoplasmic events in the absence of changes in nuclear transcription.

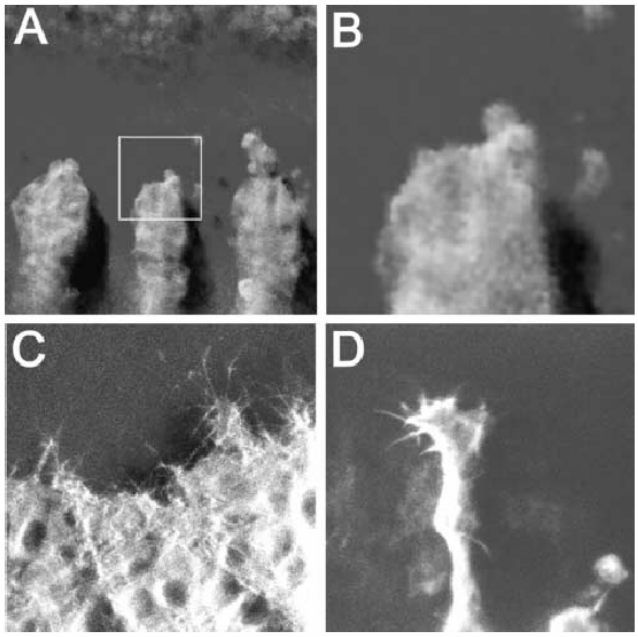

Figure 25 *Bnl/FGF signaling is responsible for filopodia formation.* 3D reconstructions of living embryos expressing the GFP-actin construct specifically in the tracheal system under the control of the btl-Gal4 driver and either lacking the FGF receptor Btl (A, B), expressing the FGFR ligand *bnl* ectopically in all tracheal cells of a wild type embryo (C), or lacking the transcription factor Pnt (D). B is a highlight of the region boxed in A. (A, B) In the absence of Bnl/FGF signaling, cells do not migrate after invagination. The actin cytoskeleton appears disorganized and cells adopt a rounded shape. No extensions protruding from these cells are visible. (C) Highlight of the dorsal trunk of an embryo expressing the FGFR ligand bnl in all tracheal cells. In contrast to wild type dorsal trunk cells, which very rarely show filopodia (see Fig. 23E), the dorsal trunk cells shown here form many filopodia protruding into all directions. (D) In embryos mutant for pnt the tip cells of the dorsal branches still form numerous filopodia. All images are anterior to the left and dorsal to the top.

Dpp signaling is required for branch outgrowth, but not for the formation of cellular extensions

The formation of tracheal branches via directed cell migration not only requires input from Bnl/FGF signaling, but also from additional signaling systems. The activation of the Dpp signal transduction cascade is essential in dorsal and ventral tracheal cells prior to migration for the subsequent formation of dorsal and ventral (ganglionic and lateral trunk anterior and posterior) branches. In the absence of the Dpp receptors Thick veins (Tkv) or Punt (Put), dorsal branches completely fail to develop and ventral branches are strongly affected (Affolter *et al.*, 1994a; Llimargas and Casanova, 1997; Ruberte *et al.*, 1995; Vincent *et al.*, 1997; Wappner *et al.*, 1997). Dpp induces the expression of the genes

kni and *knrl* in the ventral and dorsal cells of the placode; in the absence of these two nuclear proteins, dorsal branches are absent and ventral branches are strongly abnormal (Chen *et al.*, 1998). In addition, ectopic expression of *dpp* in the entire tracheal placode results in the re-specification of dorsal trunk cells to dorsal branch fates, with the consequence that a large number of cells migrate dorsally and that dorsal trunk migration is interrupted, despite the presence of Bnl/FGF in the cells that normally govern dorsal trunk outgrowth (Vincent *et al.*, 1997). These results suggest that while Bnl/FGF guidance is important and essential for tracheal cell migration *per se*, cells need to receive additional signaling information in order to properly interpret the Bnl/FGF signal and migrate successfully towards the source of the chemoattractant.

Knowing that Bnl/FGF acts as a chemoattractant for tracheal cells, and having shown above that Bnl/FGF signaling induces filopodial activity, one must wonder why cells need input from the Dpp signaling cascade for a directed movement to the Bnl/FGF source. Is the Dpp response a prerequisite for the subsequent induction of filopodia by Bnl/FGF? Or do dorsal branch cells respond to Bnl/FGF with the formation of filopodia even in the absence of Dpp signaling input, yet fail to migrate properly? This question is an important one to be addressed since, as discussed above, most or all other tracheal branches also require distinct signaling input in addition to Bnl/FGF. Apparently, none of the tracheal branches form solely under the control of the Bnl/FGF chemoattractant.

In order to find out how these different signaling systems interact *in vivo*, we wanted to investigate the cytoskeletal activity of tracheal cells in the absence of Dpp signaling, with particular emphasis on dorsal branches. However, we had previously shown that both *tkv* and *put* mutants lack dorsal expression of *bnl*; therefore, they not only lack the Dpp signaling input but also the Bnl/FGF signaling input (Vincent *et al.*, 1997). In line with the absence of dorsal *bnl* expression, cellular extensions were not observed in dorsal tracheal cells in *put* mutants when analyzed *in vivo* using the GFP-actin fusion protein (data not shown). Although this result independently confirmed our observation that *bnl* is essential for the formation of filopodial extensions (see above), this experiment did not allow us to draw any conclusions about the cellular role of Dpp signaling.

To circumvent the problem of the absence of dorsal *bnl* expression in mutants defective in Dpp signaling, we made use of the inhibitory SMAD protein encoded by the *Drosophila Daughters against dpp* (*Dad*) gene (Tsuneizumi *et al.*, 1997). Specific inhibition of Dpp signaling in tracheal cells via the trachea-specific ectopic expression of *Dad* led to the absence of dorsal branches (Fig. 26B, compare to A), despite the presence of *bnl* expression on the dorsal side of the embryo (Fig. 26C). Consistent with the absence of dorsal branches upon ectopic expression of *Dad*, *kni* expression was not detectable in dorsal tracheal cells (Fig. 26E compare to D). The loss of dorsal branches was also readily visible in the later larval stages; we did not observe dorsal branches in third instar larvae upon the expression of *Dad* in the tracheal system during embryogenesis (data

not shown; interestingly, and despite the absence of dorsal branches, ectopic *Dad* expression in the trachea did not affect the viability of embryos, larvae, pupae or adults). Both in embryos and in larvae expressing *Dad*, we occasionally observed stump-like dorsal outgrowths at positions where dorsal branches form in wild type animals (Fig. 26K-M). We will argue below that these stumps are misrouted dorsal trunk outgrowths; such outgrowths were never observed in *tkv* or *put* mutants (Fig. 26O), presumably due to the lack of *bnl* expression dorsal to the invaginating placode. We conclude from these experiments that ectopic expression of *Dad* mimics the *tkv* and *put* mutant phenotypes with regard to the lack of dorsal branch formation, and that dorsal branches fail to form through guided cell migration in this particular Dpp loss of function situation despite the presence of dorsal *bnl* expression.

To investigate the possible cell shape changes or cytoskeletal rearrangements in dorsal tracheal cells in the absence of Dpp signaling *in vivo*, we used confocal imaging of living embryos expressing both a *Dad* and a *GFP*-tagged *actin* transgene in the developing trachea (see materials and methods). Confirming the observations made in fixed embryos and in third instar larvae, the phenotype observed in late embryonic stages (stages 15 and 16) *in vivo* was the complete absence of dorsal branches (Fig. 26I). However, the analysis of a time-lapse study of 3D reconstructions, in which tracheal GFP-actin dynamics were recorded in an interval of 5 min for 135 min, revealed a strikingly different picture (selected time points in Fig. 26F-I, for a full movie, see Movie 3 in supplementary material). In sharp contrast to *put* mutants, embryos in which Dpp signaling was inhibited specifically in tracheal cells by ectopic expression of *Dad* clearly showed dorsal outgrowths and filopodial activities in positions where dorsal branches normally form. These outgrowths looked bud-like, showed dynamic filopodial extensions but never refined to single-cell-diameter, tubular dorsal branches (Fig. 26J); although tracheal cells did migrate dorsally, they never migrated over a large distance, and in most cases all the cells forming these buds eventually reintegrated into the main dorsal trunk, leading to the general absence of dorsal branches (Fig. 26I).

These results demonstrate that in the absence of Dpp signaling, tracheal cells close to the dorsal *bnl*-expressing ectodermal cells are able to form actin-containing filopodial extensions and initiate dorsal migration. However, the lack of Dpp signaling, which results in the lack of expression of the *kni*/*knrl* target genes, leads to the failure to form a dorsal branch and the short, bud-like dorsal outgrowths eventually reintegrate into the main dorsal trunk. Consistent with this interpretation, cells forming the initial dorsal outgrowth in *Dad*-expressing embryos in rare cases generated a dorsal trunk- sized lumen (Fig. 26K-L). These dorsally directed stumps of dorsal trunk were also visible in third instar larvae (Fig. 26M). Such dorsal trunk-like buds were also seen in mutants that lacked Dpp-induced *kni/knrl* in the tracheal system (Fig. 26N, for detailed genotype see Chen *et al.*, 1998 and materials and methods) indicating that dorsal migration also took place in these mutants. These buds were never observed in *put* mutants presumably due to the lack of dorsal expression of the chemoattractant Bnl/FGF (Fig. 26O).

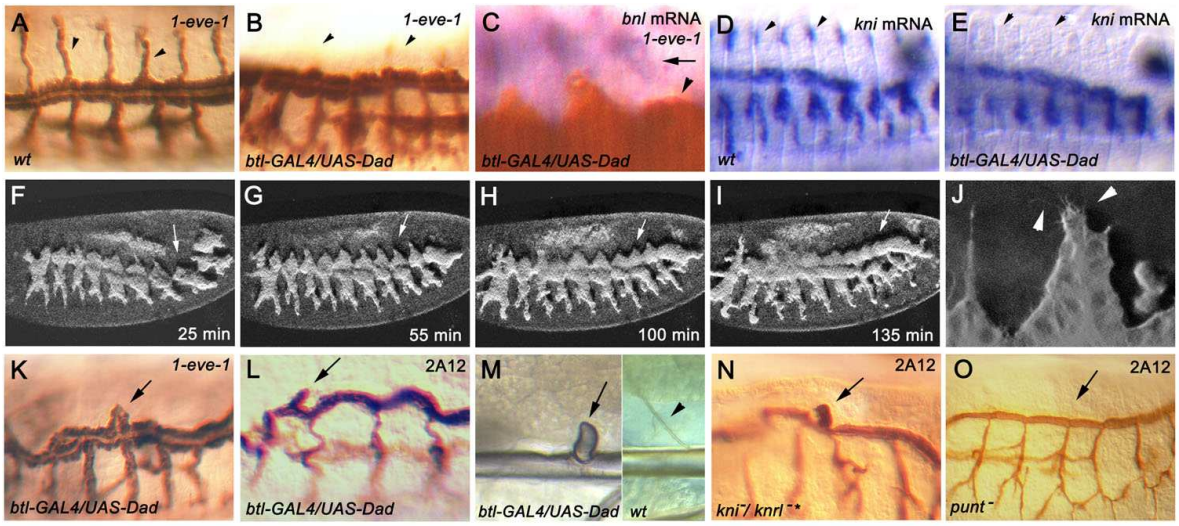

Figure 26 *Dpp signaling is required for dorsal branch outgrowth, but not for the formation of cellular extensions.* To determine the effect of Dpp signaling on dorsal branch migration, embryos expressing the Dpp signaling inhibitor *Dad* under the control of the *btl-Gal4* driver (B, C, E-M), mutants lacking Dpp-induced *kni/knrl* in the tracheal system (N) and mutants for the Dpp type II receptor *punt* (O) were analyzed (for details see materials and methods). The tracheal system was visualized using the tracheal enhancer trap line *1-eve-1* (A, B, C, K), the luminal antibody 2A12 (L, N, O) or by 3D reconstruction of living embryos expressing the *GFP-actin* construct under control of the trachea specific *btl-Gal4* driver (F-J). Bright field pictures of a third instar larva are shown in M. Embryos were recorded at stage 13 (C), stage 13-14 (D, E) and stage 15 (A, B, K, L, N, O) of development. (A, B) Embryos lacking Dpp signaling in the tracheal system (B) show absence of dorsal branches (arrowheads) when compared to the wild type embryo shown in A. (C) Visualization of *bnl* mRNA by in situ hybridization (blue) (arrow) shows that tracheal cells (brown) (arrowhead) do not form dorsal branches when Dpp signaling is interrupted despite presence of the chemoattractant. Notice that in contrast to Dpp receptor mutants, embryos overexpressing *Dad* in the tracheal system are not devoid of the dorsal *bnl* spot. (D, E) Visualization of *kni* mRNA shows that *kni* expression in the dorsal part of the tracheal tree (arrowheads) is abolished by overexpression of *Dad* in trachea when compared to the wild type situation in D. (F-I) 3D reconstruction of the tracheal actin cytoskeleton of a living embryo lacking Dpp signaling in the trachea. Selected frames from a 135 min time-lapse analysis are shown. For a full movie, see Movie 3 in the supplementary material. Surprisingly, cells start to move dorsally and form bud-like dorsal structures (arrows) (F, G) but stall (H) and eventually reintegrate into the dorsal trunk (I). (J) 3D reconstruction of the dorsal part of a tracheal tree of a living embryo overexpressing *Dad* and therefore lacking Dpp signaling. The anterior dorsal bud is reintegrating into the dorsal trunk and extends a long and thick extension dorsally. The posterior dorsal bud still extends dorsally and forms filopodia at the tip (arrowheads) showing that these cells are capable of forming filopodia even in the absence of Dpp signaling. (K-M) Rarely dorsal buds (arrows) are visible at later stages in fixed tissue (K, L) and in living third instar larvae (M) of animals overexpressing *Dad* in the trachea. Notice that, as readily visible from the 2A12 stainings in L, these buds in the larva form a lumen with a much larger diameter typical for the dorsal trunk (arrow) when compared to the wild type dorsal branch in the right inset (arrowhead). (N) These dorsal trunk-like dorsal buds are also visible in embryos lacking Dpp-induced *kni/knrl* during branch formation (* see Chen et al., 1998 and materials and methods for detailed genotype) suggesting that dorsal migration also took place in these animals. (O) Such buds are never visible in mutants for the Dpp type II receptor *put*; these findings can be readily explained by the lack of dorsal *bnl* expression in *put* mutants. All images are anterior to the left and dorsal to the top.

We conclude from these results that Bnl/FGF signaling is required and sufficient to induce cellular extensions and cell motility in tracheal cells. However, for Bnl/FGF to lead to dorsal branch formation via concerted cell migration, Dpp signaling is essential to allow productive branch outgrowth accompanied by cellular rearrangements; in the absence of either of the two signals, productive migration leading to dorsal branch formation is abolished. These finding will be discussed in the light of the genetic control of tracheal branching morphogenesis.

Discussion

Bnl/FGF is required and sufficient to induce the formation of cellular extensions

Bnl/FGF signaling is used reiteratively during tracheal development. Based on loss-of-function and gain-of-function studies and on the expression pattern of *bnl,* Bnl/FGF has been proposed to act as a chemoattractant for tracheal cells in early developmental stages; branch outgrowth is directed towards *bnl*-expressing non-tracheal target tissues via chemotactic induction of cell migration (Sutherland *et al.*, 1996). Here, we show for the first time that Bnl/FGF is indeed required and sufficient to induce filopodia in tracheal cells *in vivo*. Bnl/FGF-induced filopodia are extremely dynamic and are formed almost exclusively by the leading cells of migrating branches. It has been previously shown that Bnl/FGF-dependent phosphorylation of Map kinase (ERK) is highest in cells at the tip of branches (Gabay *et al.*, 1997). Both the number of filopodia (this study) and the amount of phosphorylated ERK dramatically increase in all cells upon ectopic expression of *bnl* (Gabay *et al.*, 1997). Together, these results strongly argue that Bnl/FGF signaling is highest in tracheal cells close to the source of the ligand and that migration is steered by the cells at the tip of the branches. Filopodia extend in all directions, suggesting that directionality in tip cell migration is controlled by events other than directional outgrowth of filopodia. Possibilities for such events include the selective adhesion of filopodia or the preferential stabilization or bundling of microtubules in the direction of the Bnl/FGF ligand.

Our results demonstrate that Bnl/FGF signaling leads to alterations in the cytoskeletal architecture of tracheal cells. Based on results mainly obtained in cultured cells, it is likely that such cytoskeletal changes are brought about via regulators and effectors of the small GTPases Cdc42, Rac and Rho, ultimately leading to local actin polymerization catalyzed by the activation of the Arp2/3 complex by WASP (Nobes and Hall, 1999). Little is known about the precise nature of the FGFR signaling pathway in *Drosophila* and its connection to the cytoskeleton. The activated FGF receptor signaling complex appears to signal through the Mitogen Activated Protein Kinase (MAPK) cascade (Gabay *et al.*, 1997), which is a signal transduction pathway common to many receptor tyrosine kinases (RTKs). A novel component specifically required for FGFR signaling in *Drosophila* has been

identified. This protein, named Downstream of FGFR (Dof), is essential for the Bnl/FGF-mediated activation of the MAPK cascade and is required during embryogenesis for tracheal cell migration as well as for mesoderm development (Vincent *et al.*, 1998); (mutations allelic to *dof* have been described and the corresponding genes called *heartbroken* or *stumps* Imam *et al.*, 1999; Michelson *et al.*, 1998). Although Dof could provide a molecular linker between FGFR activation and the cytoskeleton, it has been shown recently that the intracellular domain of the FGF receptor Btl can be functionally replaced by the intracellular domain of Torso and EGFR and that these hybrid receptors can rescue tracheal cell migration in the absence of Dof (Dossenbach *et al.*, 2001). These results demonstrate that tracheal cells respond in a certain time window to different RTK signal with migration, and that Bnl/FGF signaling triggers the inherent migratory program of tracheal cells. It will be essential to learn more about the migratory competence of tracheal cells and the link of RTK signaling to the cytoskeleton. Recent studies have provided first insight into RTK regulation of cell migration in *Drosophila* (Duchek and Rorth, 2001; Duchek *et al.*, 2001).

Bnl/FGF and Dpp signaling have distinct effects on the formation of dorsal tracheal branches

We have previously shown that Bnl/FGF signaling is not sufficient for dorsal branch formation; in the absence of Dpp signaling (Vincent *et al.*, 1997) or in mutants lacking expression of the Dpp-induced target genes *kni*/*knrl* in the trachea (Chen *et al.*, 1998), dorsal branch formation fails completely. In this study, we analyzed the effects of the absence of either of the two signals at the cellular level using confocal 4D imaging of living embryos combined with trachea-specific inhibition of Dpp signaling. Our results demonstrate that while Bnl/FGF signaling is required and sufficient for the induction of filopodial activity in tracheal cells and for cell migration in the strict sense (cells do start to migrate dorsally when Dpp signaling is inhibited by Dad), Bnl/FGF is apparently not sufficient to allow productive dorsal branch outgrowth. For dorsal branches to grow out and form, Dpp signaling input is strictly required, in addition to filopodial activity induced by Bnl/FGF. Thus, Dpp signaling does not appear to collaborate with Bnl/FGF in filopodia production and motility as such but must target cellular functions distinct from those targeted by Bnl/FGF signaling. Thus, despite the essential and crucial role of Bnl/FGF, chemoattraction is not sufficient for successful tracheal branching; and despite the requirement of Dpp for dorsal branch formation, migration *per se* is not affected.

We envision a number of potential, possibly overlapping, roles for Dpp signaling in dorsal branch formation (Fig. 27). 1.) Dpp might induce branch-specific cell rearrangements allowing the formation of an extended unicellular tube via cell intercalation (see Samakovlis *et al.*, 1996). In the

absence of this information, branch elongation can not take place and the 5-7 cells that would line up to form the dorsal branch under normal conditions start to migrate dorsally as a cell group, adopt dorsal trunk identity and later re-integrate into the resident dorsal trunk. 2.) Dpp signaling might influence the adhesion among tracheal cells, generating groups of cells with higher affinity for each other. It is possible that cell movement during branching morphogenesis is the result of a balance between the forces generated by Bnl/FGF-induced forward cell migration and the forces generated by adhesive properties among neighboring tracheal cells. Reintegration of the dorsal bud formed in the absence of Dpp signaling into the dorsal trunk could be the result of the higher affinity of the re-specified dorsal trunk cells for their own dorsal trunk "affinity-group", a force that might be stronger than the force generated by the Bnl/FGF chemoattractant. 3.) Dpp signaling could alter the adhesion between tracheal cells and migratory substrates, for example by changing the selective adhesion of extending filopodia to distinct target regions. Such a model would also be consistent with the demonstrated capability of Dpp to redirect cells towards dorsal migratory behavior (Vincent *et al.*, 1997).

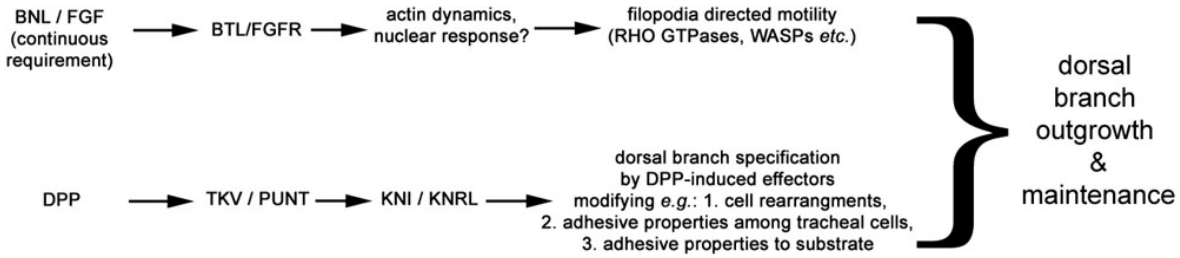

Figure 27 *Dorsal branch formation requires the control of different cellular functions by Dpp and Bnl/FGF.* Although the two signaling systems control different cellular programs, both are required in a regulated way for the formation of a stable dorsal branch by concerted cell movement. Bnl/FGF signaling controls filopodia directed motility either directly in the cytosol and/or indirectly via nuclear transcriptional control, possibly via Rho GTPases and WASPs. Dpp signaling controls dorsal branch specification via transcriptional activation of *kni/knrl* by inducing effectors, which might modify *e.g.*: 1. cell rearrangements, 2. adhesive properties among tracheal cells or 3. adhesive properties to the substrate.

In order to investigate the role of Dpp in dorsal branch formation at the molecular level, genes mediating the effect(s) of Dpp signaling in the tracheal system have to be identified. Since the target genes *kni/knrl* are capable to mediate most aspects of Dpp signaling in tracheal cells (see Chen *et al.*, 1998), many of the Dpp regulated genes might be direct or indirect targets of Kni/Knrl. In an attempt to identify such genes, we are undertaking a DNA oligonucleotide chip approach.

The models we propose for the formation of dorsal tracheal branches might also apply to other tracheal branches. Most if not all branches arise only in the presence of Bnl/FGF and an additional signal. The dorsal trunk, for example, only forms upon activation of the Wnt signaling pathway in the corresponding tracheal cells, which ultimately leads to the maintenance of sal expression (Chihara and Hayashi, 2000; Llimargas, 2000). In addition, Hh

signaling has been shown to be required for the formation of certain tracheal branches (Glazer and Shilo, 2001). Thus, it appears that the concerted development of different branches of the tracheal system might require the coordination of the control of cell motility with other, distinct cellular events. It will be interesting to find out whether the development of other branched organs, as for example the lung, also requires similar mechanisms.

FGF signaling leads to cytoskeletal changes in other developmental contexts

Bnl/FGF signaling is involved in numerous other developmental contexts that appear to be brought about by cytoskeletal changes. Subsequent to the function of Bnl/FGF as a chemoattractant for tracheal cells during primary branch formation, Bnl/FGF is required for the formation of fine terminal branches in the larva (Guillemin *et al.*, 1996; Samakovlis *et al.*, 1996). Each terminal branch arises from specified terminal cells as a long, thin (0.1-1.0 μm diameter) cytoplasmic extension that grows out on the target tissue and forms an intracellular lumen, allowing oxygen to pass through the terminal cells to reach the target tissue. Bnl/FGF also appears to act as a chemoattractant for these fine terminal extensions but the structure of these terminal extensions is dramatically different from primary branches induced earlier (Jarecki *et al.*, 1999). While the same ligand and receptor are used in both processes, some of the downstream components are different (for example Blistered/Dsrf, which is not made in time to participate in early branching processes) and this difference might account for the formation of branches of distinct structure and pattern (Guillemin *et al.*, 1996; Jarecki *et al.*, 1999). It will be interesting to uncover the molecular differences accounting for the role of Bnl/FGF signaling in the outgrowth of these fine terminal extensions, as opposed to its role in tracheal cell migration.

Bnl/FGF signaling has also been associated with the formation of actin-based cell extensions called cytonemes that project to the signaling center associated with the anterior/posterior compartment border in the wing imaginal disc (Ramirez-Weber and Kornberg, 1999). In contrast to filopodia, cytonemes are polarized with respect to their orientation to an organizing influence. Little is known about the formation and the function of cytonemes, but it will be interesting to eventually compare signaling components and targets involved in this phenomenon and the related processes discussed above.

Chapter 7

Junctional remodeling during *Drosophila* tracheal branching morphogenesis.

Carlos Ribeiro, Marc Neumann and Markus Affolter

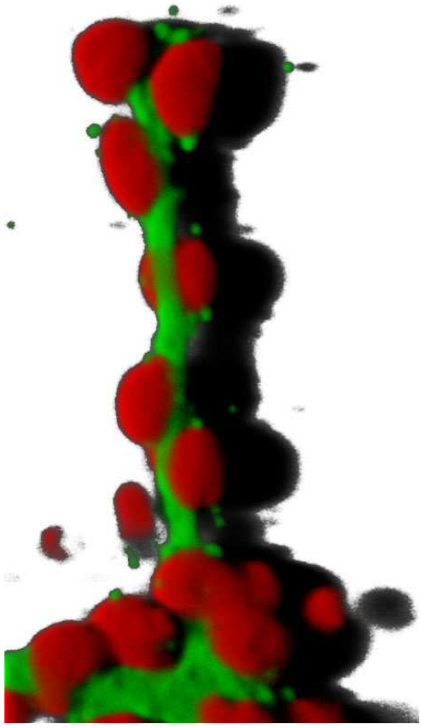

Introduction

The *Drosophila* tracheal system serves as one of the primary interfaces with which this organism is in contact with the environment. As such, it is a structure that has to be tight to prevent the intrusion of undesired substances as well as the leakage of body material from the inside while allowing normal exchange of the respiratory gases. Being of ectodermal origin it shares the shielding function with other epidermal cells, which accomplish a similar role on the exposed surface of the organism. To fulfill this task ectodermal cells are endowed with strong adhesive properties, which are mediated to a large extent by the junctional complexes (Knust and Bossinger, 2002; Tepass *et al.*, 2001). They connect adjacent cells and have a very important role in subdividing and organizing the cell membranes in multiple compartments (see introduction). The same complexes are thought to serve as barriers for extracellular material hindering uncontrolled leakage of foreign substances into the organism and *vice versa*. During morphogenetic processes, these tight connections have to be regulated in order to allow complex cell rearrangements to happen smoothly without leading to a loss of stability and integrity of the junctions.

The tracheal system of *Drosophila* is one of many tissues that are generated by a complex series of cell shape changes, migratory processes and cell rearrangements (for reviews see Affolter and Shilo, 2000; Metzger and Krasnow, 1999; Petit *et al.*, 2002; Zelzer and Shilo, 2000a). In this case, the morphogenetic process is made even more complex by the fact that the cavity that is created by the initial invagination is expanded without any interruption or breakage of the tube. In addition, the tracheal cells of the dorsal branch undergo unicellularization in which the cells rearrange themselves from a side-to-side configuration to an end-to-end configuration (Samakovlis *et al.*, 1996). During this process, which is characterized by the formation of autocellular junctions, the multicellular tube is transformed into a unicellular tube again without any spilling of the luminal content. The exact mechanisms of this transition have never been described before and even if the identification of the proteins composing the junctional complexes has advanced tremendously in the last years, the mechanisms regulating junctional remodeling still remain elusive.

The Shotgun (Shg, *D*E-cadherin), Armadillo (Arm, the β-Catenin homologue of *Drosophila*) and *D*α-Catenin (*D*α–Cat) complex is one of the major and best studied components of the adherens junctions (AJs) in *Drosophila* (see introduction). Unfortunately, it is very difficult to study genetically the role of this complex during early development as no germline clones can be obtained. Moreover, for D*α-Cat,* no mutant alleles are available and *arm* mutants show a *wingless* (*wg*) phenotype due to the additional role of Arm as a central transducer of the Wg signaling pathway. The components of this complex are very useful markers for observing the remodeling processes epithelial cell undergo during the morphogenetic movements. Especially

GFP fusions to Shg and *Dα–*Cat have proven very useful for observing and dissecting the dynamics of the Shg complex (Oda and Tsukita, 1999a; Oda and Tsukita, 1999b).

Using *Dα–*Cat-GFP (Oda and Tsukita, 1999a), we have analyzed morphogenetic rearrangements occurring during tracheal branching. Special attention was given to the intercalation of dorsal branch cells. During intercalation, the dorsal branches undergo unicellularization accompanied by the formation of autocellular AJs. This process occurs in four steps allowing the smooth transition from a multicellular to a unicellular tube without spilling of the luminal content. *Dad* overexpression specifically inhibits these AJ reorganizations by keeping the AJ network of the dorsal branch cells in a tight, mesh-like pattern, similar to the AJ organization seen in the dorsal trunk. Dorsal branch formation can however be rescued by the concomitant removal of Wnt and Dpp signaling. In this background, even complex cell rearrangements as intercalation occur in the dorsal branch, indicating that they are not controlled by Dpp signaling. Inhibition of unicellularization by *sal* overexpression corroborates the observation that Kni/Knrl exert their function largely by repressing *sal* expression in the dorsal branch. We therefore propose a model for branching morphogenesis of the tracheal system, based on the induction of different affinities for the cells of the different tracheal branches. This leads to the sorting out of the two cell populations and the establishments of two branches.

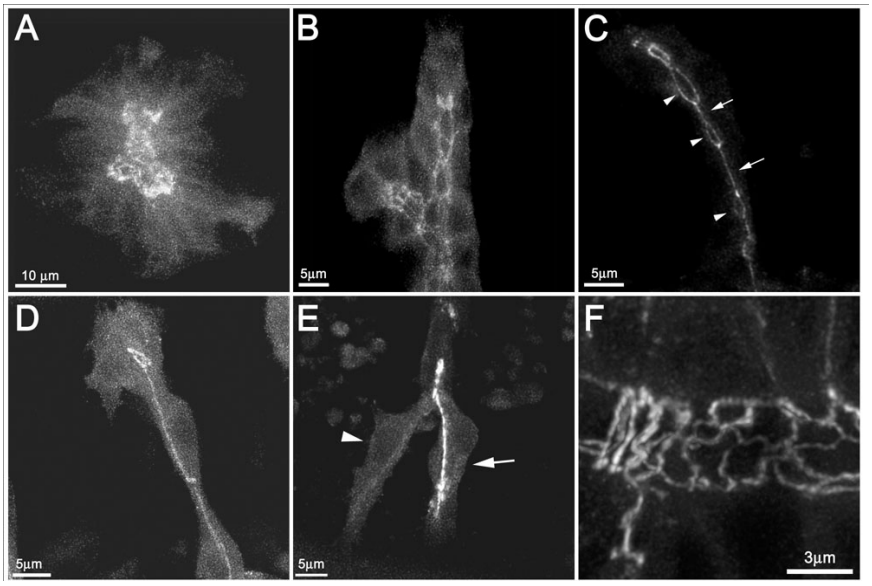

Figure 28 *Patterns of* D*α–Catenin-GFP localization during tracheal morphogenesis.* Maximum intensity projections of living embryos expressing D*α–Catenin-GFP* throughout the tracheal system. Different stages of development are depicted. In the placode, all AJs are oriented to the center (A). Later the AJs start to build a mesh-like pattern (B) and at later stages, dorsal branches undergo uni-cellularization. This process is characterized by the AJs forming circles (arrowheads) interconnectted by lines (arrows) (C). The different patterns of AJs are excellent markers for the different types of branches encountered in the tracheal system. Unicellular dorsal branches exhibit a linear pattern (D), terminal branches form autocellular tubes devoid of junction and therefore no AJs are visible in the terminal branch (arrowhead) when compared to the fusion cell (arrow) (E) and the dorsal trunk forms a mesh-like pattern specific for multicellular tubes (F).

Results

Dα-cetenin-GFP as a marker for junction remodeling during tracheal morphogenesis

We have chosen to express a *Dα*–Cat-GFP fusion protein (Oda and Tsukita, 1999a) specifically in tracheal cells in order to observe the cell rearrangements and junctional remodeling events taking place during branching morphogenesis using *in vivo* timelapse confocal microscopy. We will describe these processes with special emphasis on the development of unicellular branches.

As a consequence of the invagination process, which is thought to be driven by apical constriction (Schock and Perrimon, 2002), *Dα*–Cat-GFP is seen in early stages at the center of the placodes (Fig. 28A). Bnl/FGF mediated migration then leads to the formation of the primary branches (Ribeiro *et al.*, 2002; Sutherland *et al.*, 1996) and to an initial dilation of the apical surface (Fig. 28B). In the growing dorsal branch, the cells pair to form a row of two adjacent cells (Samakovlis *et al.*, 1996) while the AJs from a ladder like structure, which is composed of molecules originating from the AJs of the adjacent contacting cells. In this conformation two apical surfaces of two neighboring cells form a segment of the multicellular tube while the rungs of the ladder-like structure represent rings around the luminal space which connect two paired cells with the two cells lying above and below respectively (see Fig. 29).

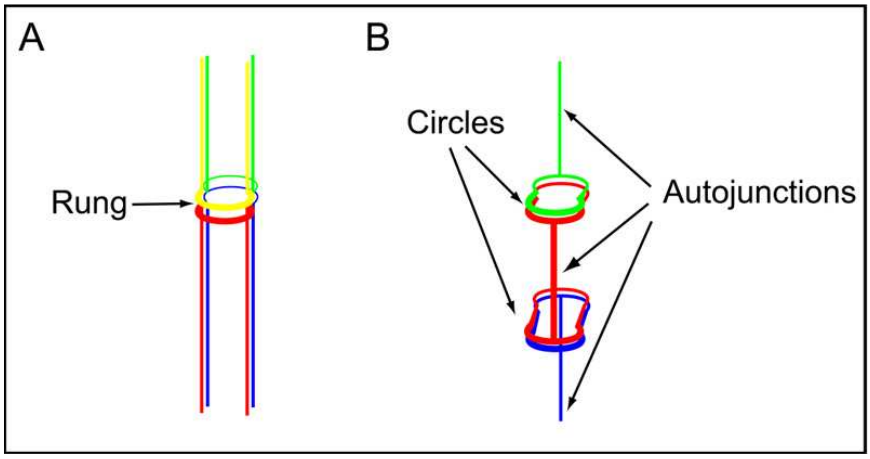

Figure 29 *Patterns of AJs as seen in the dorsal branch with* D*α-Catenin-GFP –labeling.* Different colors represent AJ complexes from the different cells. Note that for reasons of clarity the AJs are depicted separated by a space. This is not the case in reality as the AJs from adjacent cells are connected by Shg interactions and are therefore seen as a continuous line. At the beginning, cells of the dorsal branch pair and AJs form a ladder-like structure (A). During intercalation, cells form autojunctions, which are visible as one line and which are delimited by circles representing remaining multicellular stretches (B).

Subsequent elongation of the dorsal branch is accompanied by the intercalation of dorsal branch cells and the formation of a unicellular tube (Fig. 28C, Samakovlis *et al.*, 1996). The AJs start to form autocellular junctions which are specific for unicellular tubes and which are visualized by the transition from the ladder-like structure to a single line delimited by circles at its proximal and distal ends. These circles represent the points at which the dorsal branch cells still contact each other and jointly embrace the remaining bi-cellular part of the tube (Fig. 29B). While the intercalation process proceeds, the dorsal branch cells diminish their cell-cell interaction surface, leading to an increase in autocellular junctions and a shrinking of the circular structures. At the end of the process, the dorsal branch is an exclusively unicellular tube, as seen by the line formed by the AJs, which is only interrupted by small bubbles at the point of contact between two cells (Fig. 28D).

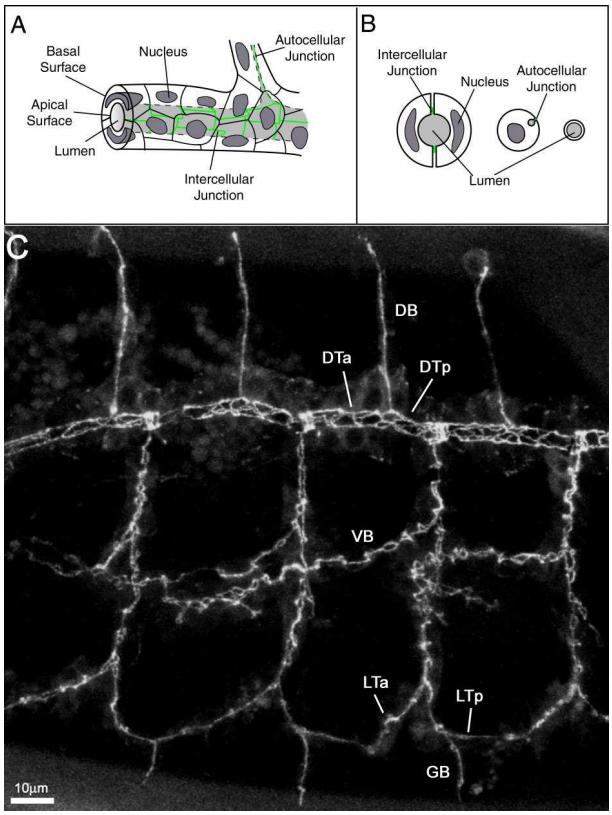

Figure 30 *Diagram showing the general structure of the AJs in the tracheal system and overview of the tracheal apical junctions.* (A) Cutaway view of a dorsal trunk and dorsal branch. (B) Cross section of the three different type of tubes in the tracheal system. On the left a multicellular tube with intercellular junctions, in the middle a unicellular tube with autocellular junctions and a terminal branch with a subcellular terminal branch without junctions. The AJs are depicted in green. (C) Maximum intensity projections of a living embryo expressing *Dα–catenin-GFP* throughout the fully developed tracheal system. (DB) dorsal branch, (DTa/p) dorsal trunk anterior and posterior, (VB) visceral branch (LTa/p) lateral trunk anterior and posterior and (GB) ganglionic branch. (According to Samakovlis *et al.*, 1996)

Changes in the pattern of *D*α–Cat-GFP visualized by *in vivo* confocal microscopy recapitulate the complex cell rearrangements that occur during tracheal branch formation (Fig. 30).

*D*α–Cat-GFP is an excellent marker for identifying the three types of tubes present in the tracheal system: multicellular tubes (*e.g.* the dorsal trunk) are perceived as a mesh of AJs (Fig. 28F), unicellular tubes (*e.g.* the dorsal branch) as single lines of AJs (Fig. 28D) and the terminal extensions are not visible as they form *de novo* and do not contain junctional complexes (Fig. 28E).

Detailed analysis of the transition from a multicellular to a unicellular tube

The *in vivo* visualization of *D*α-Cat-GFP opens the exiting possibility to analyze the junctional remodeling events taking place during the transition from a multicellular to a unicellular tube at a detailed and unprecedented level (Oda and Tsukita, 1999a). In addition, using time-lapse *in vivo* confocal microscopy, this transition can be visualized in three dimensions inside the living embryo at high temporal resolution.

Given the high complexity of this process, we have tried to extrapolate a mechanistic sequence that we think is valid for all dorsal branches. It is nevertheless clear that *in vivo* slight variation of the hereby-described paradigm can be seen. This is especially true for the exact sequence of the events as well as the exact spatial alignment of the described structures. It is however not clear whether these divergences are due to slight differences in the morphogenesis of each specific dorsal branch or if they are caused by natural variations seen in all biological systems. From the published literature and our numerous observations, we favor the second hypothesis and are confident that our model is the basic and generally used mechanism for unicellularization of dorsal branches.

In Figure 31 (see also corresponding movie 4 in supplementary material and movie 5, which is a longer and differently rendered movie of the same time-lapse), single time frames of a volumetric reconstruction of a dorsal branch undergoing unicellularization are depicted. As easily visible at the time points 0min and 3 min the connection of the dorsal branch with the dorsal trunk is already formed by only one stretch of AJs indicating that the most proximal cell has already undergone unicellularization. This fits with the observation that unicellularization starts with the cells most proximal to the dorsal trunk and continues distally in direction of the tip cells. After at the base of the dorsal branch the first intercalatory event has started, the next begins leading to a “wave of intercalatory events”.

At the beginning of the intercalatory process, when the cells are aligned in pairs, the earlier described circle-like connection of the abutting cell pairs has adopted a different form. It resembles more a tetrahedron indicating that the pulling force exerted by the Bnl/FGF chemoattraction at the tip of the branch (Ribeiro *et al.*, 2002) has lead to stretching of the branch resulting in tension forces; this might result in the distortion of the circle into the tetrahedral form (Fig. 32A). Notice however, that in spite of the shifted

position of the cellular AJs in the tetrahedron, the remaining AJs lie in one plane with the nuclei of the cells. This planar arrangement, which is only clearly visible in the interactive 3D models (see corresponding QTVR models in supplementary materials), is not seen at earlier stages (as can be observed in movie 5) and could therefore be caused by the increasing tension exerted by the pulling force of the chemoattractant. The reason for the planar alignment of the AJs is therefore not clear.

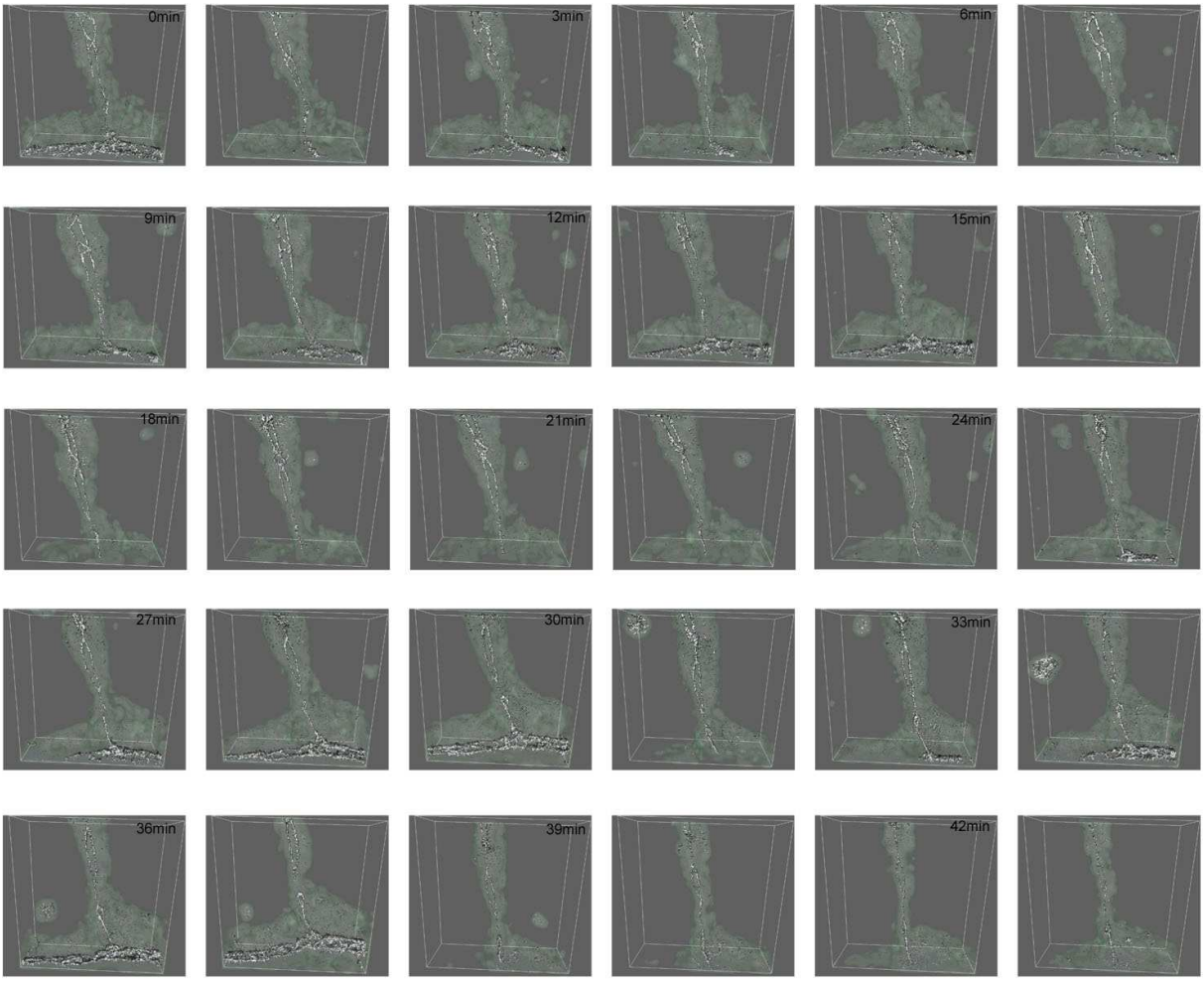

Figure 31 *Volumetric reconstruction of an intercalation timelapse analysis.* Volumetric reconstruction of a dorsal branch undergoing unicellularization and expressing *D*α-Catenin-GFP scanned every 1min and 30s. AJs are rendered in white and cell outlines are rendered in transparent green. See corresponding movie 4 in supplementary material. Movie 5 is a longer and differently rendered movie of this time-lapse.

Because two-color single cell labeling is not available at present, we cannot determine the position and cellular shape of individual cells at the same time as the dynamic behavior of the AJs. Therefore, we extrapolated their relative position from the *D*α–Catenin-GFP patterns. At the time-point 4min30s (Fig. 31 and Fig. 32B), a clear reduction in one of the hemi segmental connections (dashed line in Fig. 32B) between cells 2/4 and 1/4 starts to be

seen, indicating that the cells start to diminish their AJ connections. This reduction is continued until at time-point 15min 30s, the hemi segmental surface has disappeared leading to the formation of a circular connection between cells 1, 2 and 3, while the AJs of cells 2 and 4 are only connected in one point (at the intersection of the circle with the dashed line in Fig. 32C). This transition is accompanied and maybe even caused by the coordinated displacement of cell 4 in proximal direction while cell 3 slides upwards to take its position. This is due to the fact that cell 4 is connected via its proximal AJs to the unicellularized cell contacting the DT and is therefore not able to move upwards.

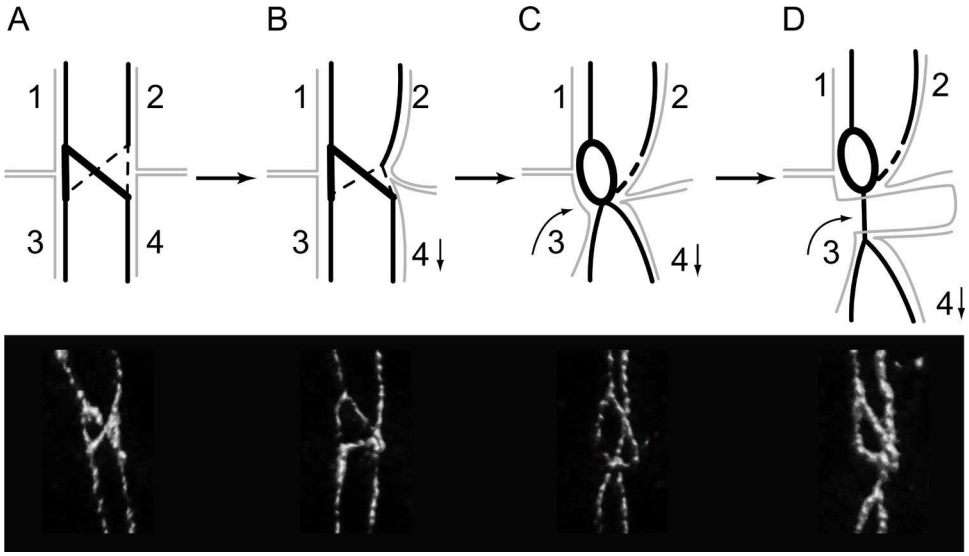

Figure 32 *Major steps of unicellularization.* Bold lines represent AJs in front and dashed lines AJs behind the focal plane. Cells are numbered and outlined in gray. Arrows beside numbers indicate directionality of displacement of the cells. Below the diagrammatic representation, the original 3D reconstructions can be seen. Note that depicted AJs are always (except for autocellular junctions of cell 3 in D) made up of interacting complexes from two cells (see Fig. 29 for details). See also corresponding QTVR models in supplementary materials. (A) corresponds to model 1, (B) to model 2, (C) to model 3 and (D) to model 4.

As it begins to be visible at time-point 24min, cell 3 starts to make an autocellular junction while cell 4 detaches from cell 2 (Fig. 32D). This leads to a smooth transition from a multicellular to a unicellular tube. The high level of coordination is visible in the fact that cell 4 starts to generate autocellular junctions on the proximal side at the same time as cell 3 on the distal side, generating the circle-like structure visible in Figure 31 and corresponding to the circles in Figure 28C and 29 B. Unicellularization is then continued by the progressive expansion of the autocellular junctions at cost of the multicellular, circular structure, which is eventually reduced to a small circle (Fig. 30 corresponding to Fig. 28D).

Effect of tracheal Dad overexpression on AJ remodeling

Up to now, we have mainly concentrated on the effect of the different signaling pathways on the basal side of the tracheal system. To do so we have analyzed the cellular dynamics of the basal actin cytoskeleton in different gain and loss of function backgrounds (Ribeiro *et al.*, 2002). It is much more difficult to visualize the effects on the apical and therefore luminal side of the tubular system *in vivo* using the described cytoskeletal and membrane markers.

Using the *D*α-Catenin-GFP construct, we can for the first time analyze *in vivo* the effects of the different signaling pathways involved in tracheal morphogenesis on AJ rearrangements. For clear reasons we did not analyze the effect of mutants in the Bnl/FGF pathway, as no morphogenetic changes were expected in these mutants due to the absence of migration. We have therefore concentrated on the effect of the Dpp pathway on AJ reorganizations in the dorsal branch.

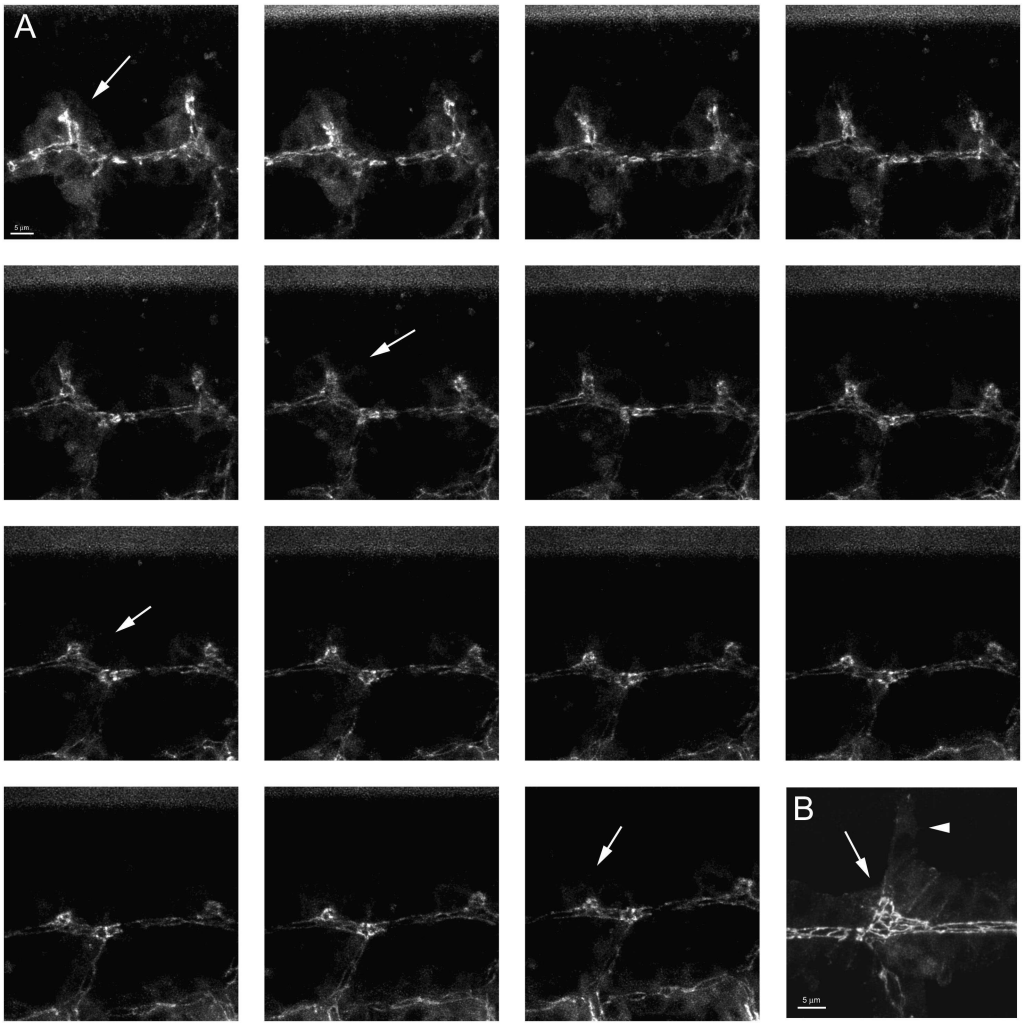

Figure 33 *Effects of* Dad *overexpression on the apical reorganization in dorsal branches.* Maximum intensity projections of a timelapse analysis of an embryo expressing *Dad* and D*α-Catenin-GFP* throughout the tracheal system, recorded at an interval of 5 minutes (A). Major steps in the reintegration of a dorsal branch are indicated by an arrow. In a different embryo, it is clearly visible how the basal (arrowhead) and apical sides (arrow) react differently to Dpp signaling suppression (B). See also movie 8 in supplementary materials, which corresponds to (A).

In Figure 33A (corresponds to movie 8 in supplementary material), a timelapse analysis of an embryo expressing *Dad* and D*α-Catenin-GFP* is illustrated. As previously described using an actin marker, the dorsal branch is not able to form correctly and reintegrates into the dorsal trunk (Ribeiro *et al.*, 2002). It is clearly visible that the AJs of the dorsal branch retain a mesh-like pattern never adopting a different conformation from the dorsal trunk, indicating that all cells express the same fate determinants (*sal*) (Kuhnlein and Schuh, 1996). Although the apical surface of the cells initially extends dorsally, this movement is later reversed and the AJs start to integrate into the dorsal trunk. As evident from the cytosolic, non-incorporated *D*α-Catenin-GFP, the basal side clearly extends much stronger in the direction of the chemoattractant. This is especially clear in Figure 33B where the basal surface of one dorsal branch cell extends wide in direction of the presumptive dorsal Bnl spot while its apical surface stays close to the dorsal trunk. This corroborates the earlier observations that the effects of the Bnl/FGF pathway and the Dpp pathway have clearly separable function in branching morphogenesis (Ribeiro *et al.*, 2002). While Bnl/FGF clearly acts by promoting basal filopodia formation, the effect of *Dad* overexpression seems to mainly affect the dynamics of the AJs.

Reintegration of dorsal buds in Dad overexpression embryos is not due to inefficient following of the dorsal Bnl spot by tracheal cells

As shown, Dpp signaling is not necessary for Bnl/FGF mediated chemoattraction as cells do grow out and form Bnl induced filopodia (Ribeiro *et al.*, 2002). It is nevertheless still possible that Dpp acts in a much more subtle way on Bnl/FGF induced migration, which is not detectable by our mode of assay. Inefficient RTK signal transduction or cytoskeletal activity would therefore lead to a slight stalling in the movement pace of the dorsal tracheal cells causing an increasing gap between the dorsal Bnl secreting cells and the tracheal cells. This would lead to a sensitive decrease of the chemoattractant and ultimately to a loss of migration triggering the reintegration of the dorsal branch cells into the dorsal trunk.

To test this possibility we have chosen to look at mutants for *kayak* (*kay*). Kayak is the *Drosophila* homologue of the transcription factor Fos and is thought to transcriptionally mediate the Jun Kinase (JNK) signal during the dorsal closure process (reviewed in Noselli and Agnes, 1999). Thus, *kayak* mutants show a strong dorsal open phenotype as the ectodermal sheets fail to extend over the amnioserosa. This failure in epithelial stretching makes it not possible for the dorsal Bnl spot to move over the same distance as it does in wildtype embryos. If the reintegration of dorsal tracheal cells in *btl-Gal/UAS-Dad* embryos is due to a “running away” of the Bnl signal this effect should be diminished in a *kay* mutant background.

In *kay* mutants, trachea form normally, showing that this transcription factor and possibly the entire JNK signaling cascade are not required for patterning of the trachea (Fig. 34A). This is of special interest since Jun is strongly expressed in tracheal cells (Zeitlinger *et al.*, 1997). Dorsal branches do form normally except for the expected shortness. Note that even if much shorter, dorsal branches retain their identity as can be seen by the smaller diameter of the dorsal branch tubes when compared to the dorsal trunk.

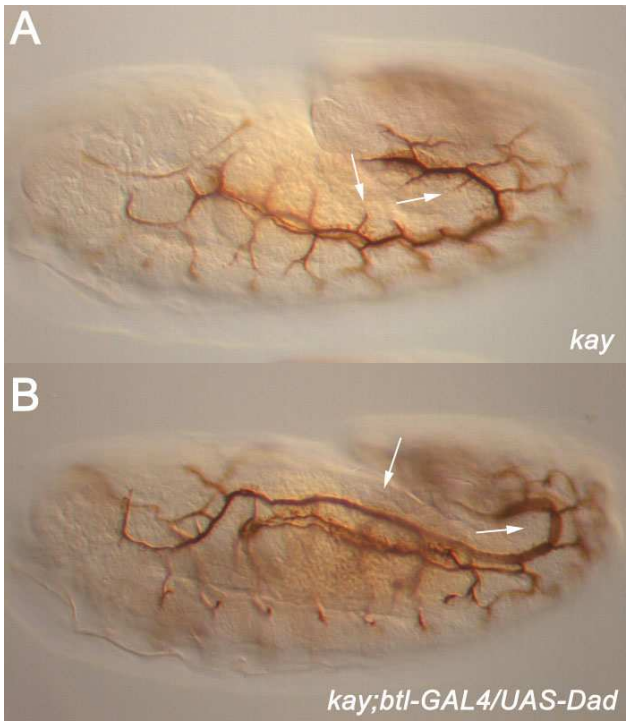

Figure 34 *Loss of* kayak *function does not rescue* Dad *induced dorsal branch reintegration. kayak* mutants with wildtype and impaired Dpp signaling stained with the tracheal luminal marker 2A12. Mutant s for *kayak* show normal albeit shortened dorsal branch formation (arrows) (A). Removal of functional Dpp signaling lads to the reintegration of dorsal branches in *kayak* mutants too (arrows) (B).

However, when in *kay* mutants Dpp signaling is cell autonomously impaired by targeted overexpression of Dad throughout the tracheal system, dorsal branches do not form, indicating that Dpp signaling is not required for a subtle modulation of Bnl/FGF signaling or its effectors, but that the dorsal bud reintegration seen in embryos lacking Dpp signaling in tracheal cells is an active process (Fig. 34B). Therefore, the effect of Dad cannot be explained by a “run away” effect of the dorsal Bnl spot due to the effect of dorsal closure.

Sal is responsible for the reintegration of the dorsal tracheal cells

Two basic mechanisms of Dpp and therefore Kni/Knrl action during dorsal branch formation are conceivable (Chen *et al.*, 1998; Ribeiro *et al.*, 2002; Vincent *et al.*, 1997). One possibility would consist in an active role of Dpp

signaling by inducing the transcription of dorsal branch specific genes necessary for the productive outgrowth of the dorsal branch cells. These genes could code for proteins necessary for cell rearrangements (*e.g.* intercalation) or for the selective adhesion between tracheal cells and dorsal specific migratory substrates. By overexpression of *Dad*, these genes would not be induced, leading to a failure of productive dorsal branch formation and ultimately to the reintegration of these cells into the DT.

The other possibility would consist in a more passive regulatory role in which Dpp induced Kni/Knrl would mainly act by repressing Sal in dorsal branch cells (Chen *et al.*, 1998; Kuhnlein and Schuh, 1996). The following cell biological mechanism would be compatible with this model: Sal target genes could confer a stronger adhesive property to dorsal trunk cells, which Kni/Knrl would counteract by repressing *sal*. In this manner, two groups of cells with different adhesive properties (high and low affinity) are formed which would lead to a sorting out of the two population of cells. In Dad overexpression embryos, Kni/Knrl cannot counteract expression of the Sal induced higher affinity adhesive proteins. This would transform dorsal branch cells into the same adhesive group as the DT cells and therefore to the reintegration of the dorsal branch cells into their new “affinity group”.

These two possibilities are easily genetically testable by the simultaneous removal of Kni/Knrl and Sal in the tracheal system. If Dpp would have an active role in productive dorsal branch formation, removal of both transcription factors would not lead to a rescue of dorsal branch formation. However if the major role of Kni/Knrl would be the repression of Sal, removal of both transcription factors would lead to the rescue of the dorsal branches.

To distinguish between the two mechanisms we analyzed the tracheal system of embryos mutant for the Wnt signal transducer *armadillo* and expressing *Dad* in all tracheal cells (further referred as double loss of function background). Note that the allele of *arm* used is a null for the signaling activity while retaining its functional activity as an important component of the AJs (Peifer and Wieschaus, 1990). To overcome the necessity of Sal for the early dorso-ventral patterning of the tracheal placodes we chose to use *arm* mutants instead of the deficiency removing *sal* and its homologues as Wnt signaling was shown only to be required for the later expression of Sal in the DT (Chihara and Hayashi, 2000; Franch-Marro and Casanova, 2002; Llimargas, 2000).

Interestingly concomitant removal of Sal and Kni/Knrl leads to the rescue of dorsal branch formation indicating that the major role of Kni/Knrl resides in the repression of
Sal in dorsal branch cells (Fig 35B, B’, C, C’, D and D’). Dorsal branch formation was almost similar to the one seen in the wildtype. The defects seen in the double loss of function background cold be due to general patterning defects of *arm* mutant embryos. Also no fusion was seen in the double loss of function background due to the lack of *esg* expression in mutants for the Wnt pathway (Chihara and Hayashi, 2000; Llimargas, 2000). Strikingly there is no big difference between the tracheal system as seen in *arm* mutants and the one seen in the

double loss of function background (compare Fig 35B,B' and C,C').

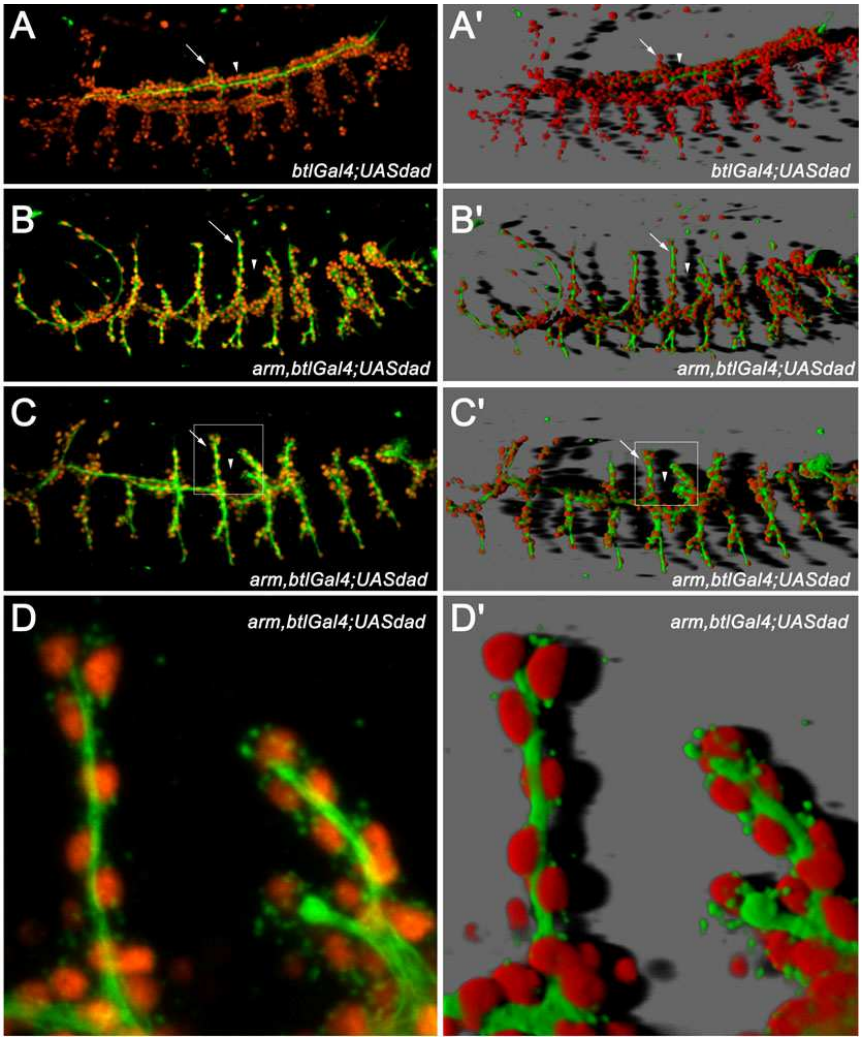

Figure 35 *Sal is responsible for the reintegration of DB cells into the DT in a Dpp signaling loss of function background.* Tracheal cells were marked by a nuclear marker (red) and the tracheal luminal antibody 2A12 (green). Left images are maximum intensity projections and right images are 3D image reconstructions. All images are taken from embryos of the same cross (see Material and Methods for details). Embryos with a wildtype copy of *arm* and expressing *Dad* in trachea show no dorsal branches (arrow) while DT formation remains as in wildtype (arrowhead) (A). Simultaneous removal of *arm* leads to the absence of DT formation (arrowhead) and rescue of DB formation (arrow in B and C). D and D' are higher magnification scans of the region boxed in C and C'). Note the striking similarity of the dorsal branches in the two different embryos in B and C.

Dpp signaling is not necessary for the intercalation of dorsal branch cells

The precise role of Dpp signaling for the morphogenesis of the dorsal branch could not be addressed before due to the central role of this signaling pathway in dorsal branch establishment (Affolter *et al.*, 1994b; Ribeiro *et al.*, 2002; Vincent *et al.*, 1997). Now the rescue of dorsal

branch formation by removal of Wnt signaling in a Dad overexpression background, opens for the first time the possibility to address this important question *in vivo*. Notwithstanding the almost complete rescue of dorsal branch formation by the removal of *sal* in a Dpp signaling loss of function background the possibility still remains that Dpp has a minor but important function as an active regulator of cell rearrangements in the dorsal branch.

As described before one of the major morphogenetic processes the dorsal branch undergoes is the intercalation of the dorsal branch cells (Samakovlis *et al.*, 1996). This highly complex and tightly regulated process is a major candidate for regulation by Dpp signaling, as it is exclusive for branches expressing *kni/knrl*. The slightly displaced arrangement of the nuclei in the dorsal branches of the double loss of function embryos as seen in Fig. 35D and D' indicates that these embryos are able to perform the transition from a multicellular to an unicellular tube. It is nevertheless very difficult to judge the correctness of this statement with the nuclear and luminal markers used in Figure 35.

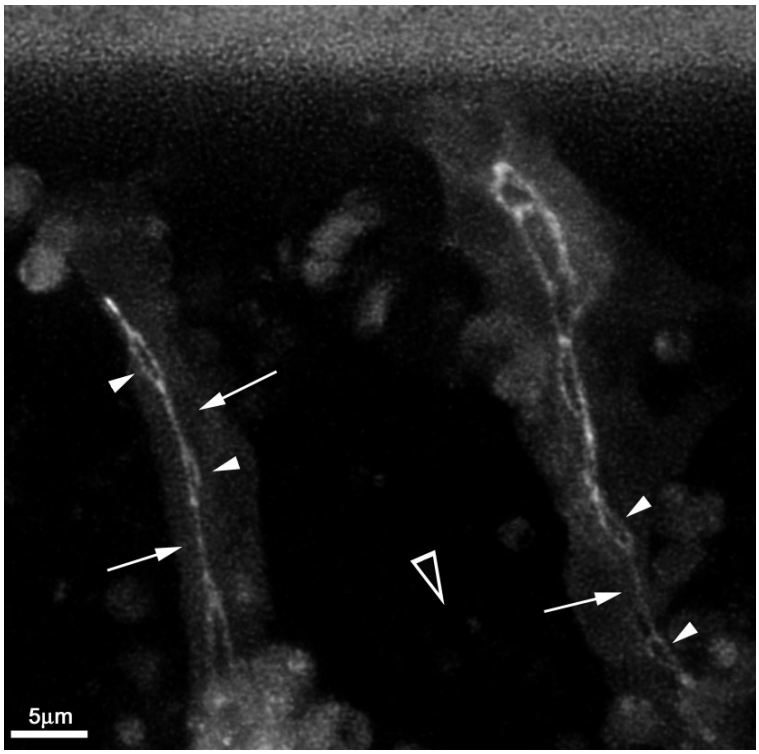

Figure 36 *Unicellularization does not require Dpp signaling.* Maximum intensity projection of a living *arm* embryo expressing D*α-Cat-GFP* and *Dad* throughout the tracheal system. Arrows mark autocellular junctions, arrowheads intercellular junctions and the empty arrowhead marks the absence of the dorsal trunk. See also movies 6 and 7 in supplementary materials.

To investigate this very important point *in vivo* in more detail, we crossed the *D*α-Catenin-GFP construct into the described double loss of function background.

Strikingly, dorsal branch cells of the tracheal system underwent normal unicellularization as observed by the transition of the AJs pattern from the ladder-like structure into a single line interrupted by circles (Fig. 36 and movies 6 and 7 in supplementary

materials). This argues again for a permissive role of Dpp signaling in dorsal branch morphogenesis. As evident from these experiments, the "ground state" of the tracheal cells is permissive for intercalation. In the absence of the pathways determining branch-specific properties, cells can undergo unicellularization. Strikingly all tested features, characteristic for the dorsal branch, can be rescued by concomitant removal of Sal and Kni/Knrl.

Sal overexpression represses unicellularization

If Kni/Knrl act mainly by repressing transcription of *sal* in unicellular tracheal branches then *sal* overexpression in these cells, should counteract the effect of Kni/Knrl and lead to an inhibition of unicellularization. To test this prediction we overexpressed *sal* together with the AJ marker in all tracheal cells and analyzed the cellular diversity of individual branches.

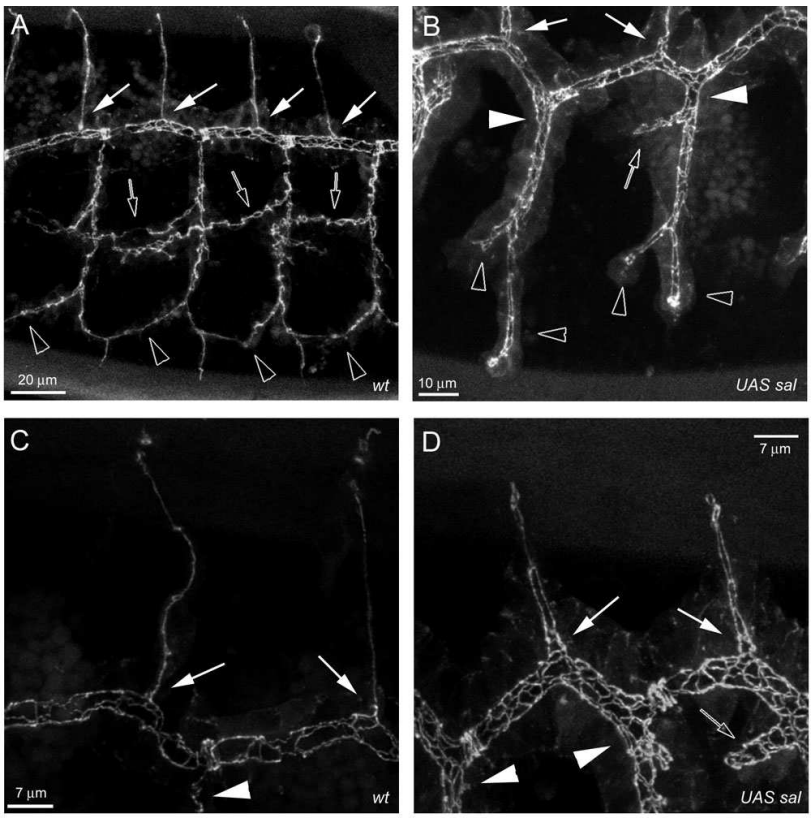

Figure 37 *Effect of* sal *overexpression on tracheal morphogenesis.* Maximum intensity projections of living embryos expressing *Dα-Catenin-GFP* in trachea. Wildtype embryos (A and C) are compared to embryos expressing *sal* ectopically throughout the tracheal system. Tracheal cells, which are always transformed from unicellular tubes to multicellular tubes are marked. Filled arrows mark the transitions from the dorsal trunk to the dorsal branch, filled arrowheads the transition from the dorsal trunk to the ventral tracheal system, empty arrows the visceral branch and empty arrowheads the ventral branches (lateral connectives and the ganglionic branches).

As published previously the effect of *sal* overexpression on tracheal patterning is a very strong one as it interferes with dorsal branches extension (Chen *et al.*, 1998). This becomes more evident when visualized with the AJs marker. In Fig. 37A, we see the wildtype distribution of unicellular and multicellular tubes in the tracheal system. Dorsal branches, ganglionic branches and lateral connectives as well as the visceral branch and the connection of the dorsal trunk to the ventral part of the tracheal system are made up of cells forming autocellular junctions. In the case of *sal* overexpression embryos, the majority of dorsal branch cells do not intercalate (Fig. 37B and C) and the transition from the dorsal trunk is never unicellular (filled arrows). Additionally the transition from the dorsal trunk to the ventral tracheal system (filled arrowhead) is multicellular the visceral branch (empty arrow), the lateral connectives and the ganglionic branches (empty arrowheads) are multicellular and do therefore not fully expand. Thus, Sal clearly interferes with the cellular rearrangements necessary for the conversion of multicellular into unicellular tubes.

In addition, the shape of the dorsal trunk does change dramatically. In wildtype embryos, the dorsal trunk forms a long, almost straight tube, while tracheal *sal* overexpression embryos present a wriggled dorsal trunk. This indicates that more cells have joined the dorsal trunk leading to a lengthening and bending of the dorsal trunk. This surplus of dorsal trunk cells is also visible as a compression of the apical surfaces circumscribed by the AJs signal, which are much smaller in the *sal* overexpression embryos when compared with the wildtype embryos. Interestingly the diameter of the dorsal trunk remains unaffected confirming that the regulation of the tube diameters is independent of the number of cells (Beitel and Krasnow, 2000).

Discussion

Adherens junction remodeling during unicellularization

Morphogenetic processes are accompanied by changes in cell shapes and positions, which are thought to be mainly driven by the cytoskeleton. Less attention has been given to the fine regulation of the junctional complexes, which ensure the integrity of the organism. These tight connections have to be regulated during development in order to allow the morphogenetic processes to take place without endangering the stability of the ectodermal structures.

This is especially obvious for branching morphogenesis. While cells undergo dramatic rearrangements and cell shape changes to maximize their apical surface the continuity and tightness of the tubular network has to be guaranteed. This demands a high degree of contact flexibility while requiring an absolute stability of the cell junction complexes. Unfortunately, almost no information is available on the precise nature of these AJ

rearrangements during branching morphogenesis: neither on the cellular mechanisms underlying this sequence of events, nor on the regulatory networks controlling it, or its molecular nature.

Using confocal four-dimensional imaging of living embryos expressing *D*α-Catenin-GFP as an *in vivo* marker for the adherens junctions, we analyzed the transition from a multicellular to a unicellular tube in the dorsal branch. Unicellularization proceeds from proximal to distal and is characterized by four main stages. In the first stage, the cells of the dorsal branch pair, leading to the formation of a ladder-like arrangement of their AJs. In the next stage proximal displacement of one of the two lower cells leads to the diminishment of the AJ contacts between that cell and the cells lying above it. The third stage is characterized by the formation of a circular AJ structure, which surrounds the lumen and connects the three cells with exception of the cell sliding in proximal direction, which is only connected at one knot-like point with the ring.

The continuing proximal movement of the one cell leads to the breakage of the remaining knot-like contact and therefore to the loss of AJs contact with the remaining cells. To prevent the spilling of luminal content during the fourth step this loss in AJ contacts is compensated by the formation of autocellular junctions by the neighboring cell, leading to the formation of a unicellular tube. Intercalation is accompanied by the extension of the autocellular junctions until two cells lying in an end-to-end arrangement are only connected by a small circular AJs ring.

Bnl/FGF induced migration seems to be the main driving force for this intercalatory process (Ribeiro *et al.*, 2002; Sutherland *et al.*, 1996). It becomes apparent that the cells have to sustain strong pulling forces. As the AJ have to remain flexible to allow cell rearrangements to occur, an additional system may be required to ensure the structural stability of branch undergoing unicellularization. Mutants for genes fulfilling this function would show a loss of integrity of unicellular branches. The phenotype would consist of breaks in the dorsal and ventral branches as well as the absence of other unicellular tubes. Such mutants have been described and shown to encode ZP proteins. They are expressed throughout the tracheal system and are secreted into the luminal space (Jazwinska, A, Ribeiro, C and Affolter, M submitted).

It remains unclear if the intercalatory process requires a specialized machinery, responsible for mediating the smooth transition from a multicellular to a unicellular tube. Further analyses are required to characterize the precise molecular mechanisms of unicellularization.

The effect of Dad *overexpression is mainly visible on the AJs and reminiscent of* ribbon

As previously described using basal cytoskeletal markers inhibition of Dpp signaling leads in a first step to the normal dorsal outgrowth of dorsal branch cells but the final establishment of the branch is not possible and these cells reintegrate into the dorsal trunk (Ribeiro, 1998). The mechanisms of this reintegration were nevertheless still elusive.

The same effect of *Dad* overexpression is also observed when analyzed with *D*α-Cat-GFP. It becomes clear that this effect is especially strong on the apical side while the basal side of the dorsal branch cells tries to follow the chemoattractant. Because the AJs stay tightly connected in a mesh-like pattern as seen for the ones of the dorsal trunk, the cells are not able to follow the dorsal Bnl/FGF spot and eventually reintegrate into the dorsal trunk. This corroborates the already observed fact that the function of Bnl/FGF and Dpp can be separated functionally. While the effect of *Dad* overexpression is mainly seen on the apical side, the effect of FGF seems to be concentrated on the basal side.

These differences between apical and basal behavior are reminiscent of the observations made by (Shim *et al.*, 2001) in *ribbon* loss of function backgrounds. In mutants, lacking Ribbon tracheal morphogenesis is strongly affected. First analyses indicate that Ribbon could be necessary for coordinating basal and apical cell movements as in *ribbon* mutants the basal surface of the tracheal cells show signs of strong reorganizations while the cell body and especially the apical surface of the cells remain unchanged. Unfortunately, ribbon encodes a transcription factor and does therefore not allow for the understanding of the cellular mechanisms underlying its function.

Kni/Knrl exert their function to a large extent by repressing sal

The identification of the targets of the transcription factors Kni/Knrl in the tracheal system have always been thought to be very helpful for the elucidation of the cellular roles of Dpp signaling. From the beginning however, *sal* had been shown to be one of the main targets of Kni/Knrl as the absence of *sal* in the dorsal trunk is dependent on its repression by Kni/Knrl (Chen *et al.*, 1998). Due to the complex rearrangements the dorsal branch undergoes and the fact that the effect of loss of Dpp signaling on the patterning of the dorsal branch could not be analyzed (as no dorsal branch is formed), this was thought not to be the only role of Kni/Knrl during dorsal branch morphogenesis.

To further clarify the relation between Kni/Knrl and Sal, we analyzed the effect of concomitantly removing both factors during tracheal development. The rescue of dorsal branch formation in the absence of both Kni/Knrl and Sal indicates that the main if not sole function of Dpp and therefore Kni/Knrl during dorsal branch formation is the removal of Sal and thereby its target genes in dorsal branch cells. Strikingly even unicellularization, one of the most complex morphogenetic events the tracheal system undergoes, does not require Dpp signaling as it is unaltered

in the double loss of function background.

"Affinity group model" of tracheal branch formation

From the data presented in this study, we propose the following general model for branching morphogenesis of the tracheal system. Even if this paradigm is mainly based on observations of the dorsal branch and the dorsal trunk, we think that this represents a general mechanism for branching morphogenesis.

All tracheal cells are intrinsically capable to react to the chemoattractant by migration, to adhere strongly to each other, ensuring the integrity of the tube, and to undergo unicellularization. Activation of the FGF pathway by Bnl/FGF induces cytoskeletal rearrangements (*e.g.* filopodia) enabling the receiving cells to move in direction of the chemoattractant. Given the adherent force among all tracheal cells, these migrating cells drag the attached cells with them, leading to the formation of the initial tracheal buds.

Sal controls the expression of proteins in dorsal trunk cells, which modulate the adhesive properties of these cells and augment the affinity of their AJs to each other. The resulting higher rigidity of the junctions prevents these cells from undergoing complex cell rearrangements and promotes the formation of contacts with cells of the same affinity group. This ensures the formation of a thick, multicellular, main tracheal trunk. The higher affinity of the dorsal trunk cells for cells of the same affinity group is also visible in the cuboidal shape these cells adopt, which indicates a high contact surface with other dorsal trunk cells.

Branching morphogenesis requires however that multiple tubes are formed in order to expand the available oxygen exchange surface and to ensure that all cells of the organism are adequately provided with oxygen. For dorsal branch formation, the tracheal system solves this problem by creating two different affinity groups.

Kni/Knrl repress the expression of *sal* in dorsal branch cells leading to the loss of the described high affinity properties. Only the intrinsic adhesiveness of all tracheal cells remains ensuring the integrity of the tracheal system. This is again visible in the shape of the dorsal branch cells. These exhibit are more columnar shape in which only the smaller proximal and distal surfaces of the cells contacts other tracheal cells indicating a lower affinity for cells of the own branch. This way, two cell groups are formed: one with a high self-affinity (the dorsal trunk) and one with a lower self-affinity (the dorsal branch). As in the wing imaginal disc, due to their different affinity properties the two populations sort out leading to the formation of two distinct branches (Tepass *et al.*, 2002). This process is reminiscent of the hydrophobic effect, which leads to the formation of two phases in a water oil mixture. The lower AJs rigidity also enables the dorsal branch cells to undergo complex cell rearrangements, as for example unicellularization.

The pulling force of the tip cells leads to the formation of a high tension in the few cells of the dorsal branch. Their intrinsic adhesive properties are too weak to resist to the force exerted by Bnl/FGF (as it is the case when Kni/Knrl are removed by *Dad* overexpression) but strong enough to grant the preservation of the contacts

among the tracheal cells and therefore the integrity of the lumen. This equilibrium in adhesive properties leads to the shift in the positions of the cells from a side-to-side to an end-to-end conformation. It is not clear, if these complex rearrangements are performed without the help of any specialized molecules or if unicellularization requires a dedicated machinery. It is however clear that this machinery would not be controlled by Dpp signaling.

Multiple evidences support this model. When Kni/Knrl are removed, *sal* expands into the dorsal branches, leading to the formation of only one affinity group and therefore the loss of dorsal branch morphogenesis, while concomitant removal of Sal rescues the effect of the absence of Kni/Knrl, as cells do not express the high affinity molecules anymore enabling the dorsal branch cells to move dorsally. Overexpression of *sal* throughout the dorsal trunk, leads to an inhibition of unicellularization. Almost all AJs adopt a mesh like pattern indicating an increase in cell-cell contacts. In addition, the dorsal trunk changes its shape from an almost straight tube into a zig zag form indicating that more cells have integrated the dorsal trunk in order to increase their contact surface with other tracheal cells. Further observations as the high number of cell-cell contacts in the dorsal trunk, the shape of dorsal trunk cells as well as the perpendicular direction of outgrowth of the dorsal branch to the dorsal trunk indicate the correctness of the “affinity group model”.

This model also explains other aspects of tracheal morphogenesis. The bridge cell is for example a mesodermal cell, which is required for correct dorsal trunk formation (Wolf and Schuh, 2000). It is thought to serve as an intermediate adhesion step for the dorsal trunk cells on their migratory path. Why do dorsal trunk cells require such a mechanism if the way they have to travel is much shorter than the way other branches migrate without requiring such a structure? If one stipulates that Sal induces the expression of a strong adhesion molecule it is imaginable that the pulling force exerted by the chemoattractant is less efficient in dragging the dorsal trunk cells as they stick more strongly together. Therefore, an additional mechanism is required to stabilize the short way the cells have traveled to enhance the effect of the chemoattractant.

But why does the dorsal trunk then not form in *arm* mutants? *arm* mutant dorsal trunk cells form normal filopodia and are therefore capable of following the anterior Bnl/FGF spot analogous to *Dad* overexpressing dorsal branch cells (data not shown). In *arm* mutants, however *esg* is not expressed leading to a loss of fusion capacity (Chihara and Hayashi, 2000; Llimargas, 2000). Therefore, even if filopodia are extended and the putative fusion cells contact each other using these extensions no stable connection and subsequent anastomosis can be initiated leading to a lack of dorsal trunk formation.

The identification of the Sal effectors in the dorsal trunk as well as of the tracheal intrinsic factors, which allow tracheal specific morphogenetic processes like unicellularization and chemoattraction to take place, will shed more light on the precise molecular nature of the cellular mechanisms underlying branching

morphogenesis in *Drosophila melanogaster*.

Given the poor cellular and molecular understanding of the adhesive properties in *e.g.* vertebrate morphogenesis processes, it is very difficult to validate the applicability of our “affinity group” model for other branching morphogenetic processes. We feel however confident that this paradigm could serve as a general strategy to sculpt branched and other complex patterned organs.

Chapter 8

Transcriptional profiling of different branching morphogenesis programs

Carlos Ribeiro, Alain C. Jung, Lydia Michaut, Ulrich Certa and Markus Affolter

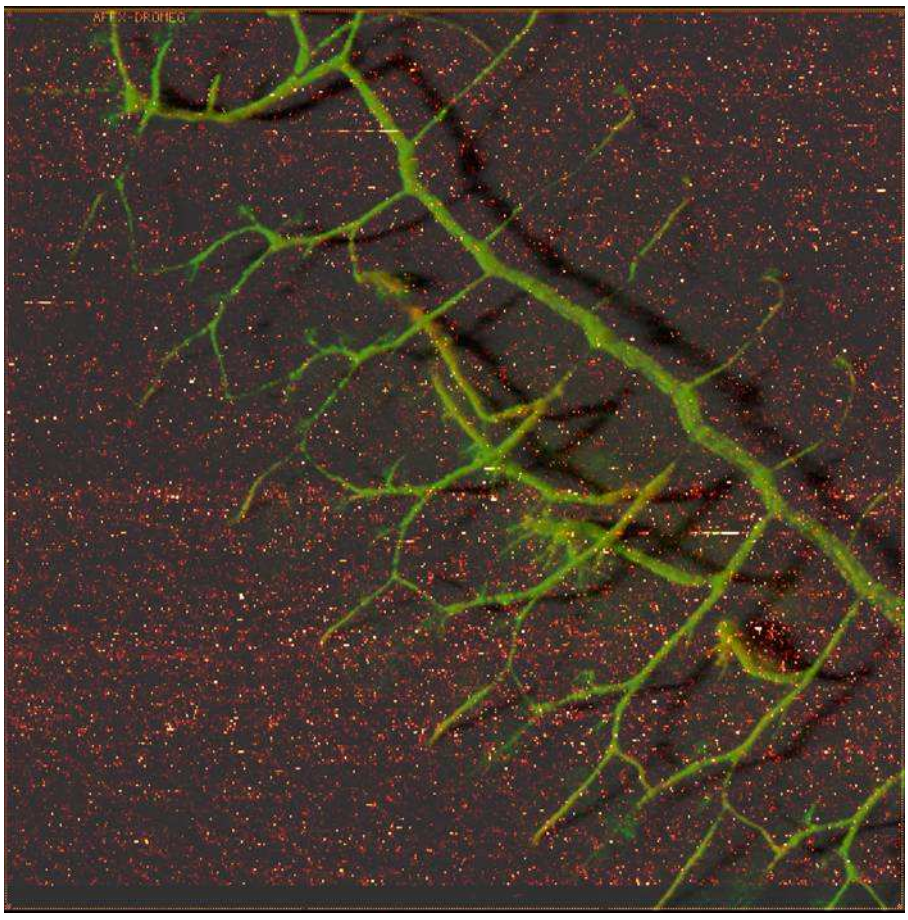

Introduction

As shown in the previous chapters, two main signaling systems control the morphogenesis of the tracheal network. One relies on the chemoattractive action of Bnl/FGF to sculpt the tracheal system by guiding the direction of outgrowth of the primary branches. The second, superimposed system relies on the transcription factors Kni/Knrl and Sal, induced by Dpp and Wnt signaling respectively, to confer a unique identity and morphology to the different branches.

However, the exact nature of the molecules whose tracheal expression is controlled by Kni/Knrl and Sal is not clear. Only the elucidation of these effectors can clarify the exact molecular mechanisms controlling branch identity and morphology.

Unfortunately, no systematic saturated genetic screen has been undertaken addressing the development of the tracheal system. In addition, all previous studies using reverse genetics, available mutations, deficiencies and other approaches did not lead to the identification of a single target gene of Kni/Knrl and Sal. Moreover, as one has to expect that the effector genes regulated by the two transcription factors are either highly redundant and/or maternal, zygotic loss of function genetic screens may not be the approach of choice.

We have therefore decided to screen for target genes of Kni/Knrl and Sal by performing a whole genome transcriptional profiling of embryos, whose tracheal system has been modified by constitutively activating or inactivating the Dpp signaling system. In collaboration with F. Hoffmann-La Roche, we took advantage of the recently sequenced *Drosophila* genome to design the first *Drosophila* whole genome oligonucleotide array, which was then produced by Affymetrix. In an initial attempt, we tried to isolate and purify tracheal cells using Fluorescence Activated Cell Sorting (FACS) from embryos of interest, in order to have a purified tracheal cell population containing a minimum of other embryonic cells. Unfortunately, due to technical problems, we had to give up this approach. We therefore compared the RNA populations isolated from whole embryos in which we modified the activity of the Dpp pathway throughout the tracheal system. 303 genes were found to have significant differences in their expression levels when compared across both populations. Regrettably, we were not able to confirm by *in situ* hybridization any of the most promising candidates as being expressed in the tracheal system, for reasons outlined at the end.

Results

Cell isolation and sorting

Transcriptional profiling using oligonucleotide arrays is an exquisitely sensitive method (Lockhart and Winzeler, 2000), and thus encloses the

risk that fluctuations and variations that occur in all biological system significantly amplify the noise of the experimental setup. This danger is furthermore increased by the heterogeneity of the cell population encountered in a complex organism, as for example the developing embryo. Therefore, great care has to be taken in selecting the cells from which to extract the RNA that one intends to compare. While exploiting the strengths of the fruitfly, based on the powerful genetics and the fact that one can analyze developmental processes in the context of the developing multicellular organism, one has also to accept that in the case of the *Drosophila* embryo, it is very difficult or even impossible to dissect manually cell groups or organs.

To circumvent these difficulties, we have decided to isolate the cells of the tracheal system by specifically labeling the desired cells with a fluorescent marker (*e.g.* Green Fluorescent Protein, GFP) followed by the dissociation of the cells of stage-selected embryos and subsequent automated sorting by FACS (Bryant *et al.*, 1999; Krasnow *et al.*, 1991). This would allow us not only to sort purified cells from Dpp signaling gain- and loss-of-function trachea, but also to compare the transcriptional profile of purified tracheal cells with a control population of embryonic cells (devoid of tracheal cells), thereby allowing us to define a list of trachea-specific genes.

As we were afraid that the available tracheal driver line would not be strong enough to drive a clear fluorescent signal at early stages of tracheal development, we generated a strain in which GFP is directly driven by the B123 fragment of the *btl* enhancer (Ohshiro and Saigo, 1997). However, this line was never used since the fluorescence signal from recombinants of *btl-GAL4* with a *tau-GFP* fusion construct under UAS control was shown to be strong enough to be used for our experiments.

In a series of experiments, we developed a quick, robust and reproducible cell dissociation protocol starting from the published Whole Animal Cell Sorting (WACS) and the imaginal discs cell sorting protocol (Jasper *et al.*, 2002; Krasnow *et al.*, 1991; Neufeld *et al.*, 1998). Our procedure is based on trypsin treatment of dechorionated embryos with subsequent mechanical dissociation and multiple filtering and purification steps. Due to the weakening of the cell integrity by trypsin treatment, the quite harsh mechanical stress and the subsequent very careful filtration steps (to absolutely avoid cell clumps, which could jam the sorter), the efficiency of the protocol is very low. Less than 2% of all embryonic cells are recuperated by this method. This is a relatively low number, but given that one can very easily scale up the amount of dissociated embryos, the sorting rate is the actual limiting factor in the efficiency of the procedure. For a detailed protocol, see materials and methods.

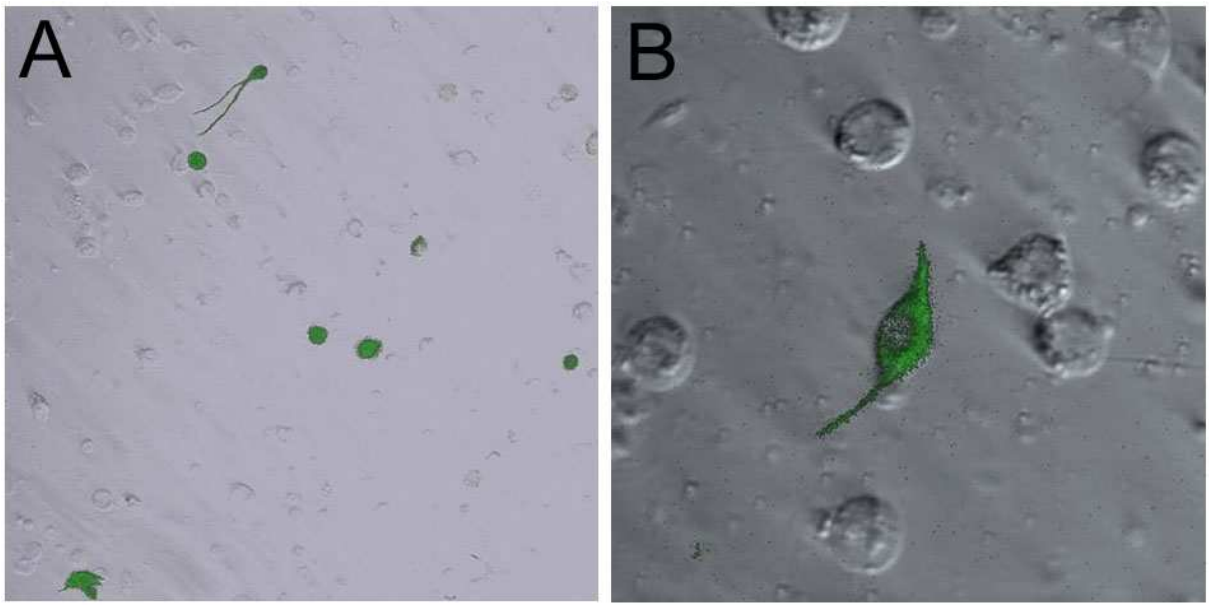

Figure 38 *Images of dissociated embryonic cells.* Overlays of confocal image projections (green, tau-GFP) and DIC images, of embryos expressing *tau-GFP* under *btl-Gal4* control.

Multiple analyses were performed to control the quality of the dissociation of the embryonic cells. First, dissociated cells were analyzed under the confocal microscope for the degree of separation, signal intensity of the marked cells and cell morphology. As it is clearly visible in Fig. 38, cells were nicely dissociated, had a rounded morphology (as expected after trypsinization) and GFP positive cells were readily visible. Interestingly some GFP positive cells were presenting long protrusions nicely highlighted by the Tau-GFP fusion.

To test for the viability of the cells, the dissociation suspension was incubated with the cell viability maker Propidium Iodide (PI) and analyzed by FACS. Less than 10% of the sorted cells were PI positive indicating that more than 90% of the cells were still alive (data not shown). We also checked for the proportion of GFP positive cells in the dissociation suspension. It is possible that our cells of interest are especially susceptible to the dissociation protocol. If that would be the case, these cells would be underrepresented in our preparation. We expected the tracheal cells to represent approximately 10% of all embryonic cells. Multiple FACS analyses revealed a ratio between 5% and 10% (data not shown). The lower percentage can be explained by the fact that we used overnight, unstaged embryo collections for these tests. Therefore, some embryos had not yet developed a tracheal system and were therefore devoid of GFP positive cells, diminishing the ratio of GFP positive to negative cells.

After these initial tests, we sorted different preparations of dissociated embryos. Cells were sorted into FCS coated polystyrene tubes (to decrease the sticking of the cells to the tube wall). Subsequently, cells were centrifuged, resuspended in Trizol and immediately frozen. For details, see materials and methods.

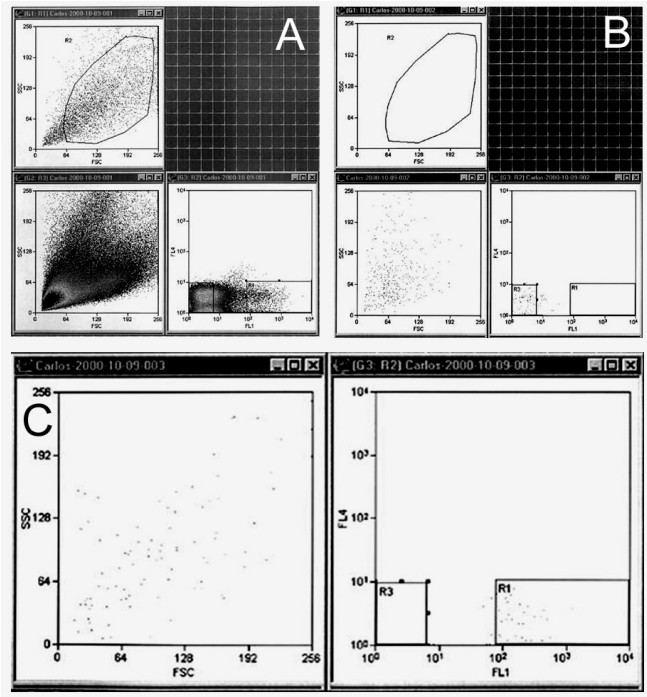

Figure 39 *Sorting profile of dissociated cells.* A, cells profile during the sorting. In the lower left window is a side-scatter/forward-scatter diagram of all cells, in the lower right window, a fluorescence intensity diagram of the sorted cells with the right square indicating the sorting window for the GFP positive cells and the left square the sorting window for the GFP negative control cells and in the top left window the backgated side-scatter/forward-scatter diagram of the GFP positive cells with the marked area indicating the sorting window for this condition. B, sorting profile of the reanalyzed GFP negative cells. Note that all cells are in the left square in the fluorescence diagram. C, sorting profile of the reanalyzed GFP positive cells. Note that with some rare exceptions all cells are in the right square of the fluorescence diagram indicating that they are really GFP positive cells.

A small sample of the purified cells was retested on the FACS to assess the purity of the sorted GFP positive cell population (Fig. 39C). Purity of the GFP positive cells was more than 95%. Note that this does not mean that we obtained a more than 95% pure tracheal cell population, as the *btl-Gal4* driver is also strongly expressed in the ventral midline.

We were able to isolate in average 150'000 to 200'000 cells per two hours of sorting by this procedure. From control RNA extractions of dissociated non-sorted cells, we calculated that 200'000 cells would yield 200 ng of total RNA, which would be enough material to perform a labeling reaction using a linear amplification method (Hoffmann *et al.*, 2002). Additionally, we made sure that the total RNA is not degraded by the dissociation protocol by testing its quality using an Agilent 2100 Bioanalyzer. These tests revealed that, except for very rare cases, the isolated total RNA was of excellent quality.

We did however not succeed in isolating enough RNA from the sorted cells. We suspect that the problems rely in the large volume into which the cells were sorted (approximately 15 ml) and which make the recuperation very difficult and inefficient. Regrettably, due to the inability to perform this essential step, this approach was abandoned.

Oligonucleotide analysis of whole embryos expressing Dad or a constitutive active form of the Dpp receptor throughout the tracheal system

Due to the unexpected technical problems in extracting the total RNA from the sorted cells, we decided to use a different approach to address our question of interest. In order to circumvent the encountered problem, we chose to use whole embryos instead of the sorted cells. Except for the disadvantages mentioned earlier, this procedure also presents clear advantages. First of all, the tracheal cells are not submitted to the isolation and sorting procedure which could lead to artifacts. Secondly, one can perform the labeling reaction without the use of linear amplification steps, as the collection of embryos is easily scalable, and therefore the isolation of enough total RNA is not as much a problem as when using FACS sorted cells.

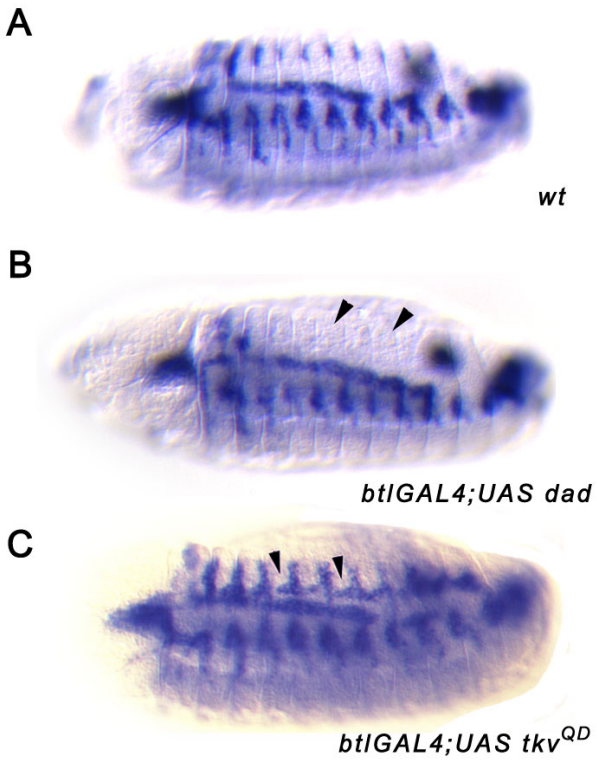

Figure 40 *Confirmation of our paradigm for modifying* kni *expression in the tracheal system. In situ* hybridization using a probe for the *kni* gene (blue) on wildtype embryos (A) as well as on embryos expressing *Dad* (B) and tkv^{QD} (C) throughout the tracheal system. Arrowheads mark the differences in the expression pattern of *kni* in the different genetic backgrounds.

For this purpose, we crossed a homozygous tracheal driver line with a homozygous *UAS-Dad* line (leading to the repression of *kni* expression, Fig. 40B) or a homozygous *UAS-*tkv^{QD} line (leading to an expansion of *kni* expression, Fig. 40C) (for details see materials and methods). Embryos were then staged by performing a one-hour precollection and a one-hour subsequent collection, after which embryos were allowed to develop for an additional nine hours before they were transferred to Trizol,

homogenized and frozen at -70℃. For each RNA isolation, this procedure was performed on different days, with flies from independent crosses, to minimize the influence of external experimental effects.

Total RNA from these embryos was then extracted in parallel on the same day and analyzed on the Agilent 2100 Bioanalyzer. 20 μg from samples that showed no degradation were used to perform the labeling reaction. Four samples from the *btl-Gal4/ UAS-Dad* and four samples from the *btl-Gal4/ UAS-tkv^{QD}* crosses were chosen for the experiment.

	btl-Gal4/ UAS-Dad C9	*btl-Gal4/ UAS-Dad* C10	*btl-Gal4/ UAS-Dad* C11	*btl-Gal4/ UAS-Dad* C12	*btl-Gal4/ UAS-tkv^{QD}* C13	*btl-Gal4/ UAS-tkv^{QD}* C14	*btl-Gal4/ UAS-tkv^{QD}* C15	*btl-Gal4/ UAS-tkv^{QD}* C16
btl-Gal4/ UAS-Dad C9	-	0.983	0.990	0.976	0.979	0.982	0.973	0.961
btl-Gal4/ UAS-Dad C10	-	-	0.976	0.960	0.967	0.967	0.963	0.951
btl-Gal4/ UAS-Dad C11	-	-	-	0.980	0.982	0.978	0.961	0.944
btl-Gal4/ UAS-Dad C12	-	-	-	-	0.977	0.975	0.965	0.941
btl-Gal4/ UAS-tkv^{QD} C13	-	-	-	-	-	0.990	0.980	0.969
btl-Gal4/ UAS-tkv^{QD} C14	-	-	-	-	-	-	0.986	0.977
btl-Gal4/ UAS-tkv^{QD} C15	-	-	-	-	-	-	-	0.988
btl-Gal4/ UAS-tkv^{QD} C16	-	-	-	-	-	-	-	-

Table 1 *Correlation coefficients for arrays.*

The probes were hybridized on the prototypical *Drosophila* whole genome oligonucleotide array roDROMEGa (see materials and methods), which was then scanned, and the extracted data compared and analyzed using the RACE-A software from F. Hoffmann-La Roche (see materials and methods). The correlation coefficients of the arrays (Table 1), as well as all other values used to assess the quality of the experiment indicated a high confidence value for the results obtained by this series of comparisons.

Overview of the differentially regulated genes obtained by the comparison of both genetic backgrounds

Transcripts showing an expression level fold change of ≥ 2 or ≤ -2 at significance values of P≤0.01 (t-test) were considered to be differentially expressed. 303 genes were found to fall in this category. 130 being expressed at higher levels in the *btl-Gal4/ UAS-tkv^{QD}* background when compared to *btl-Gal4/ UAS-Dad* and 173 at lower levels. Genes were defined as unregulated by Dpp signaling when their expression levels were higher in the *tkv^{QD}* experiment when compared to the *Dad* overexpression background.

As a first confirmation, we checked for the genes whose expression levels we expected to be changed by the manipulation of the Dpp pathway in the tracheal system. These control genes were *gal4*, *Dad*, *salm* (Kuhnlein and Schuh, 1996), *tkv*, *kni* and *knrl* (Chen *et al.*, 1998) (Table 2). *gal4*, the gene we use as ectopic activator is barely detected by the chip (threshold for detection is 50) indicating that the ectopic expression signal from the tracheal cells is strongly diluted by the signals of the other embryonic cells present in our experimental setup. *Dad* however behaves as expected. In the comparison it is a gene strongly downregulated by Dpp signaling because its overexpression triggers the shutoff of the Dpp pathway in our paradigm. It is one of the most strongly regulated genes in our experiment and has a very good confidence value. This is especially encouraging as in the case of ectopic *tkv^{QD}* expression, endogenous *Dad* should also be induced (as negative feedback loop) and therefore the difference seen in this comparison should be attenuated by this effect.

sal (represented here by *spalt major* one of the homologues) was also detected as a gene regulated by ectopic Dpp signaling activation and inhibition. As expected from the literature it is downregulated by Dpp signaling and has a very good confidence value (Kuhnlein and Schuh, 1996).

Unfortunately, none of the known tracheal Dpp target genes was detected by our experimental setup. Test *in situ* hybridizations with *kni* show that this is not due to a flaw in the experimental paradigm (Fig. 40). In the case of *tkv* it had already been shown that the gene is tightly regulated in trachea (Affolter *et al.*, 1994b) and therefore this strong regulatory mechanisms could have kept the expression level lower than in the case of *Dad*. In the cases of *kni* and its homologue *knrl,* we detect almost no difference when comparing the expression levels in both situations. As both genes behave similarly to Dpp signaling in trachea and both show no change in expression level when monitored using oligonucleotide arrays, we ruled out a problem in the design of the array probes. These two genes are also strongly expressed in other tissues of the embryo, and we suppose that the signal change in the few transformed tracheal cells was buffered by the expression signal in the remaining non-tracheal cells. As expected, the signal to noise ratio when using whole embryos was not good enough to detect such slight alterations in expression levels.

Gene	Average Difference in ectopic *tkv*^{QD}	Average Difference in ectopic *Dad*	Changefold	t-test p value
Control: *gal4*	54	37	1.46	0.67165
Dad	143	1526	-10.69	0.00001
salm	575	1159	-2.01	0.002
tkv	4178	3282	1.27	0.06715
kni	1464	1750	-1.2	0.15881
knrl	489	551	-1.13	0.4521

Table 2 *Overview of control genes.*

To further analyze the obtained data, the list of candidate genes was connected with the information available from FlyBase (Consortium, 2003). The complete annotated list of genes can be found as HTML and Excel tables in supplementary materials.

Table 3 shows how many of our candidate genes have homologies with genes in other species according to their annotation in FlyBase. In other words, these numbers indicate how many of these genes have remained conserved throughout evolution. Conserved genes have a higher likeliness to fulfill central functions in the biological process in which they participate. Interestingly, the table also reflects the state of sequence information available in the databases at the time of the comparison (October 2001). As the *C. elegans* genome was the only other sequenced genome of a higher eukaryote at the time of the comparison, a further analysis is only justified with the worm data (1998). The ratio from our sample of 51% of homologous genes in both species is nevertheless an overproportionally high ratio when one considers that 30% of all fly proteins have homologues in the worm genome (Rubin *et al.*, 2000). Therefore, we conclude that our candidate genes have an overproportionally high likeliness to be involved in conserved and therefore core functions of the fly.

Candidate genes with homologues in other species	**195 (64%)**
Candidate genes with *C. elegans* homologues	156 (51%)
Candidate genes with Human homologues	114 (38%)
Candidate genes with Mouse homologues	32 (11%)
Candidate genes with Rat homologues	8 (3%)
Candidate genes with Zebrafish homologues	3 (1%)

Table 3 *Overview of the homologies of our candidate genes with genes from other species.*

From the distribution of the annotated functions of the candidate genes, we see immediately that most groups belong to genes, which could have an

obvious mechanistic role in the process of branching morphogenesis (Table 4). This is especially the case for the cell adhesion molecules, the proteases, motor proteins and actin binding proteins. These results are too preliminary to implicate these genes in the Dpp controlled branching morphogenesis processes in trachea. First and most importantly, this list of genes represents only a list of candidate genes, which first has to be confirmed to be expressed in trachea. Secondly, it is widely recognized that the annotations, which in many cases do not rely on functional studies, but on homologies with genes having described functions, are very often misleading and do not reflect the real nature of the protein product of the gene.

Transcription factors	13 (4%)
Kinases	13 (4%)
Structural proteins	7 (2%)
Transporters	7 (2%)
Cell adhesion molecules	6 (2%)
Signal transducers	4 (1%)
RNA binding	4 (1%)
Proteases	4 (1%)
Phosphatases	3 (1%)
Motor proteins	3 (1%)
Actin binding	2 (1%)
Defense/ Immunity	2 (1%)
Others functions	66 (22%)
Genes with annotated functions	**134 (44%)**
Function unknown	**169 (56%)**

Table 4 *Overview of the annotated functions of the candidate genes.*

In situ *hybridization of candidate* genes

From the 303 genes, approximately 30 genes, which showed strong upregulation/downregulation, excellent confidence values (t-test) and with annotated functions of interest were selected. Additionally some genes, which showed no strong relative upregulation/ downregulation (fold) but very strong absolute upregulation/ downregulation values (large absolute difference of Average Differences) were selected. As many genes had already been cloned and characterized an extensive literature search was done for all these candidates.

Given that our experiment was aimed at identifying genes downstream of transcription factors expressed in a subset of the tracheal branches, the rescreening assay was based on the identification of genes recapitulating the same expression pattern. Therefore, the minimum requirement for the confirmation of a candidate gene was its expression in the trachea. Ideally, the gene should only be expressed in a subset of the tracheal cells.

Unfortunately, none of these genes could be confirmed as being expressed in the tracheal system. Most

genes showed either a ubiquitous expression pattern, or no expression pattern at all. According to their expression patterns, the remaining genes were grouped in three different classes:

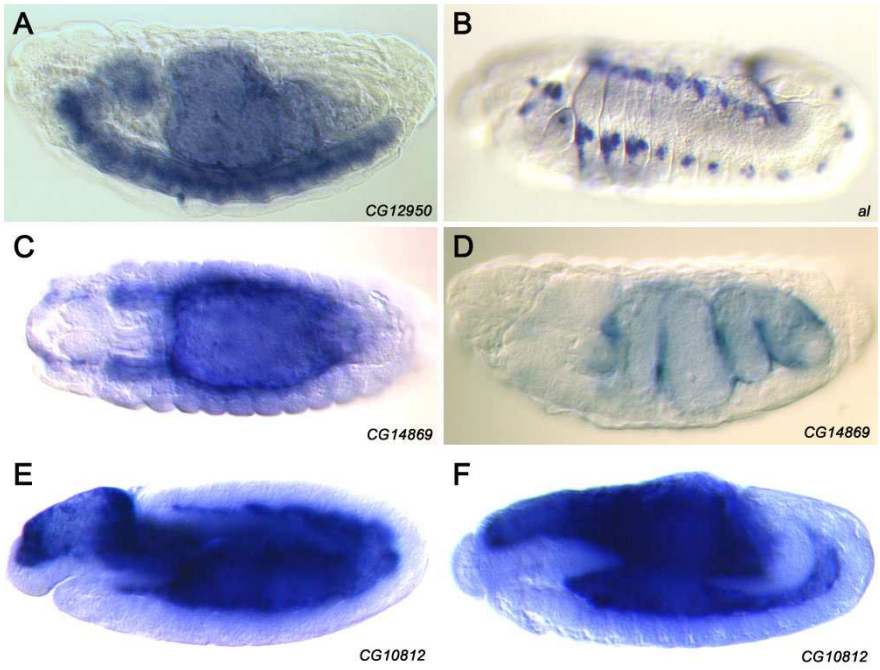

Figure 41 ***Some expression patterns of the tested candidate genes. CG12950*** **is strongly expressed in the CNS (A) while** ***al*** **is expressed in the leading edge cells and in a segmentally repeated pattern (B).** ***CG14869*** **viewed dorsally shows strong expression in the gut and in the salivary glands (C). A lateral view nicely shows that the gene seems to be expressed at higher levels in the folds (D).** ***CG10812*** **is very strongly expressed in the amnioserosa (E) and in the embryonic fat body (F).**

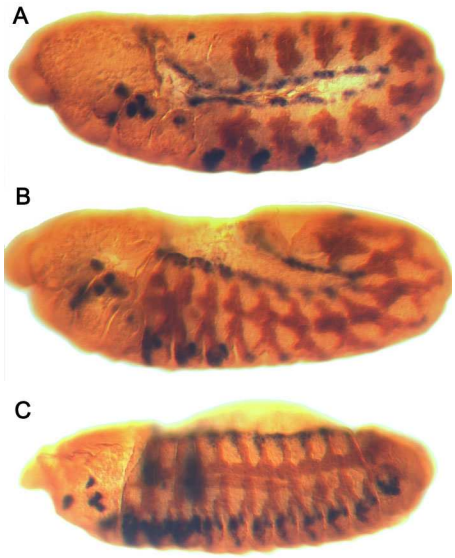

Figure 42 *Trachea and* al *double labeling experiment.* The tracheal system was labeled using the 1-eve-1 enhancer trap line (brown) while *al* was visualized by *in situ* hybridization (blue). Before and during germband retraction, part of the *al* expression pattern recapitulates the *dpp* expression pattern (A, B). After germband retraction, the expression in the endoderm becomes more evident (blue stripes under the first two tracheal metameres) while partial overlap with the tracheal system indicates the possibility of tracheal expression (C).

One class contained genes expressed in the central nervous system (CNS). This had been expected due to the strong expression of the driver in the midline glia cells. Most genes had already been characterized as expressed in the CNS (*e.g. slit*, *off-track*, *scabrous*, *grain* and *unc-5*). Additionally, our *in situ* assays revealed one gene with a nice expression in the embryonic CNS: *CG12950*, which has homologies to the *Bos taurus* N-CAM 140 and to the *Homo sapiens* Nephrin gene. Therefore the CNS expression comes as no surprise (Fig. 41A).

A further large class showed expression in the gut. The gut is a tissue, which is known to often produce artifactual *in situ* hybridization signals. The control hybridization with the reverse strand probes and the overproportional high number of genes showing an endodermal expression pattern however indicates that these are *bona fide* endodermal genes. A good example for this class is gene *CG14869*. It encodes for a protein with similarities to the human ADAMTS14 with an ADAM Cysteine-Rich Domain and several Thrombospondin type 1 repeats, and is expressed in the gut and in the salivary glands (Fig. 41C and D).

The last class consists of genes expressed in the amnioserosa or the leading edge cells. This is the region of the embryo which is defined by high Dpp levels during early dorso-ventral patterning (Rusch and Levine, 1996). Additionally, the leading edge cells express Dpp, which is one of the key players involved in the process of dorsal closure. Two genes exemplify this class of genes and will be discussed in more details due to their interesting expression patterns: *aristaless* (*al*) and *CG10812*. *al* encodes a homeobox transcription factor playing a major role in establishing the proximodistal axis of adult appendages (Campbell *et al.*, 1993). Even if it is embryonic lethal and presents an exquisite expression pattern in the embryo the exact role during embryonic development is not known (Schneitz *et al.*, 1993). In the embryo, *al* is expressed in the head and in a segmentally repeated pattern, as well as in the imaginal disc primordia, the leading edge cells and the gut (Fig. 41B). As the *in situ* hybridization looked like their could be some tracheal expression, we performed a double labeling experiment in which we visualized the tracheal system together with the *al* expression pattern (Fig. 42). From the light microscopy images, after germband retraction, a colocalization in the dorsal and ventral tracheal system could not be ruled out. To finally clarify this issue, we performed additional fluorescent double labeling experiments. 3D reconstructions show that *al* is not expressed in the trachea but in ectodermal cells just above it (Fig. 43).

CG10812 encodes a defense immunity protein belonging to the drosomycin family. It is expressed at very high levels in the amnioserosa and the embryonic fat body (Fig. 41E and F). Due to this high level of expression, we were afraid that the embryonic fat body expression could mask a tracheal signal. Therefore, we tested the expression pattern of *CG10812* in a *serpent* mutant background, which lacks mesodermal derivates, and consequently the fat body. Nevertheless, also in this background, no expression could be seen in the tracheal system (Ribeiro, C and Jung, AC, unpublished result).

As none of the candidate genes could be confirmed as expressed in the tracheal system, we chose to terminate the project.

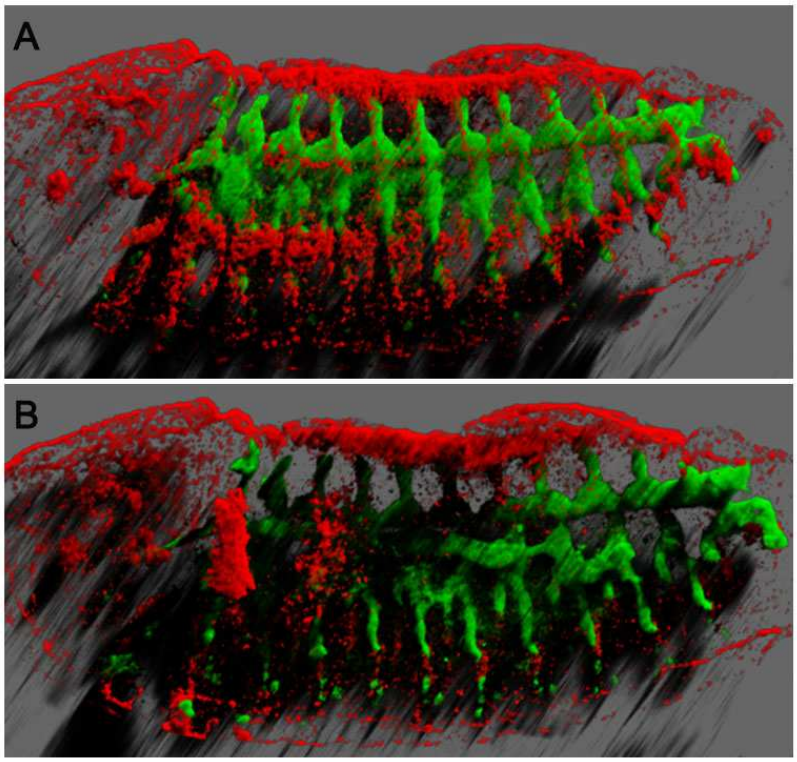

Figure 43 al *is not expressed in trachea.* 3D reconstructions of the tracheal system visualized by the *1-eve-1* enhancer trap line (green) and *al* by *in situ* hybridization (red). "Outside-in" view shows that *al* is expressed in ectodermal cells over the tracheal system (A). "Inside-out" view shows that also the cells expressing *al* in the inside the embryo (mostly endoderm) do not overlap with the tracheal system.

Discussion

Even if the use of whole genome oligonucleotide arrays is a promising tool for the survey of the transcriptional changes occurring during experimental perturbations of a system, in our case, its use has not led to a satisfying result. We think that multiple reasons can be advanced for this regrettable outcome. First of all, the experiment was performed by comparing the RNA pools of whole organisms, even if we were only interested in a defined population of cells. Additionally, only a subset of the tracheal system was changed by our experimental setup, leading to and even further decrease in the signal to noise ratio. We think that this effect is nicely exemplified in the case of *kni* and *knrl*.

But why did we get so many similar expression patterns which did not correlate with the expression pattern of *btl-Gal4*? Careful analysis of the expression pattern of *btl-Gal4* revealed that its expression is slightly leaky (for an example partially visible in Fig. 1). Indeed, in addition to its expression in the trachea and the midline glia, very weak *Gal4* expression can be detected in the region of the endoderm and the leading edge cells (data not shown).

Since these tissues are endogenously very sensitive to Dpp, we think that the very slight expression of *Dad* and constitutive active *tkv* in those regions of the embryo was enough to strongly modify the expression levels of Dpp target genes. Unfortunately, btl-*Gal4* is the best driver line available for the tracheal system and since there is no other driver line suited for the type of experiments we wanted to perform, even in the case of the cell sorting approach, we would have had this problem. Actually, we were from the beginning on aware of non-tracheal expression of the driver (in the midline glia) and accepted this disadvantage knowing that there was no alternative.

Finally, large scale gene expression monitoring is still a method with many pitfalls (Knight, 2001). As any method, chips produce many false negative and unfortunately false positive data. In the case of such large amount of data however, this is reflected in a much larger number of false candidate genes, dramatically increasing the amount of work one has to invest to experimentally asses the correctness of the data. Scientists are used to face such problems as they arise with most high throughput approaches. Saturating genetic screens for example produce innumerous mutants, which have to be discarded as erroneous candidates. The difference however is that the hype, which has surrounded large-scale expression monitoring in the last years, has praised this method as almost infallible. Using sophisticated computational and statistical tools one is supposed to be able to extract any kind of information from the data. The truth however is that this method is only an extremely fast and powerful method to perform a first molecular screen and only after having tested ALL candidates using a secondary independent screening method, it is possible to assess if the approach was successful. In our opinion, investing time in careful experimental confirmation should be preferred to refining the statistical and computational treatment of the data

Even if we were not successful in finding new tracheal target genes for Kni/Knrl and Sal, the *in vivo* imaging experiments described before reveal that possibly very few genes are controlled by these transcription factors in trachea. Possibly, Kni/Knrl only have *sal* as a repressive target in the dorsal branch while Sal could perform its function by only inducing few adhesion molecules. In this light, the likeliness to find target genes for these two transcription factors is even slimmer.

We have however found some interesting genes with very interesting expression patterns. Given that some of these are expressed in tissue sensitive to Dpp, it is conceivable that the identified candidate genes are *bona fide* Dpp targets outside of the tracheal system. Further analyses are required to clarify this point.

Also is it possible that some of the genes which show no or ubiquitous expression have a function in tracheal morphogenesis without having a notably different expression pattern in the tracheal system. Deficiencies removing some of the most promising candidates (*e.g. CG8811*, a Muskelin homologue, Adams *et al.*, 1998) have therefore been analyzed for tracheal defects; unfortunately, without success. Even if the absence of a tracheal phenotype could be due to maternal contribution of these genes, we believe that none of the tested candidates has a detectable function during tracheal morphogenesis.

Chapter 9

Final discussion, conclusions and outlook

Summary of the in vivo microscopy data

Bnl/FGF Is Required and Sufficient to Induce the Formation of Cellular Extensions

Bnl/FGF signaling is used reiteratively during tracheal development. Based on loss-of-function and gain-of function studies and on the expression pattern of *bnl*, Bnl/FGF has been proposed to act as a chemoattractant for tracheal cells in early developmental stages; branch outgrowth is directed toward *bnl*-expressing non tracheal target tissues via chemotactic induction of cell migration (Sutherland *et al.*, 1996). Here, we show that Bnl/FGF is indeed necessary and sufficient to induce filopodia in tracheal cells *in vivo*. Bnl/FGF-induced filopodia are extremely dynamic and are formed almost exclusively by the leading cells of migrating branches. It has been shown previously that Bnl/FGF-dependent phosphorylation of Map kinase (ERK) is highest in cells at the tip of branches (Gabay *et al.*, 1997). Both the number of filopodia (this thesis) and the amount of phosphorylated ERK dramatically increase in all cells upon ectopic expression of *bnl* (Gabay *et al.*, 1997). Together, these results strongly argue that Bnl/FGF signaling is highest in tracheal cells close to the source of the ligand and that migration is steered by the cells at the tip of the branches. Filopodia extend in all directions, suggesting that directionality in tip cell migration is controlled by events other than directional outgrowth of filopodia. Possibilities for such events include the selective adhesion of filopodia or the preferential stabilization or bundling of microtubules in the direction of the Bnl/FGF ligand.

Bnl/FGF and Dpp Signaling Have Distinct Effects on the Formation of Dorsal Tracheal Branches

We have previously shown that Bnl/FGF signaling is not sufficient for dorsal branch formation; in the absence of Dpp signaling (Vincent *et al.*, 1997) or in mutants lacking expression of the Dpp-induced target genes *kni*/*knrl* in the trachea (Chen *et al.*, 1998), dorsal branch formation fails completely. In this thesis, we analyzed the effects of the absence of either of the two signals at the cellular level using confocal four-dimensional imaging of living embryos combined with trachea-specific inhibition of Dpp signaling. Our results demonstrate that while Bnl/ FGF signaling is necessary and sufficient for the induction of filopodial activity in tracheal cells and for cell migration in the strictest sense (cells do start to migrate dorsally when Dpp signaling is inhibited by Dad), Bnl/ FGF is apparently not sufficient to allow productive dorsal branch outgrowth. For dorsal branches to grow out and form, Dpp signaling input is strictly required, in addition to filopodial activity induced by Bnl/FGF. Thus, Dpp signaling does not appear to collaborate with Bnl/ FGF in filopodia production and motility, but instead to target cellular functions distinct from those targeted by

Bnl/FGF signaling. Thus, despite the essential and crucial role of Bnl/FGF, chemoattraction is not sufficient for successful tracheal branching and, despite the requirement of Dpp for dorsal branch formation, migration *per se* is not affected.

Intercalation of the dorsal branches is a highly complex junctional remodeling process

Branching morphogenesis is characterized by multiple, complex cell rearrangements that lead to the formation of the tubular tracheal structure. One of these rearrangements is the intercalation of the dorsal branch cells. This process is characterized by the formation of autocellular junctions, which are unique for unicellular branches (Samakovlis *et al.*, 1996). Additionally, these rearrangements have to take place without breaking the tube, which would lead to spilling of the luminal content.

Using confocal four-dimensional imaging of living embryos expressing *D*α-Catenin-GFP as an *in vivo* marker for the adherens junctions (Oda and Tsukita, 1999a), we analyzed the transition from a multicellular to a unicellular tube in the dorsal branch. Initiation of unicellularization proceeds from proximal to distal and is characterized by four main stages. In the first stage, the cells of the dorsal branch pair, leading to the formation of a ladder-like arrangement of their AJs. In the next stage proximal displacement of one of the two lower cells leads to the diminishment of the AJ contacts between that cell and the cell lying above it. The third stage is characterized by the formation of a circular AJ structure, which surrounds the lumen and connects the three cells with exception of the cell sliding in proximal direction, whose AJs are only connected at one knot-like point with the ring.

The continuing proximal movement of the one cell leads to the breakage of the remaining knot-like contact and therefore to the loss of AJs contact with the remaining cells. To prevent the spilling of luminal content during the fourth step this loss in AJ contacts is compensated by the formation of autocellular junctions by the neighboring cell leading to the formation of a unicellular tube. Intercalation is accompanied by the extension of the autocellular junctions until two cells lying in an end-to-end arrangement are only connected by a small circular AJs ring.

Dad overexpression inhibits reorganization of the adherens junctions but Dpp signaling is not required for unicellularization

As *Dad* overexpression inhibits the productive formation of a unicellular branch, we analyzed the effect of Dpp signaling loss on the AJs dynamics of the dorsal branch (Ribeiro *et al.*, 2002; Vincent *et al.*, 1997). In *Dad* overexpression embryos the cells of the dorsal branch do not pair, to form the ladder-like AJs pattern observed in wildtype. Instead, the AJs retain the same mesh-like pattern as the dorsal trunk cells. Additionally, the basal side

of the dorsal branch cells is seen to extend in the direction of the chemoattractant while the apical surface stays tightly associated with the dorsal trunk, finally leading to the reintegration of the dorsal branch cells into the dorsal trunk.

To assess if Dpp signaling is an instructive or permissive factor for dorsal branch formation and unicellularization we analyzed the effect of simultaneously removing Sal and Kni/Knrl in tracheal cells. Surprisingly dorsal branch formation was rescued indicating that the reintegration of the dorsal branch cells into the dorsal trunk in *Dad* overexpression embryos was due to ectopic *sal* expression in the dorsal branch cells.

To further analyze, the requirement of Dpp signaling for correct dorsal branch morphogenesis, we assessed the effect of the concomitant removal of Sal and Kni/Knrl on intercalation. As shown using *D*α-Cat-GFP, unicellularization proceeds normally without Dpp signaling in a *sal* loss of function background.

Kni/Knrl exert their function to a large extent by repressing **sal**

From these data, we conclude that Kni/Knrl exert their function largely by inhibiting *sal* expression in the dorsal branch. Not Kni/Knrl target genes are responsible for the morphogenesis of the dorsal branch. Instead, Sal leads to the transcription of dorsal trunk specific genes, which inhibit dorsal branch specific AJs reorganizations. Therefore, Kni/Knrl act by permitting dorsal branch cells to undergo pairing and intercalation as they would in the absence of *sal*.

Open questions in branching morphogenesis of the tracheal system

The challenges still ahead in the study of tracheal morphogenesis, can be divided in two major types: technical problems and biological questions. As well exemplified by the work presented in this thesis, both topics strongly influence each other. Advances in methodologies will lead to advances in the understanding of biological processes and the requirements of the biological question will influence the development of novel technical approaches to solve it (Amos, 2000). Therefore, it is not possible to strictly separate both aspects. In the next two sections, an overview over the major remaining topics in these two aspects of tracheal research will be attempted.

Technical challenges

Multiple color labeling

The most urgent technical advance necessary is the establishment of *in vivo* multiple color labeling. Using this method one could finally study the interplay of actin and microtubular filaments during guided cell migration. In addition, the interplay of tracheal cells with the surrounding tissue (Boube *et al.*, 2001; Franch-Marro and Casanova, 2000) and the relation of the cell body to the adherens junctions during intercalation could be studied. We have undertaken first efforts to solve this problem using CFP/YFP labeling. However, due to difficulties in efficiently exciting CFP using our laser setup, this approach has not led to satisfying results. Theoretically, one could specifically filter out the YFP signal from a GFP/YFP coexpression background (we term this one and a half labeling) but this is not the method of choice for multiple labeling and should therefore only be used as a temporary solution until real double labeling works (Neumann, M. and Ribeiro, C., unpublished results). The remaining possibilities to solve this problem are the use of GFP in combination with red fluorescent proteins (see introduction) or the use of an additional “blue” laser to excite CFP.

Alternatively, computational approaches to separate multiple fluorescent signals (spectral unmixing) as used by the new Zeiss LSM 510 META microscopes would allow the visualization of multiple, very close signals (Dickinson *et al.*, 2001).

Paired with the ability to mark single cells, this approach promises dramatic improvements in our understanding of many cellular processes inside the living organism.

Spinning disc confocal microscopy

Even if the temporal resolution of the confocal laser scanning microscopy (CLSM) approach used in our studies was high enough to answer the questions asked, we could not rule out that the structure seen in one time point were not distorted due to the required image recording time. Using this approach one can only make qualitative statements about highly dynamic structures such as filopodia. For analyses that are more detailed, a microscope setup is required which allows much faster image recording. The spinning disk or Nipkow disk microscope connects the advantages of the CLSM with the speed of a wide field fluorescence microscope (Fig. 44). Until recently, technical problems with the irradiation intensity impeached this setup to be used as a standard imaging approach. Lately however, advances in material technologies have led to the development of spinning disc microscopes suited for the standard use in the laboratory (Nakano, 2002).

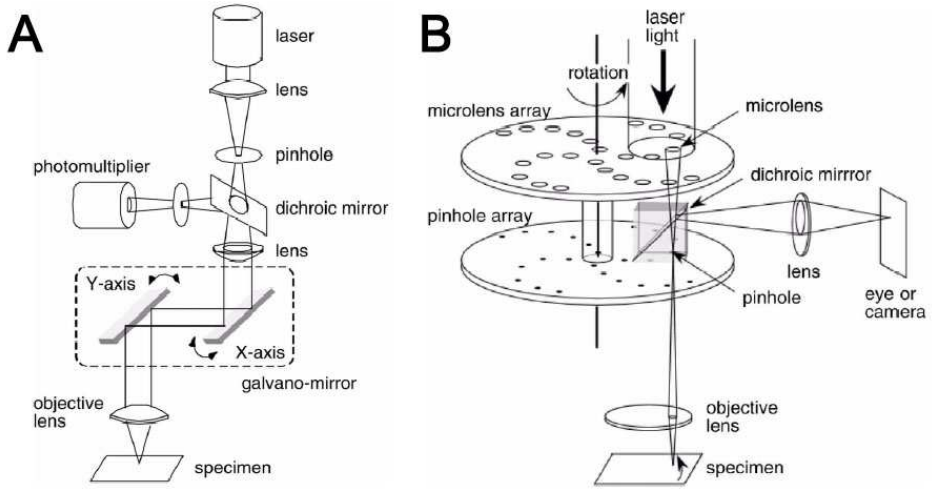

Figure 44 *Comparison of a conventional laser scanning confocal microscope and a confocal Nipkow disk laser scanning microscope.*(A) In the conventional laser scanning confocal microscope the laser beam that passes through the pinhole is focused on the specimen as a light point. This point is scanned over the x- and y-axis by a mechanical way. The demerit of this method is the slowness of scanning. (B) The confocal Nipkow disk laser scanning microscope uses a spinning disk with multiple pinholes. The problem of irradiation efficiency is markedly improved by the use of microlenses. This method has enabled scanning at as fast as 100 frames/sec. Since the light axis never moves during scanning, fluorescent signals produce an image, which can be directly captured by cameras. (From Nakano, 2002)

Fluorescence recovery after Photobleaching (FRAP)

As outlined in the introduction FRAP allows the assessment of the mobility of proteins inside a living cell. This can be used to measure the fluidity of molecules inside of cellular structures and therefore indirectly the physical properties of these structures. Especially in the study of the different structural properties of the AJs FRAP could be a potent tool. If the rigidity of the AJs is a major factor in controlling morphogenetic processes, the measurement of the fluidity of AJ components could give important indications about the correctness of this assumption. We are currently performing preliminary FRAP experiments on the AJs of the dorsal branch.

Fluorescence resonance energy transfer (FRET)

One of the main unanswered questions of research on guided migration is how signaling of chemoattractant pathways is mediated onto the cytoskeleton. This is due due to the fact, that knowledge on the exact cellular dynamics of these pathways have only started to emerge recently (Mochizuki *et al.*, 2001). Receptors seem not to act on the whole surface of the cell but only in specific microdomains of the plasma membrane and to act highly specifically by the targeted vesicular delivery of the activated receptor complex to subcellular targets. Understanding where and how the signal is conveyed inside the cell could be crucial to understand how chemoattractants control motility. In

addition, FRET could be used to analyze the subcellular dynamics of all kind of protein-protein interactions. Unfortunately, it is a technically very challenging technology making its use inside the embryo even more difficult. We have tried to detect a FRET signal using the small GTPases probes in the tracheal system. However due to the limitations in exciting CFP with our CLSM setup we were not able to detect any specific FRET signal. Eventually the use of the spectral unmixing approaches could solve this problem.

New subcellular markers and protein traps

The main cell biological use of *in vivo* microscopy is the observation of experimental perturbations on cellular components of interest. As such, it is a very sensitive approach to detect subtle phenotypes at the subcellular level. The use of this approach very much depends on the capability to generate subcellular markers for the structures of interest. Therefore, the best way to improve the opportunities offered by *in vivo* microscopy is the generation of new and better GFP fusion proteins. hCLIP-170-GFP (microtubular dynamics, Perez *et al.*, 1999) and SLAM-GFP (junction polarity, Lecuit *et al.*, 2002) fusion proteins for example harbor great potential for understanding cellular processes controlling morphogenesis inside the living organism.

Even if the directed fusion of characterized proteins is mostly the method of choice, this approach has three main drawbacks. First, it is relatively slow, secondly, it does not allow the identification of new localized proteins and third, this approach relies on overexpression of the construct and can therefore lead to artifacts. Protein trapping has proven to be an excellent approach to overcome these limitations (Morin *et al.*, 2001). Especially when performed in combination with fluorescent embryo sorting this can be an extremely powerful method to generate new subcellular markers.

Biological questions

How is the chemoattractive signal of Bnl/FGF mediated on the cytoskeleton?

As outlined in the introduction, research on migration using cell culture systems has greatly improved our understanding of how guided migration is controlled by signaling. Especially small GTPases have been shown to play a major role in mediating the signal on the cytoskeletal machinery (Bishop and Hall, 2000; Van Aelst and D'Souza-Schorey, 1997). Unfortunately it is very difficult to genetically asses the importance of small GTPases for tracheal branch formation. Precise analyses of the effects of constitutive active and dominant negative versions of these molecules, on filopodia formation could however help to clarify this issue.

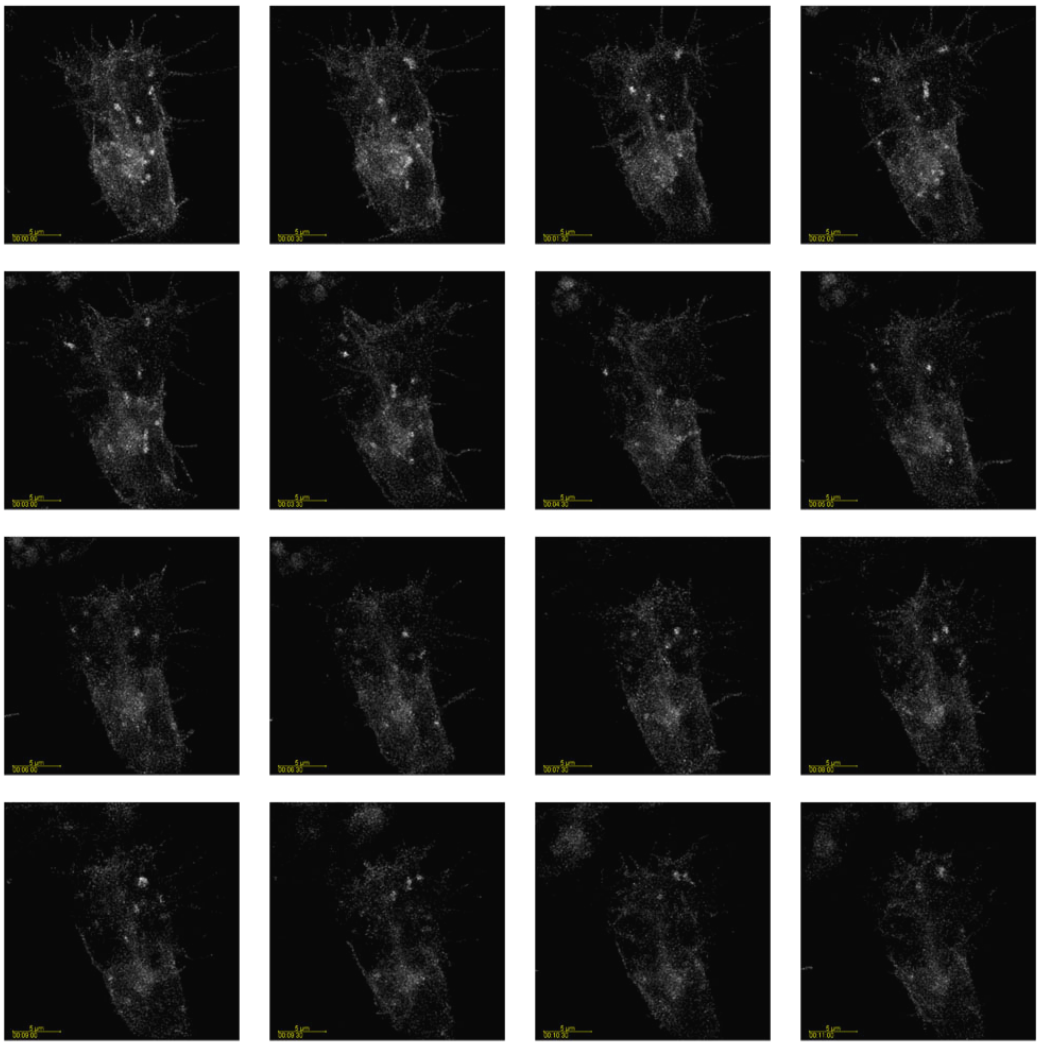

Figure 45 *Btl dynamic in tracheal tip cells.* Maximum intensity projections of a time-lapse of a living embryo expressing *btl-GFP* in the tracheal system. Two tip cells of the dorsal branch are visible. Frames were acquired at an interval of 30 seconds. See also corresponding movie 9 in supplementary materials.

Also, the precise analysis of the dynamics of Bnl/FGF signaling components using GFP fusion proteins or even better, FRET could help in our understanding of the precise role of the chemoattractant in guiding cell migration. First analyses at the pupal stage, on the subcellular localization of the receptor Btl, indicate that Btl is localized at the tip of filopodia (Sato and Kornberg, 2002). This would suggest that filopodia are indeed cellular sensors, which scan the surroundings for the availability of the chemoattractive signal. These studies however were performed on dissected tissue using widefield microscopes and very strong exposure. We favor the hypothesis, that the extensions analyzed represent the already stabilized fraction of filopodia. As stabilization is maybe due to Bnl/FGF signaling this would explain the observation of the receptor at the tip of the filopodia.

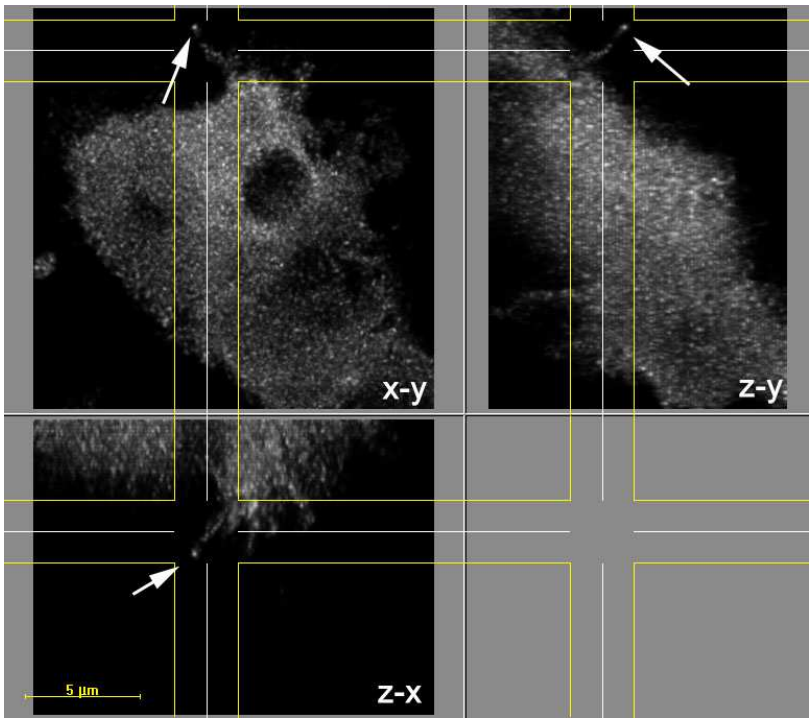

Figure 46 *Dof localization in trachea.* Maximum intensity projection in three planes of tip cells expressing Dof-GFP. Arrow marks the accumulation of Dof-GFP at the tip of a filopodium.

Own preliminary analyses indicate that Btl is indeed highly localized in the cell. Btl can be found in vesicular structures, which show a very dynamic behavior within the cell. We could however not observe any stable enrichment of Btl at the tips of the filopodia (Fig. 45 and movie 9 in supplementary materials).

We also analyzed the localization of a Dof-GFP fusion protein when expressed in trachea. In contrast to Btl, Dof does not present any specific localization within the cell. However, as filopodia are visible using Dof-GFP, Dof could also mediate Bnl/FGF signaling inside these extensions. In rare cases, we even observed an accumulation at the tip of a filopodium (Petit, V. and Ribeiro C. unpublished observation; Fig. 46).

The *Drosophila* ERM protein Dmoesin could play a key function in mediating FGF signaling on the actin cytoskeleton. ERM proteins are thought to constitute a bridge between the actin cytoskeleton and the plasma membrane. It is strongly expressed in the tracheal system (McCartney and Fehon, 1996), controls actin-based morphogenetic processes and is regulated by phosphorylation (Polesello *et al.*, 2002). For these reason, it is a prime candidate as a mediator of Bnl/FGF induced actin rearrangements.

How do filopodia control migration?

Actin dynamics are a reoccurring theme in migration of cells. Filopodia or lamellipodia are observed in almost all migrating cells and thought to be one of the main driving forces of motility. How filopodia mediate guided cell migration remains however unclear. They have been postulated to

fulfill their role by differential adhesion, generating mechanical force or transducing distal signals. It is very likely that all three possibilities apply. It is however unclear if analyses based on the tracheal system will be able to answer these complex questions. The integration of the cell biological knowledge gained from cell culture studies and theoretical models (Meinhardt, 1999) into the context of the living organism could help to asses the relevance of these observations for the morphogenesis of a complex organ.

Can Bnl/FGF induce migration in all ectodermal cells?

As shown Bnl/FGF is a very potent inducer of filopodia in tracheal cells. It is however unclear if the migratory response seen in tracheal cells is not an intrinsic property of all ectodermal cells, or if tracheal cells express specific components required for Bnl/FGF mediated motility. Clearly, the lack of Btl and Dof outside the tracheal system is an important regulatory mechanism but is there a trachea specific migratory machinery? This important question could be answered by ectopically coexpressing an activated form of *btl* together with *dof* and *GFP-actin* in ectodermal cells and observing if ectopic filopodia are observed.

Why are filopodia confined to the tip cells?

One of the most striking observations made in our studies is the confinement of cytoskeletal activity to the migrating tip cells. The reasons for this phenomenon are however still unclear. Multiple possibilities are conceivable.

Given that Bnl is an extracellular diffusible factor, the concentration past the tip cells could be too low to trigger the induction of filopodia.

Similarly, the levels of Btl and Dof could be regulated in order to be higher in the tip cells making these more sensitive to the chemoattractive signal. This possibility is strengthened by the observation that Dof is indeed observed to be expressed stronger in the tip cells (Vincent *et al.*, 1998). In addition, the transcription of *btl* was recently shown to be regulated by an autocatalytic loop leading to the concentration of the receptor in the tip cells (Ohshiro *et al.*, 2002). As in this study, Pointed is required to activate the transcription of *btl*, this model also explains why the rate of filopodia formation was reduced in *pointed* mutants.

However, the possibility remains that additional mechanisms are responsible for confining the chemoattractive response to the tip cells.

What is the contribution of the microtubules in guiding migration in the tracheal system?

Guided migration has always been associated with the interplay of the actin and microtubular cytoskeleton. Our studies have however been mainly focused on the analysis of actin dynamics. This is mainly due to the fact, that the tracheal microtubules only show a reduced dynamic behavior. We have nevertheless to assume that an important role has to be played by this essential cytoskeletal component (Small *et al.*, 2002). Possibly the examination of the interplay of the actin cytoskeleton with the microtubules using *in vivo* multiple color labeling could shed more light on this essential question.

Is Bnl/FGF induced motility the only driving force of morphogenesis of the tracheal system?

The chemoattractant Bnl/FGF is the main factor sculpting the primary pattern of the tracheal system. The pulling force generated by the two tip cells in the tracheal branch could be sufficient to mechanically drive cell rearrangements such as intercalation. It is however possible that additional mechanisms exist that mediate these morphogenetic events.

One of these mechanisms could be intracellular calcium signaling. Based on the observation of the simultaneous requirements of calcium and FGF signaling during *Xenopus* gastrulation, it has been proposed that FGF could mediate its morphogenetic effect via calcium signaling (Wallingford *et al.*, 2002). We are currently analyzing calcium dynamics in the tracheal system using a permutated GFP based calcium probe. (Nakai *et al.*, 2001).

We can however rule out that a molecular mechanism similar to convergent extension in vertebrates (Keller *et al.*, 2000) is involved in tracheal morphogenesis. Analyses of the subcellular localization, as well as loss- and gain-of-function effects of known components of the planar cell polarity (PCP) pathway in flies (Mlodzik, 2002), have led us to conclude that this pathway does not have a function in tracheal morphogenesis (Neumann, M. and Ribeiro, C.).

How is *bnl* expression regulated?

Bnl/FGF is the main factor sculpting the tracheal system by controlling the outgrowth of the primary branches (Sutherland *et al.*, 1996 and this thesis). Therefore, the pattern of *bnl* expression encodes the basic shape of this organ. Unfortunately, we do not to understand how *bnl* expression is regulated. This is however, a key question to understand tracheal morphogenesis and should be one of the main directions of tracheal research.

How is a new tube formed?

Tube formation is a biological process that has obtained a lot of attention recently. Different types of tube formation can be distinguished (Affolter *et al.*, 2003; Hogan and Kolodziej, 2002; Lubarsky and Krasnow, 2003). The tracheal system creates a cavity by invagination, which is then extended into different tubular branches by migration. Additionally, *de novo* tube formation occurs in the terminal branches and during anastomosis. Especially, the process of branch fusion is an excellent, accessible and already partially studied system to dissect *de novo* tube formation and apicalization. Therefore, further analyses of this process should lead to an understanding of the molecular mechanisms underlying tube formation.

How do tracheal cells interact with the surrounding tissue?

The main interest of studying morphogenesis *in vivo* is the consideration of the biological context in which such complex processes occur. Also tracheal morphogenesis is highly dependent on the surrounding tissue as it relies on signaling factors (Bnl/FGF, Dpp, Wg, *etc.*) secreted by surrounding cells. Physical interactions with the surrounding tissues were however also shown to be necessary for the morphogenesis of the tracheal system (Boube *et al.*, 2001; Franch-Marro and Casanova, 2000; Wolf and Schuh, 2000). The cells of these tissues are thought to serve as migratory substrates. Studying the dynamics of these cell-cell interactions could shed more light on the regulation of tracheal morphogenesis by these cell contact mechanisms.

How does Sal control cell rearrangements?

Dpp and Wnt signaling play an essential role in the correct patterning of the tracheal system (Chihara and Hayashi, 2000; Llimargas, 2000; Vincent *et al.*, 1997). By inducing Kni/Knrl and Sal in specific branches, they confer different identities to these branches (Chen *et al.*, 1998; Kuhnlein and Schuh, 1996). This leads to the patterning of the tracheal system into different branches with different tubular properties.

As the morphogenetic processes undergone by the cells expressing *kni/knrl* and *sal*, are very specific, it was thought that both transcription factors induce sets of different genes mediating these different events. Kni/Knrl and Sal were however characterized as repressive transcription factors and as shown in this thesis the main if not sole mode of action of Kni/Knrl in tracheal morphogenesis is the repression of *sal*. It is however still conceivable, that Kni/Knrl induce target genes in the dorsal branch and that the function of these transcription factors in tracheal morphogenesis is less straight forward than these studies indicate.

If the sole role of Kni/Knrl in tracheal morphogenesis is the repression of *sal,* would it not be conceivable that also Sal, having been characterized as

a repressor, represses genes in the dorsal trunk instead of inducing them? Especially as Wnt signaling, seems not only to be required for *sal* induction but also for *esg* expression in the tracheal system (Chihara and Hayashi, 2000; Kuhnlein and Schuh, 1996; Llimargas, 2000) and could therefore be responsible for inducing other dorsal trunk specific genes than *sal*.

But which are the cell biological mechanisms mediating the Sal effect on the dorsal trunk? It is now clear that Dpp and Wnt signaling do not act by interfering with Bnl/FGF induced migration. Instead, they seem to control AJ rigidity: Sal by inhibiting rearrangements and Kni/Knrl by repressing this inhibitory role of Sal and allowing therefore these morphogenetic processes to occur in the dorsal branch.

Dpp and Wnt signaling are however also required for the proper establishment of both branches. We favor the “affinity group” model for branch establishment. From different observations, we would like to propose, that a cell sorting mechanism based on differential adhesion properties, is responsible for separating both cell populations (Tepass *et al.*, 2002). *sal* expression in the dorsal trunk leads to a higher homophilic affinity among these cells. This effect is counteracted by the suppression of *sal* by Kni/Knrl in the dorsal branch. The higher homophilic affinity of the dorsal trunk cells causes these cells to maximize their adhesion surface with the cells of the same affinity group, leading to the formation of a thick trunk. The lower homophilic affinity of the dorsal branch cells allows these cells to undergo cell rearrangements, as intercalation for example, which lead to the diminishment of the cell-cell interaction surface. The differences in the adhesive properties lead to the formation of a tissue boundary and subsequent cell sorting (Tepass *et al.*, 2002). This mechanism would explain many of the phenomena observed in tracheal branching morphogenesis.

Finding new factors involved tracheal morphogenesis is the way to go.

What is the best way to approach the remaining questions and to test the proposed models? Only the identification of new tracheal genes involved in the processes described before can lead to a deeper understanding of tracheal branching morphogenesis. Multiple approaches are possible.

Genetic screens: The most obvious approach is the use of genetic screens. Either loss of function (EMS) or gain of function (EP) screens are suited to identify new genes involved in tracheal development. As no systematic loss of function screen for tracheal morphogenesis has been performed this should be the method of choice. Additionally, a maternal loss of function screen should be envisaged, as many cell biologically interesting genes will be maternally provided. The direct visualization of subcellular markers in trachea has the potential to greatly increase the sensitivity of the screens, allowing very subtle phenotypes to be detected (*e.g.* AJs patterns).

An alternative approach would be the identification of tracheal genes according to their expression pattern. Even if the use of oligonucleotide

arrays was not successful in our case, they could help to identify target genes of Trh in the trachea. Improvements in the cell sorting approach (*e.g.* use of magnetic cell sorting) could also help in this direction. Additionally systematic large scale *in situ* hybridization approaches are sure to reveal new genes expressed in the tracheal system.

Our Final model

From the data presented in this thesis, we propose the following general model for branching morphogenesis of the tracheal system. Even if this paradigm is mainly based on observations of the dorsal branch and the dorsal trunk, we think that this represents a general mechanism for branching morphogenesis.

All tracheal cells are intrinsically capable to react to the chemoattractant by migration, to adhere strongly to each other, ensuring the integrity of the tube, and to undergo unicellularization. Activation of the FGF pathway by Bnl/FGF induces cytoskeletal rearrangements (*e.g.* filopodia) enabling the receiving cells to move in direction of the chemoattractant. Given the adherent force among all tracheal cells, these migrating cells drag the attached cells with them, leading to the formation of the initial tracheal buds.

Sal controls the expression of proteins in dorsal trunk cells, which modulate the adhesive properties of these cells and augment the affinity of their AJs to each other. The resulting higher rigidity of the junctions prevents these cells from undergoing complex cell rearrangements and promotes the formation of contacts with cells of the same affinity group. This ensures the formation of a thick, multicellular, main tracheal trunk. The higher affinity of the dorsal trunk cells for cells of the same affinity group is also visible in the cuboidal shape these cells adopt, which indicates a high contact surface with other dorsal trunk cells.

Kni/Knrl repress the expression of *sal* in dorsal branch cells, leading to the loss of the described high affinity properties. Only the intrinsic adhesiveness of all tracheal cells remains, which ensures the integrity of the tracheal system. This is again visible in the shape of the dorsal branch cells. These exhibit are more columnar shape, in which only the smaller proximal and distal surfaces of the cells contact other tracheal cells, indicating a lower affinity for cells of the own branch.

This way, two cell groups are formed: one with a high self-affinity (the dorsal trunk) and one with a lower self-affinity (the dorsal branch). As in the wing imaginal disc, due to their different affinity properties, the two populations sort out leading to the formation of two distinct branches (Tepass *et al.*, 2002). This process is reminiscent of the hydrophobic effect, which leads to the formation of two phases in a water oil mixture. The lower AJs rigidity also enables the dorsal branch cells to undergo complex cell rearrangements, as for example unicellularization.

Concluding remarks

Nature has always fascinated men. With its inexhaustible repertoire of shapes and forms, it has stimulated the fantasy of our artists while challenging engineers to match the perfect balance between form and function observed in living organisms.

It is almost unconceivable that three-dimensional structures of such high complexity and beauty as our lungs are encoded genetically as a one-dimensional sequence of four chemical compounds. We have nevertheless started to understand how genetic information could generate such esthetic patterns. But how does the nascent organism transform this patterning information into morphogenetic processes which ultimately lead to the three dimensional sculpting of the animal's tissues?

This question is comparable with the challenges archeologists face when trying to understand how our ancestors achieved the construction of buildings and structures as complex and gigantic as the great Egyptian pyramids, the massive statues of Easter Island or the tomb of the first Chinese emperor.

Two main differences exist however: On the one side, in contrast to the relatively primitive means at the disposal of our ancestors, nature draws from an unlimited catalogue of tools it has developed as the universe's unchallenged engineer. It is like comparing the carving of a tool by humans at the Stone Age with the construction of the Space Shuttle by NASA engineers. On the other side, biologists have a tremendous advantage when compared with archeologists: The miracle of development occurs constantly around us giving us the opportunity to analyze it while it happens. Archeologists cannot send a camera team back in time in order to film the Egyptians while building the great Pyramids. Developmental biologists however start to have the possibility to record the cells while they perform morphogenetic processes leading to the formation of a living being.

We are presently entering a time in which key developmental processes will be capturable as they take place in their native environment. Thus, imaging provides a powerful testing ground for results from molecular investigations and a much-needed bridge between studies at different scales. *In vivo* live imaging is enabling biologists to move out of the culture dish into the real jungle of the living developing organism and to face the challenges of understanding morphogenesis as it happens inside the nascent embryo.

Materials and methods

Drosophila Strains and Genetics

Targeted gene expression was achieved using the Gal4/UAS system (Brand and Perrimon, 1993). A *btl-Gal4* strain, which drives *Gal4* expression in all tracheal cells to high levels from late stage 10 onwards, was kindly provided by Shigeo Hayashi (Shiga *et al.*, 1996); the *UAS-GFP-actin #2-2* strain was kindly provided by Vladislav V. Verkhusha (Verkhusha *et al.*, 1999). To facilitate the visualization of the actin cytoskeleton in the trachea a recombinant *btl-Gal4*, *UAS-GFP-actin/CyO* chromosome was generated. A *UAS-Src-GFP* line was kindly provided by Nicholas H. Brown and was used to highlight the membrane of tracheal cells (Kaltschmidt *et al.*, 2000). Adherens junctions were visualized using the *UAS-*Dα*-cat-GFP* lines kindly provided by Hiroki Oda (Oda and Tsukita, 1999a). As the *btl-Gal4, UAS-*Dα*-cat-GFP#3* recombinant from Oda *et al.* showed unspecific ectodermal expression, a new recombinant line was generated using the *UAS-*Dα*-cat-GFP#8* line. Tracheal nuclei were visualized using the *UAS-GFPN-lacZ (2-1)/CyO; btl-Gal4 (3-1)/TM3, Sb, Ser* line (Shiga *et al.*, 1996). Microtubuli were labeled using the *btl-Gal4, UAS-GFP-tau/CyO* line (Brand, 1995) provided by Ben Zion Shilo. *spalt* overexpression was achieved using the *UAS-salX; If/CyO, ftz-lacZ* line provided by Reinhard Schuh (Kuhnlein and Schuh, 1996). The second chromosome homozygous *UAS-tkv^{QD} 1A 8B3* line was provided by Theodor E. Haerry.

Dpp signaling was blocked cell autonomously using a homozygous *UAS-Dad* line on the second chromosome (Tsuneizumi *et al.*, 1997). When crossed to the *btl-Gal4*, *UAS-GFP-actin/CyO* line, all embryos with *GFP-actin* expression in the tracheal tree also expressed *Dad*.

Embryos lacking Dpp and Wnt signaling in trachea were generated by first crossing *arm^{XM19}* virgins to *btl-Gal4, UAS-*Dα*-cat-GFP#8* or *UAS-GFPN-lacZ (2-1)/CyO; btl-Gal4 (3-1)/TM3, Sb, Ser* males. Virgins carrying the *arm* allele and the reporter constructs were then crossed to a homozygous *UAS-Dad* line. Embryos lacking Dpp and Wnt signaling in trachea were recognized by the expression of the reporter constructs and the lack of dorsal trunk formation.

An *UAS-bnl* line was used to ectopically activate FGFR signaling (Sutherland *et al.*, 1996). The *trachealess* enhancer trap line *1-eve-1* was used to visualize the tracheal tree using conventional immunostaining methods (Perrimon *et al.*, 1991). The *kni-transgene/CyO;Df(3L)riXT1/TM2* line kindly provided by Reinhard Schuh (bearing a *kni* transgene on the second chromosome, that rescues the *kni* segmentation phenotype and the *kni* early tracheal phenotype) was used in this study (Chen *et al.*, 1998). *Df(3L)riXT1* is a deletion, which uncovers both *kni* and *knrl*.

The *punt^{P}* allele (Ruberte *et al.*, 1995), the *btl$^{H82\Delta3}$* allele (Klambt *et al.*, 1992), the *arm^{XM19}* (Peifer and Wieschaus, 1990), the *kay^{9B} (Riesgo-Escovar and Hafen, 1997)* and the *pnt$^{\Delta88}$* allele (Scholz *et al.*, 1993) were used.

Immunostainings and whole-mount in situ hybridization

The following primary antibodies were used: a tracheal lumen specific monoclonal antibody 2A12 (used at 1:5 dilution; kindly provided by N. Patel) and anti-β-Galactosidase (diluted 1:500; Promega). Embryos were fixed and immunostained according to (Patel, 1994) with minor modifications, followed by a secondary antibody conjugated with biotin or alkaline phosphatase. The distribution of the secondary antibody was revealed either by using horseradish peroxidase ABC kit (Vectastain) or by staining for alkaline phosphatase activity.

For confocal analysis, the signal was amplified. We used as secondary antibodies peroxidase-conjugated antibodies followed by biotinylated-tyramide (NEN Life Science Product), which is recognized by streptavidin-fluorescein or streptavidin-Texas Red. When performing fluorescent immunostainings using 2A12, IgG antibodies were hybridized before the 2A12 IgM antibody.

mRNA was detected by in situ hybridization to whole-mount embryos as described by (Tautz and Pfeifle, 1989) and (Hauptmann and Gerster, 2000) with minor modifications. In the case of double stainings, horseradish peroxidase stainings were performed after the alkaline phosphatase staining.

Embryo mounting for *in vivo* visualization

Embryos for *in vivo* visualization were mounted in two different ways.

Standard mounting of living embryos

After standard collection and dechorionation, embryos were washed with water and collected on a mesh. A drop of halocarbon oil (Voltalef 10s) was placed on a standard glass microscopy slide and embryos were transferred into the drop of oil using a standard laboratory spatula. To distribute the embryos evenly the embryos were mixed by stirring them in the drop using the spatula.

Two small coverslips were then slightly moisten and placed on the left and right side of the drop of oil to serve as spacers. A large coverslip was then gently placed over the oil and the coverslips and this setup was then imaged.

This was the first method used for *in vivo* visualization. It has the advantage to require only standard microscopy equipment and to be rapidly and easily usable. The embryos normally stay alive for at least two hours and can stay alive for over six hours. This is normally long enough for standard recordings and analysis. Especially, if no timelapse analyses have to be performed. For longer recordings however, this method is only of limited use. It has also been observed to induce artifacts in protein localizations,

which we have interpreted as hypoxia reactions (Valerie Petit unpublished observations). The activity of the actin cytoskeleton is however an excellent marker to asses if the embryos are still alive. No dynamics indicate that the embryo is dead.

Multiple factors affect the survival rate of the embryos. First, great care has to be taken not to overcrowd the slide. As easily visible when looking at two touching embryos the GFP luminosity tends to decrease at the point of contact indicating a competition for oxygen. One has also to take care not too use the laser beams at high intensity settings and not to scan at small intervals. Ideally, at least one minute of time is awaited before initiating the next scanning round. The survival rate can also be increased by previously saturating the oil with air. This is can be done by blowing air or oxygen through the oil for some hours before use.

"Hanging drop" mounting of living embryos

This method has several advantages over the standard mounting method. Foremost the fact that embryo survival is almost unaffected makes this a much superior method and it has completely replaced the standard method for our studies. It requires however a special support slide which has to be manufactured. This is however not a major hurdle as it is very easy to build.

For this method, embryos are prepared in the same way as for the standard method. A drop of halocarbon oil (Voltalef 10s) is placed on a large coverslip. The amount of oil should not be too big in order to avoid that it drips on the condenser of the microscope but enough to avoid drying of the embryos. The embryos are then transferred and evenly distributed on the coverslip. The oil has to be evenly distributed to cover the embryos. This preparation is then inverted and placed on a special support, which consists of a metal plate with a hole in the middle (Fig. 47). The plate should have the same dimensions as standard microscopy slides in order to fit on the microscope stage. The oil drop is placed into the hole of the support to allow for imaging. The coverslip can be fixed on the support using standard adhesive tape. One has to wait some minutes for the mounting medium to equilibrate in its drop-form in order to allow for imaging.

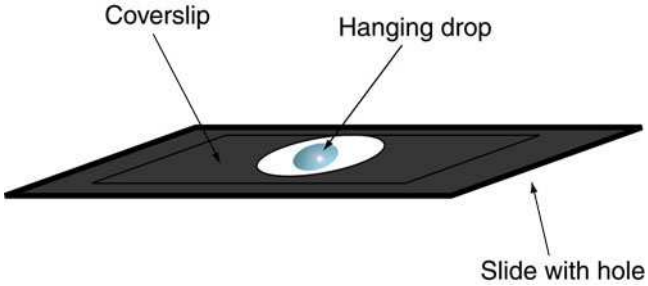

Figure 47 *Diagram of the hanging drop setup*

The great advantage of the hanging drop method is that the mounting medium has a large surface for oxygen exchange. Therefore, the amount of oxygen is not as limiting as in the standard method. Normally no lethality

with this method is observed. Great care has however to be taken not to spill oil into the microscope. We have never observed any hypoxic artifacts using this method. To decrease the likeliness of any lethality air saturated oil can be used.

Time-lapse Confocal Microscopy

Embryos expressing the *GFP* construct of interest were collected over night, dechorionated for three minutes using 3-4% chlorax and mounted in 10s Voltalef oil Images were collected on a Leica TCS SP2 confocal system using the Leica TCS NT software (Version 1.6.578) and the Leica Confocal Software (Version 2.00). For excitation the 488nm emission line of an Argon laser was (laser power was usually set between 20% and 40% on the laser box and at 100% in the scanning software). GFP emission was detected between 500nm and 570nm using a RSP 500 dichroic filter. Scans were performed at the highest available scan speed (fast2 in the 1.6 and bidirectional high scan speed in the 2.00 software). Time-lapse recordings using the version 1.6 software were performed using the Timelapse/ bleach function (in the settings menu). Time-lapse recordings using the version 2.0 software were performed in the XYZT mode using the time series function (not time-lapse function!).

For the studies in chapter 6 typically 20 to 30 focal sections were recorded for each time point (each averaged 4-8 times) with a spacing of 0.5 to 1.5 µm between each focal plane. This procedure was repeated with an interval of typically 2 minutes.

For the studies in chapter 7, the number focal sections were selected according to the number required for scanning the structure of interest. The spacing of the focal sections was chosen in order to comply with the critical sampling distance of the objective (see section on deconvolution). For the Detailed analysis of the transition from a multicellular to a unicellular tube, the focal plane was constantly readjusted after five time points to ensure that the structure of interest was not lost.

Deconvolution

Images were deconvoluted using Huygens Essential (Version 2.3.0) from SVI. For an overview on deconvolution, see the corresponding chapter of the introduction. Huygens Essential is an easy to use software, which deconvolutes microscopy images without the requirement of previously generating a PSF. Its wizard guides one through the processing steps, making its use very easy. One has only to be careful in collecting the images with a high enough sampling rate in order not to loose any image information and to enter the correct values into the wizard.

Image collection for deconvolution

In order to generate the PSF and for the subsequent deconvolution treatment the image data have to be collected without any loss of information (McNally *et al.*, 1999). The optical properties of the microscope define the maximal resolution one can achieve with the chosen setup. According to the information theorem of Nyquist, one can extract the maximal information available, by sampling the specimen at an interval, which is three times smaller than the maximal resolution of the optics. This sampling interval is called critical sampling distance. It is especially dependent on the imaging method used (widefield or confocal), the numerical aperture (NA) of the objectives as well as the excitation wavelength used. The Nyquist diagram nicely shows this dependencies (Fig. 48).

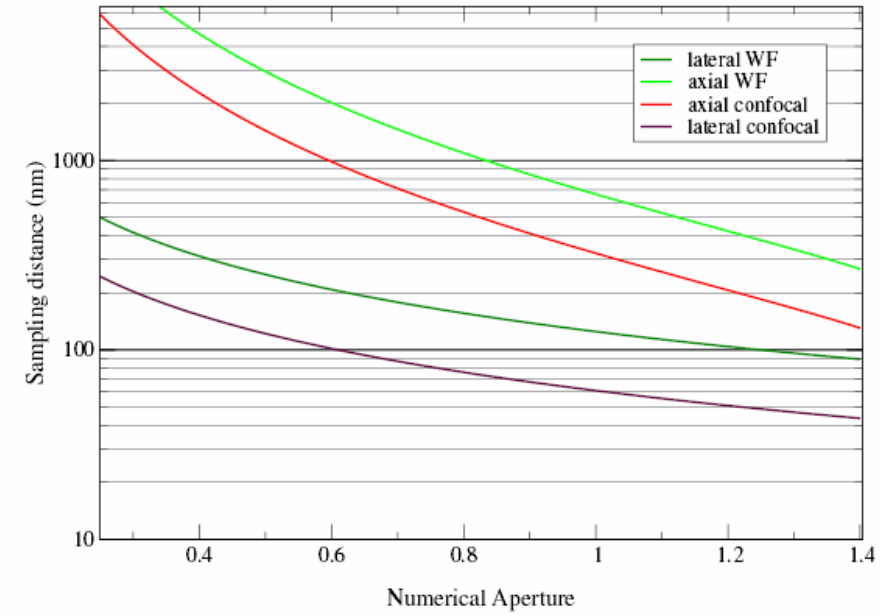

Figure 48 *Critical sampling distance versus NA.* The curves above show the critical sampling distance in axial and lateral directions for Widefield (WF) and confocal microscopes. The emission wavelength in the WF case was 500nm; the excitation wavelength in the confocal case is 488nm. From the Huygens Essential User Guide.

Due to limitations in the optics, the axial resolution (in z-axis) is always smaller than the lateral resolution (x- and y-axis). Taking samples at a smaller distance than the critical sampling distance is termed oversampling, while taking them at a greater distance is termed undersampling.

The robust Huygens algorithms generate acceptable results using slightly undersampled data but this should be avoided.

Deconvolution procedure using Huygens Essential

The wizard interface of Huygens Essential guides the user through the data entering process. These are normally correctly extracted from the microscope files. Due to constant changes in the file standards one should nevertheless control if the data are imported correctly. It is very important to enter the correct data as mistakes can lead to no convergence of the deconvolution algorithm or even the generation of artifacts.

The following procedure has to be followed to deconvolute an image of an embryo mounted according to the described procedures, expressing GFP and imaged using the Leica TCS NT setup of the cell biology department. For more information see the Huygens Essential User Guide or (McNally *et al.*, 1999).

Images are loaded into Huygens Essential by opening them from the running program or by dragging an image file of the stack of interest onto the program icon. Huygens Essential can load single stacks or complete time-lapse sequences. While the program has a system to manage large datasets from one time point (it will offer to deconvolute the image as bricks; accept this option and continue with the procedure) it does not have one for large time-lapse data sets. Therefore, depending on the memory of the used hardware the amount of time points, which can be processed, can vary. Usually ten to fifteen time points are no problem. For larger sets, the data can be reduced directly in Huygens Essential by selecting “time>select frames” from the launched cropper (is launched by selecting “Image>launch cropper”) or using an image processing software (*e.g.* Imaris).

In the first window of the wizard, the microscope type (normally “confocal”), the numerical aperture of the used objective (see Table 5) as well as the refractive index of the lens medium (0 for air and 1.518 for immersion oil) and the mounting medium (1.410 for Voltalef 10s) are entered.

Objective	NA
HC PL APO 10x	0.40
HC PL APO 20x	0.70
HCX PL APO 40x	0.85
PL APO 100x oil	1.4-0.7

Table 5 *NA of our objectives.*

In the second window, additional optical parameters are defined. The voxel and pinhole dimensions are normally correct but should be checked. They correspond to the sampling resolution, defined when recording the image. If a number is marked in yellow, the image is

undersampled in that dimension, while red indicates heavy undersampling. For GFP the excitation and emission wavelengths should be corrected to, 488 nm for the excitation and to 510nm for the emission wavelength.

The following image histogram is of no practical use and can be skipped without special notice.

In the last step, the background has to be defined. Huygens Essential uses this information to subtract the noise from the image information. This setting has strong effects on the efficiency of the deconvolution algorithm. The more background one selects the less information will have to be processed by the algorithm. If too many pixels are subtracted, real information will be lost. Unfortunately, the different algorithms Huygens Essential uses to calculate the background, perform very poorly and most times a too low background value is calculated (maybe a conservative value is chosen in order not to loose any information). This value however can be changed. To do so, double click on the upper panel representing your loaded images. Select an area of the image that only shows background, and move your mouse over that area. The intensity of the voxels in that area is displayed below the image and is used to estimate the background. Normally, I take the average of the values and divide it by two or three. This step however requires some experience. Have the program estimate the background without modifying the settings. In the result window though replace the calculated value (usually 0) by your estimate. For very good images, I usually use a value of 5, for normal images a value of 10 and for noisy images a value of 20.

Now the program has all the optical information required to begin with the deconvolution. Before running the algorithm, it will now ask you to define the parameters for the calculations.

First Huygens asks at which step the process should be stopped in case the iterative calculations do not converge (*i.e.* do not reach a satisfying quality). Images that reach that limit can still be of use, even if the calculations did not reach their optimum. In very rare cases, when using very difficult data sets, this number can be increased in order to give the program more time to find a satisfactory solution. This is however very rare and therefore this value is normally left unchanged.

The signal to noise (S/N) ratio, defines the overall quality of the input data. A very noisy image gets a value around 10, moderately noisy images between 10 and 20 and very good images a value above 20. This is a very important setting as it defines the accuracy with which the program treats every voxel. If the S/N value is set very low, the algorithm will tend to neglect problematic information. Like this, the algorithm minimizes the danger of introducing artifacts by treating erroneous information. Clearly, this leads to a lower quality deconvolution and a slightly blurred result. It is however, wise to use this value with a certain respect as an overestimate can seriously affect the efficiency of the algorithm and dramatically delay the convergence, while introducing artifacts into the image. Normally, I set a value of 15 for our data. Good images get a value of 20 or as a maximum 25 (integrated, high signal to noise images, recorded with the oil immersion objective).

Next, the quality threshold is defined. This is the interval, the algorithm uses

to decide if it has reached the convergence point. During deconvolution, Huygens Essential computes a quality value for the newly calculated image. This image is then retreated and a new quality value is calculated. If two quality values in a row present a difference that is lower than the defined threshold, the algorithm decides that it has converged and that the image cannot be further improved. Usually, 0.1 is a very sensitive value and this setting can therefore be left unaltered. If an image of even better quality is desired this number can be reduced. This is however no guarantee for a better result.

The iteration mode defines the accuracy and performance of the algorithm. This value is usually left on the fast mode.

Bleaching correction is only applicable when treating time-lapse data. As GFP normally shows no bleaching when correctly imaged and this correction can seriously slow down the deconvolution process, we tend to turn off the bleaching correction. When treating longer, short-interval time-lapse data, it can however be advisable to turn on the bleaching correction.

After setting all these parameters, the calculations can be initiated. This may take from some minutes to some hours. It is advisable to observe the progression of the image treatment and to stop the algorithm if one observes that no convergence occurs or that a serious deterioration instead of an improvement is achieved. In these cases stop the algorithm and change some of the parameters. If this does not change, the behavior of the algorithm the image is not suited for deconvolution (for example due to undersampling or wrong optical parameters).

When the deconvolution job is finished, the treated image appears as a new window beside the loaded image in the upper part of the program. The result can be inspected by double clicking the new window. The viewer appears as a split window. By clicking on the name above one of the two parts of the window, the original image can be loaded and thereby the original and the treated images can be compared.

If one want to save the treated image, one can click on the window representing it and select “save as” from the file menu. Alternatively, the “accept” button can be pressed. We always save the images in the Imaris format.

If one is not satisfied with the result, one can click on the “again” button to restart the process.

Huygens Essential allows the easy and fast deconvolution of almost all correctly recorded samples. As the increase in quality is spectacular, we deconvolute almost all collected images. In 90% of the cases, the use of Huygens Essential requires only the input of the standard parameters and therefore almost no knowledge on the details of the procedure.

In addition, it affects the way we collect our data by giving us more flexibility in the constructs we can use and the recording parameters. As it eliminates almost all background signal and significantly improves the contrast and resolution, one can use very weak constructs and high photomultiplier settings while avoiding high intensity laser illuminations. One can also improve the temporal resolution of the timelapse data, as almost no

integration is needed and less recovery time is required due to the lower laser intensity used.

3D and 4D Reconstructions

For the studies in chapter 6, images from the Leica TCS NT software (Version 1.6.578) were subsequently processed using the Imaris 2.7 software (Bitplane) running on a Silicon Graphics O_2 workstation. Images were manually cropped into single stacks representing each time point, treated to reduce the background noise and 3D reconstructed using the Shadow Projection function of this software. For some images, the same procedure was performed using the Easy 3D and Full 3D functions of the Imaris 3.0.6 software (Bitplane). The 3D reconstructed images were treated with the Photoshop 5.5 software (Adobe) and time-lapse series were assembled using the Premiere 6.0 software (Adobe).

For the studies in chapter 7, images from the Leica Confocal Software (Version 2.00) were deconvoluted using the Huygens Essential software (SVI) (see section on deconvolution) and subsequently processed using the Imaris 3.3.0 software (Bitplane) or the Volocity 1.6 to 2.0 software (Improvision) running on a desktop PC. Maximum intensity projections were produced using the easy 3D function of Imaris 3.3.0. Volumetric reconstructions were produced using the Surpass module of Imaris 3.3.0. Cell outlines were visualized by generating an IsoSurface using a threshold of 1 with the resampling and smoothing options turned on. AJs were visualized by generating an IsoSurface using a threshold corresponding to the average intensity of the D*α-Cat-GFP* signal with the resampling and smoothing options turned off. Time-lapse series were assembled directly in Imaris and then processed using the Premiere 6.0 software (Adobe). Stills were treated with the Photoshop 5.5 software (Adobe). Volocity was mainly used to interactively analyze the time-lapse data and to generate interactive 3D Quicktime Virtual Reality models. Volocity movies were generated using the movie sequence function. 3D Quicktime Virtual Reality models were generated by selecting Create QTVR Movie in the Render menu.

Cell dissociation

Embryos from an overnight collection were dechorionated using 3-4% chlorax for 3-5 minutes, collected on a mesh and rinsed thoroughly with H_2O.

Embryos were transferred into a 15 ml polystyrene tube containing 1ml of 10x Trypsin-EDTA which contains 5g Porcine Trypsin and 0.2 g EDTA per liter in 0.9% NaCl. Afterwards the suspension was passed approximately 10 times through a 27 ½ G needle and a 1ml syringe to “break up” the embryos in order to make the embryonic cells accessible to the Trypsin. Then the treated suspension was incubated at 25º C for an hour on a shaker running at 800 rpm.

Following steps were performed at 4ºC. After incubation, cells were homogenized by passing again

approximately 30 times through a 27 ½ G needle and a 1ml syringe. This suspension was pressed through a cell strainer with a mesh diameter of 40 µm and pelleted at 188 g (1000 rpm on a Heraeus Megafuge 10R) for 5 minutes. The supernatant was subsequently discarded and the pellet was gently resuspended in PBS and 2mM EDTA. This suspension was refiltered using the same cell strainer with a 40µm mesh diameter to remove any clumps left, which could cause problems in the FACS procedure.

After the cell sorting, the highly diluted cell suspension was transferred to a coated 15 ml polystyrene round bottom tube. The coating was performed by incubating the tube O/N at 4ºC on a rotating rotor using ~2 ml of a PBS, 10% FCS and 2mM EDTA solution which was removed after coating. This treatment is important to prevent the cells from sticking to the tube, which would greatly reduce the amount of recovered cells. The cells are then centrifuged at 999 g (2400 rpm on an Heraeus Megafuge 10R) for 5 minutes and the supernatant is removed VERY CAREFULLY. The pellet is immediately resuspended in 800 µl of Trizol and frozen at –70℃ or directly used to extract RNA.

Total RNA extraction from limited amount of material (according to Lydia Michaut)

Remember that extreme care has to be taken to work in an RNAse free environment.

Material was homogenized by passing multiple times through a G27 ¾ needle using a 1ml syringe. 10µg of Glycogen were added (1µl of a 20mg/ml stock) and the mix incubated for 5 minutes at room temperature. After adding 160 µl of chloroform the mix was vigorously shaken by hand for 15 seconds, incubated for 3 minutes at room temperature and then centrifuged at maximum speed on a table centrifuge for 15 minutes at 4℃. The colorless upper phase was then transferred to a fresh tube and 400 µl of isopropanol were added. This mixture was then incubated at room temperature for 15 minutes and afterwards centrifuged on a table centrifuge at 4° C at maximum speed for 10 minutes. The pellet was washed with 800 µl 75% ethanol, mixed by vortexing and centrifuged for 5 minutes at 4° C at 7500 rpm. The pellet was dried (not too long!) and resuspended in 10µl DEPC water. To facilitate the resuspension of the sample the suspension was heated up to 65° C for 5 minutes and vortexed vigorously.

Embryo collection and RNA extraction for array analysis

btl-Gal4/ UAS-Dad and *btl-Gal4/ UAS-tkv^{QD}* embryos were staged by performing a one-hour precollection and a one-hour subsequent collection, after which embryos were allowed to develop for an additional nine hours before they were transferred to Trizol, homogenized and frozen at -70℃. For each RNA isolation, this procedure was performed on different days, with flies from independent crosses, to

minimize the influence of external experimental effects.

Total RNA from these embryos was then extracted in parallel on the same day (see before) and analyzed on the Agilent 2100 Bioanalyzer using the RNA 6000 kit. 20 μg from samples that showed no degradation were used to perform the labeling reaction. Four samples from the *btl-Gal4/ UAS-Dad* and four samples from the *btl-Gal4/ UAS-tkv^{QD}* crosses were chosen for the experiment.

High-density oligonucleotide arrays and hybridization

In this study, a custom-designed Drosophila oligonucleotide array (roDROMEGAa, Affymetrix, Santa Clara, CA) was used (Montalta-He *et al.*, 2002). It contains 14,090 sequences representing Drosophila-specific transcripts, prokaryotic control sequences and custom chosen sequences for transgenes such as *Gal4*, *GFP*, and *lacZ*. Of the sequences included, 13,998 correspond to *Drosophila* specific transcripts annotated by Celera Genome Release 1 (Adams *et al.*, 2000) and deposited in SWISS-PROT/TrEMBL databases. These 13,998 sequences represent approximately 13,400 genes in the *Drosophila* genome and therefore some genes are represented by more than one probe set. Each sequence is represented on the array by a set of 14 oligonucleotide probes (25mers) matching the sequence. To control the specificity of hybridization, the same probes are represented on the array with a single nucleotide mismatch in a central position. As such, each sequence is represented by 14 perfect match and 14 mismatch probes. The average difference (Avg Diff) between the perfect-match hybridization signal and the mismatch signal is proportional to the abundance of a given transcript. RNA was labeled, and hybridized to the arrays as described (Egger *et al.*, 2002; Leemans *et al.*, 2000; Montalta-He *et al.*, 2002) with minor modifications.

Data analysis

Probe arrays were scanned with a commercial confocal laser scanner (Hewlett-Packard). Pixel intensities were measured, and expression signals were analyzed with commercial software (GENECHIP 3.1, Affymetrix). Data processing was carried out using RACE-A (F. Hoffmann-La Roche), Access97 and Excel 97 (Microsoft) software. For quantification of relative transcript abundance, Avg Diff value was used. Four replicates were carried out for each experimental condition. All arrays were normalized against the mean of the total sums of Avg Diff values across all 8 arrays. In order to avoid huge fold changes, genes with a normalized Avg Diff below 20 were automatically assigned an Avg Diff of 20 (RACE-A protocol). An unpaired t-test for each individual gene was carried out. For differential transcript imaging, only transcripts that had highly significant or significant changes in Avg Diff ($P \leq 0.01$ and $P \leq 0.01$, respectively) and whose changes were in the twofold and above range are presented. Additionally, the higher

mean Avg Diff of a pairwise comparison for a given transcript had to be above or equal to 50.

References

(1998). Genome sequence of the nematode C. elegans: a platform for investigating biology. The C. elegans Sequencing Consortium. Science *282*, 2012-2018.

Adams, J. C., Seed, B., and Lawler, J. (1998). Muskelin, a novel intracellular mediator of cell adhesive and cytoskeletal responses to thrombospondin-1. Embo J *17*, 4964-4974.

Adams, M. D., Celniker, S. E., Holt, R. A., Evans, C. A., Gocayne, J. D., Amanatides, P. G., Scherer, S. E., Li, P. W., Hoskins, R. A., Galle, R. F.*, et al.* (2000). The genome sequence of Drosophila melanogaster. Science *287*, 2185-2195.

Affolter, M., Bellusci, S., Itoh, N., Shilo, B., Thiery, J. P., and Werb, Z. (2003). Tube or not tube. Remodeling epithelial tissues by branching morphogenesis. Dev Cell *4*, 11-18.

Affolter, M., and Mann, R. (2001). Development. Legs, eyes, or wings--selectors and signals make the difference. Science *292*, 1080-1081.

Affolter, M., Montagne, J., Walldorf, U., Groppe, J., Kloter, U., LaRosa, M., and Gehring, W. J. (1994a). The Drosophila SRF homolog is expressed in a subset of tracheal cells and maps within a genomic region required for tracheal development. Development *120*, 743-753.

Affolter, M., Nellen, D., Nussbaumer, U., and Basler, K. (1994b). Multiple requirements for the receptor serine/threonine kinase thick veins reveal novel functions of TGF beta homologs during Drosophila embryogenesis. Development *120*, 3105-3117.

Affolter, M., and Shilo, B. Z. (2000). Genetic control of branching morphogenesis during Drosophila tracheal development. Curr Opin Cell Biol *12*, 731-735.

Ahmad, S. M., and Baker, B. S. (2002). Sex-specific deployment of FGF signaling in Drosophila recruits mesodermal cells into the male genital imaginal disc. Cell *109*, 651-661.

Amano, M., Ito, M., Kimura, K., Fukata, Y., Chihara, K., Nakano, T., Matsuura, Y., and Kaibuchi, K. (1996). Phosphorylation and activation of myosin by Rho-associated kinase (Rho-kinase). J Biol Chem *271*, 20246-20249.

Amos, B. (2000). Lessons from the history of light microscopy. Nat Cell Biol *2*, E151-152.

Anderson, M. G., Perkins, G. L., Chittick, P., Shrigley, R. J., and Johnson, W. A. (1995). drifter, a Drosophila POU-domain transcription factor, is required for correct differentiation and migration of tracheal cells and midline glia. Genes Dev *9*, 123-137.

Bagrodia, S., and Cerione, R. A. (1999). Pak to the future. Trends Cell Biol *9*, 350-355.

Beccari, S., Teixeira, L., and Rorth, P. (2002). The JAK/STAT pathway is required for border cell migration during Drosophila oogenesis. Mech Dev *111*, 115-123.

Beiman, M., Shilo, B. Z., and Volk, T. (1996). Heartless, a Drosophila FGF receptor homolog, is essential for cell migration and establishment of several mesodermal lineages. Genes Dev *10*, 2993-3002.

Beitel, G. J., and Krasnow, M. A. (2000). Genetic control of epithelial tube size in the Drosophila tracheal system. Development *127*, 3271-3282.

Bellen, H. J., O'Kane, C. J., Wilson, C., Grossniklaus, U., Pearson, R. K., and Gehring, W. J. (1989). P-element-mediated enhancer detection: a versatile method to study development in Drosophila. Genes Dev *3*, 1288-1300.

Bilder, D. (2001). PDZ proteins and polarity: functions from the fly. Trends Genet *17*, 511-519.

Bishop, A. L., and Hall, A. (2000). Rho GTPases and their effector proteins. Biochem J *348 Pt 2*, 241-255.

Bloor, J. W., and Kiehart, D. P. (2002). Drosophila RhoA regulates the cytoskeleton and cell-cell adhesion in the developing epidermis. Development *129*, 3173-3183.

Boube, M., Llimargas, M., and Casanova, J. (2000). Cross-regulatory interactions among tracheal genes support a co-operative model for the induction of tracheal fates in the Drosophila embryo. Mech Dev *91*, 271-278.

Boube, M., Martin-Bermudo, M. D., Brown, N. H., and Casanova, J. (2001). Specific tracheal migration is mediated by complementary expression of cell surface proteins. Genes Dev *15*, 1554-1562.

Brand, A. (1995). GFP in Drosophila. Trends Genet *11*, 324-325.

Brand, A. H., and Perrimon, N. (1993). Targeted gene expression as a means of altering cell fates and generating dominant phenotypes. Development *118*, 401-415.

Bretscher, M. S., and Aguado-Velasco, C. (1998). Membrane traffic during cell locomotion. Curr Opin Cell Biol *10*, 537-541.

Brown, S., Hu, N., and Hombria, J. C. (2001). Identification of the first invertebrate interleukin JAK/STAT receptor, the Drosophila gene domeless. Curr Biol *11*, 1700-1705.

Bryant, Z., Subrahmanyan, L., Tworoger, M., LaTray, L., Liu, C. R., Li, M. J., van den Engh, G., and Ruohola-Baker, H. (1999). Characterization of differentially expressed genes in purified Drosophila follicle cells: toward a general strategy for cell type-specific developmental analysis. Proc Natl Acad Sci U S A *96*, 5559-5564.

Campbell, G., Weaver, T., and Tomlinson, A. (1993). Axis specification in the developing Drosophila appendage: the role of wingless, decapentaplegic, and the homeobox gene aristaless. Cell *74*, 1113-1123.

Campbell, R. E., Tour, O., Palmer, A. E., Steinbach, P. A., Baird, G. S., Zacharias, D. A., and Tsien, R. Y. (2002). A monomeric red fluorescent protein. Proc Natl Acad Sci U S A *99*, 7877-7882.

Chen, C. K., Kuhnlein, R. P., Eulenberg, K. G., Vincent, S., Affolter, M., and Schuh, R. (1998). The transcription factors KNIRPS and KNIRPS RELATED control cell migration and branch morphogenesis during Drosophila tracheal development. Development *125*, 4959-4968.

Chen, H. W., Chen, X., Oh, S. W., Marinissen, M. J., Gutkind, J. S., and Hou, S. X. (2002). mom identifies a receptor for the Drosophila JAK/STAT signal transduction pathway and encodes a protein distantly related to the mammalian cytokine receptor family. Genes Dev *16*, 388-398.

Chihara, T., and Hayashi, S. (2000). Control of tracheal tubulogenesis by Wingless signaling. Development *127*, 4433-4442.

Cho, N. K., Keyes, L., Johnson, E., Heller, J., Ryner, L., Karim, F., and Krasnow, M. A. (2002). Developmental control of blood cell migration by the Drosophila VEGF pathway. Cell *108*, 865-876.

Chung, C. Y., Funamoto, S., and Firtel, R. A. (2001). Signaling pathways controlling cell polarity and chemotaxis. Trends Biochem Sci *26*, 557-566.

Consortium, T. F. (2003). The FlyBase database of the Drosophila genome projects and community literature. Nucleic Acids Res *31*, 172-175.

Cooper, J. A., and Schafer, D. A. (2000). Control of actin assembly and disassembly at filament ends. Curr Opin Cell Biol *12*, 97-103.

Critchley, D. R. (2000). Focal adhesions - the cytoskeletal connection. Curr Opin Cell Biol *12*, 133-139.

Curtiss, J., Halder, G., and Mlodzik, M. (2002). Selector and signalling molecules cooperate in organ patterning. Nat Cell Biol *4*, E48-51.

de Celis, J. F., Llimargas, M., and Casanova, J. (1995). Ventral veinless, the gene encoding the Cf1a transcription factor, links positional information and cell differentiation during embryonic and imaginal development in Drosophila melanogaster. Development *121*, 3405-3416.

de Curtis, I. (2001). Cell migration: GAPs between membrane traffic and the cytoskeleton. EMBO Rep *2*, 277-281.

Dickinson, M. E., Bearman, G., Tilie, S., Lansford, R., and Fraser, S. E. (2001). Multi-spectral imaging and linear unmixing add a whole new dimension to laser scanning fluorescence microscopy. Biotechniques *31*, 1272, 1274-1276, 1278.

Dickson, B., and Hafen, E. (1994). Genetics of signal transduction in invertebrates. Curr Opin Genet Dev *4*, 64-70.

Dossenbach, C., Rock, S., and Affolter, M. (2001). Specificity of FGF signaling in cell migration in Drosophila. Development *128*, 4563-4572.

Duchek, P., and Rorth, P. (2001). Guidance of cell migration by EGF receptor signaling during Drosophila oogenesis. Science *291*, 131-133.

Duchek, P., Somogyi, K., Jekely, G., Beccari, S., and Rorth, P. (2001). Guidance of cell migration by the Drosophila PDGF/VEGF receptor. Cell *107*, 17-26.

Egger, B., Leemans, R., Loop, T., Kammermeier, L., Fan, Y., Radimerski, T., Strahm, M. C., Certa, U., and Reichert, H. (2002). Gliogenesis in Drosophila: genome-wide analysis of downstream genes of glial cells missing in the embryonic nervous system. Development *129*, 3295-3309.

Englund, C., Steneberg, P., Falileeva, L., Xylourgidis, N., and Samakovlis, C. (2002). Attractive and repulsive functions of Slit are mediated by different receptors in the Drosophila trachea. Development *129*, 4941-4951.

Fehon, R. G., Oren, T., LaJeunesse, D. R., Melby, T. E., and McCartney, B. M. (1997). Isolation of mutations in the Drosophila homologues of the human Neurofibromatosis 2 and yeast CDC42 genes using a simple and efficient reverse-genetic method. Genetics *146*, 245-252.

Fodor, S. P., Read, J. L., Pirrung, M. C., Stryer, L., Lu, A. T., and Solas, D. (1991). Light-directed, spatially addressable parallel chemical synthesis. Science *251*, 767-773.

Franch-Marro, X., and Casanova, J. (2000). The alternative migratory pathways of the Drosophila tracheal cells are associated with distinct subsets of mesodermal cells. Dev Biol *227*, 80-90.

Franch-Marro, X., and Casanova, J. (2002). spalt-induced specification of distinct dorsal and ventral domains is required for Drosophila tracheal patterning. Dev Biol *250*, 374-382.

Freeman, M. (1997). Cell determination strategies in the Drosophila eye. Development *124*, 261-270.

Fulga, T. A., and Rorth, P. (2002). Invasive cell migration is initiated by guided growth of long cellular extensions. Nat Cell Biol *4*, 715-719.

Gabay, L., Seger, R., and Shilo, B. Z. (1997). MAP kinase in situ activation atlas during Drosophila embryogenesis. Development *124*, 3535-3541.

Gehring, W. J. (1998). Master control genes in development and evolution : the homeobox story (New Haven, Yale University Press).

Geisbrecht, E. R., and Montell, D. J. (2002). Myosin VI is required for E-cadherin-mediated border cell migration. Nat Cell Biol *4*, 616-620.

Gisselbrecht, S., Skeath, J. B., Doe, C. Q., and Michelson, A. M. (1996). heartless encodes a fibroblast growth factor receptor (DFR1/DFGF-R2) involved in the

directional migration of early mesodermal cells in the Drosophila embryo. Genes Dev *10*, 3003-3017.

Glazer, L., and Shilo, B. Z. (1991). The Drosophila FGF-R homolog is expressed in the embryonic tracheal system and appears to be required for directed tracheal cell extension. Genes Dev *5*, 697-705.

Glazer, L., and Shilo, B. Z. (2001). Hedgehog signaling patterns the tracheal branches. Development *128*, 1599-1606.

Golic, K. G., and Lindquist, S. (1989). The FLP recombinase of yeast catalyzes site-specific recombination in the Drosophila genome. Cell *59*, 499-509.

Gordon, G. W., Berry, G., Liang, X. H., Levine, B., and Herman, B. (1998). Quantitative fluorescence resonance energy transfer measurements using fluorescence microscopy. Biophys J *74*, 2702-2713.

Guillemin, K., Groppe, J., Ducker, K., Treisman, R., Hafen, E., Affolter, M., and Krasnow, M. A. (1996). The pruned gene encodes the Drosophila serum response factor and regulates cytoplasmic outgrowth during terminal branching of the tracheal system. Development *122*, 1353-1362.

Gupta, T., and Schupbach, T. (2001). Two signals are better than one: border cell migration in Drosophila. Dev Cell *1*, 443-445.

Gurskaya, N. G., Fradkov, A. F., Terskikh, A., Matz, M. V., Labas, Y. A., Martynov, V. I., Yanushevich, Y. G., Lukyanov, K. A., and Lukyanov, S. A. (2001). GFP-like chromoproteins as a source of far-red fluorescent proteins. FEBS Lett *507*, 16-20.

Hafen, E., Basler, K., Edstroem, J. E., and Rubin, G. M. (1987). Sevenless, a cell-specific homeotic gene of Drosophila, encodes a putative transmembrane receptor with a tyrosine kinase domain. Science *236*, 55-63.

Hall, A. (1994). Small GTP-binding proteins and the regulation of the actin cytoskeleton. Annu Rev Cell Biol *10*, 31-54.

Harris, H. (1995). The cells of the body : a history of somatic cell genetics (Cold Spring Harbor, NY, Cold Spring Harbor Laboratory Press).

Hauptmann, G., and Gerster, T. (2000). Multicolor whole-mount in situ hybridization. Methods Mol Biol *137*, 139-148.

Heim, R., Prasher, D. C., and Tsien, R. Y. (1994). Wavelength mutations and posttranslational autoxidation of green fluorescent protein. Proc Natl Acad Sci U S A *91*, 12501-12504.

Heino, T. I., Karpanen, T., Wahlstrom, G., Pulkkinen, M., Eriksson, U., Alitalo, K., and Roos, C. (2001). The Drosophila VEGF receptor homolog is expressed in hemocytes. Mech Dev *109*, 69-77.

Hing, H., Xiao, J., Harden, N., Lim, L., and Zipursky, S. L. (1999). Pak functions downstream of Dock to regulate photoreceptor axon guidance in Drosophila. Cell *97*, 853-863.

Hoffmann, R., Seidl, T., Neeb, M., Rolink, A., and Melchers, F. (2002). Changes in gene expression profiles in developing B cells of murine bone marrow. Genome Res *12*, 98-111.

Hogan, B. L., and Kolodziej, P. A. (2002). Organogenesis: molecular mechanisms of tubulogenesis. Nat Rev Genet *3*, 513-523.

Hotchin, N. A., and Hall, A. (1995). The assembly of integrin adhesion complexes requires both extracellular matrix and intracellular rho/rac GTPases. J Cell Biol *131*, 1857-1865.

Huttenlocher, A., Ginsberg, M. H., and Horwitz, A. F. (1996). Modulation of cell migration by integrin-mediated cytoskeletal linkages and ligand-binding affinity. J Cell Biol *134*, 1551-1562.

Iijima, M., Huang, Y. E., and Devreotes, P. (2002). Temporal and spatial regulation of chemotaxis. Dev Cell *3*, 469-478.

Imam, F., Sutherland, D., Huang, W., and Krasnow, M. A. (1999). stumps, a Drosophila gene required for fibroblast growth factor (FGF)-directed migrations of tracheal and mesodermal cells. Genetics *152*, 307-318.

Isaac, D. D., and Andrew, D. J. (1996). Tubulogenesis in Drosophila: a requirement for the trachealess gene product. Genes Dev *10*, 103-117.

Jacinto, A., Martinez-Arias, A., and Martin, P. (2001). Mechanisms of epithelial fusion and repair. Nat Cell Biol *3*, E117-123.

Jacinto, A., Wood, W., Balayo, T., Turmaine, M., Martinez-Arias, A., and Martin, P. (2000). Dynamic actin-based epithelial adhesion and cell matching during Drosophila dorsal closure. Curr Biol *10*, 1420-1426.

Jacinto, A., Wood, W., Woolner, S., Hiley, C., Turner, L., Wilson, C., Martinez-Arias, A., and Martin, P. (2002). Dynamic analysis of actin cable function during Drosophila dorsal closure. Curr Biol *12*, 1245-1250.

Jaglarz, M. K., and Howard, K. R. (1995). The active migration of Drosophila primordial germ cells. Development *121*, 3495-3503.

Jarecki, J., Johnson, E., and Krasnow, M. A. (1999). Oxygen regulation of airway branching in Drosophila is mediated by Branchless FGF. Cell *99*, 211-220.

Jasper, H., Benes, V., Atzberger, A., Sauer, S., Ansorge, W., and Bohmann, D. (2002). A genomic switch at the transition from cell proliferation to terminal differentiation in the Drosophila eye. Dev Cell *3*, 511-521.

Jockusch, B. M., Bubeck, P., Giehl, K., Kroemker, M., Moschner, J., Rothkegel, M., Rudiger, M., Schluter, K., Stanke, G., and Winkler, J. (1995). The molecular architecture of focal adhesions. Annu Rev Cell Dev Biol *11*, 379-416.

Kaltschmidt, J. A., and Brand, A. H. (2002). Asymmetric cell division: microtubule dynamics and spindle asymmetry. J Cell Sci *115*, 2257-2264.

Kaltschmidt, J. A., Davidson, C. M., Brown, N. H., and Brand, A. H. (2000). Rotation and asymmetry of the mitotic spindle direct asymmetric cell division in the developing central nervous system. Nat Cell Biol *2*, 7-12.

Keely, P. J., Westwick, J. K., Whitehead, I. P., Der, C. J., and Parise, L. V. (1997). Cdc42 and Rac1 induce integrin-mediated cell motility and invasiveness through PI(3)K. Nature *390*, 632-636.

Keller, R., Davidson, L., Edlund, A., Elul, T., Ezin, M., Shook, D., and Skoglund, P. (2000). Mechanisms of convergence and extension by cell intercalation. Philos Trans R Soc Lond B Biol Sci *355*, 897-922.

Kiehart, D. P., Galbraith, C. G., Edwards, K. A., Rickoll, W. L., and Montague, R. A. (2000). Multiple forces contribute to cell sheet morphogenesis for dorsal closure in Drosophila. J Cell Biol *149*, 471-490.

Kim, A. S., Kakalis, L. T., Abdul-Manan, N., Liu, G. A., and Rosen, M. K. (2000). Autoinhibition and activation mechanisms of the Wiskott-Aldrich syndrome protein. Nature *404*, 151-158.

Kimura, K., Ito, M., Amano, M., Chihara, K., Fukata, Y., Nakafuku, M., Yamamori, B., Feng, J., Nakano, T., Okawa, K.*, et al.* (1996). Regulation of myosin phosphatase by Rho and Rho-associated kinase (Rho-kinase). Science *273*, 245-248.

Klambt, C., Glazer, L., and Shilo, B. Z. (1992). breathless, a Drosophila FGF receptor homolog, is essential for migration of tracheal and specific midline glial cells. Genes Dev *6*, 1668-1678.

Knight, J. (2001). When the chips are down. Nature *410*, 860-861.

Knust, E., and Bossinger, O. (2002). Composition and formation of intercellular junctions in epithelial cells. Science *298*, 1955-1959.

Krasnow, M. A., Cumberledge, S., Manning, G., Herzenberg, L. A., and Nolan, G. P. (1991). Whole animal cell sorting of Drosophila embryos. Science *251*, 81-85.

Kuhnlein, R. P., and Schuh, R. (1996). Dual function of the region-specific homeotic gene spalt during Drosophila tracheal system development. Development *122*, 2215-2223.

Lauffenburger, D. A., and Horwitz, A. F. (1996). Cell migration: a physically integrated molecular process. Cell *84*, 359-369.

Lecuit, T., Samanta, R., and Wieschaus, E. (2002). slam encodes a developmental regulator of polarized membrane growth during cleavage of the Drosophila embryo. Dev Cell *2*, 425-436.

Lecuit, T., and Wieschaus, E. (2002). Junctions as organizing centers in epithelial cells? A fly perspective. Traffic *3*, 92-97.

Leemans, R., Egger, B., Loop, T., Kammermeier, L., He, H., Hartmann, B., Certa, U., Hirth, F., and Reichert, H. (2000). Quantitative transcript imaging in normal and heat-shocked drosophila embryos by using high-density oligonucleotide arrays [In Process Citation]. Proc Natl Acad Sci U S A *97*, 12138-12143.

Leung, Y. F., Lam, D. S., and Pang, C. P. (2001). The miracle of microarray data analysis. Genome Biol *2*, REPORTS4021.

Lewis, E. B. (1978). A gene complex controlling segmentation in Drosophila. Nature *276*, 565-570.

Lichtman, J. W., and Fraser, S. E. (2001). The neuronal naturalist: watching neurons in their native habitat. Nat Neurosci *4 Suppl*, 1215-1220.

Lin, M. Z., and Greenberg, M. E. (2000). Orchestral maneuvers in the axon: trio and the control of axon guidance. cell *101*, 239-242.

Lin, X., Buff, E. M., Perrimon, N., and Michelson, A. M. (1999). Heparan sulfate proteoglycans are essential for FGF receptor signaling during Drosophila embryonic development. Development *126*, 3715-3723.

Lippincott-Schwartz, J., Snapp, E., and Kenworthy, A. (2001). Studying protein dynamics in living cells. Nat Rev Mol Cell Biol *2*, 444-456.

Lipshutz, R. J., Fodor, S. P., Gingeras, T. R., and Lockhart, D. J. (1999). High density synthetic oligonucleotide arrays. Nat Genet *21*, 20-24.

Llimargas, M. (2000). Wingless and its signalling pathway have common and separable functions during tracheal development. Development *127*, 4407-4417.

Llimargas, M., and Casanova, J. (1997). ventral veinless, a POU domain transcription factor, regulates different transduction pathways required for tracheal branching in Drosophila. Development *124*, 3273-3281.

Llimargas, M., and Casanova, J. (1999). EGF signalling regulates cell invagination as well as cell migration during formation of tracheal system in Drosophila. Dev Genes Evol *209*, 174-179.

Lockhart, D. J., Dong, H., Byrne, M. C., Follettie, M. T., Gallo, M. V., Chee, M. S., Mittmann, M., Wang, C., Kobayashi, M., Horton, H., and Brown, E. L. (1996). Expression monitoring by hybridization to high-density oligonucleotide arrays. Nat Biotechnol *14*, 1675-1680.

Lockhart, D. J., and Winzeler, E. A. (2000). Genomics, gene expression and DNA arrays. Nature *405*, 827-836.

Lubarsky, B., and Krasnow, M. A. (2003). Tube morphogenesis. Making and shaping biological tubes. Cell *112*, 19-28.

Lukyanov, K. A., Fradkov, A. F., Gurskaya, N. G., Matz, M. V., Labas, Y. A., Savitsky, A. P., Markelov, M. L., Zaraisky, A. G., Zhao, X., Fang, Y.*, et al.* (2000). Natural animal coloration can Be determined by a nonfluorescent green fluorescent protein homolog. J Biol Chem *275*, 25879-25882.

Machesky, L. M., Atkinson, S. J., Ampe, C., Vandekerckhove, J., and Pollard, T. D. (1994). Purification of a cortical complex containing two unconventional actins from Acanthamoeba by affinity chromatography on profilin-agarose. J Cell Biol *127*, 107-115.

Machesky, L. M., and Gould, K. L. (1999). The Arp2/3 complex: a multifunctional actin organizer. Curr Opin Cell Biol *11*, 117-121.

Machesky, L. M., and Insall, R. H. (1999). Signaling to actin dynamics. J Cell Biol *146*, 267-272.

Machesky, L. M., and May, R. C. (2001). Arps: actin-related proteins. Results Probl Cell Differ *32*, 213-229.

Manning, G., and Krasnow, M. A. (1993). Development of the Drosophila tracheal system. In The development of Drosophila melanogaster, M. Bate, and A. Martinez Arias, eds. (Cold Spring Harbor Laboratory press), pp. 609-685.

Manser, E., Huang, H. Y., Loo, T. H., Chen, X. Q., Dong, J. M., Leung, T., and Lim, L. (1997). Expression of constitutively active alpha-PAK reveals effects of the kinase on actin and focal complexes. Mol Cell Biol *17*, 1129-1143.

Matz, M. V., Lukyanov, K. A., and Lukyanov, S. A. (2002). Family of the green fluorescent protein: journey to the end of the rainbow. Bioessays *24*, 953-959.

McCartney, B. M., and Fehon, R. G. (1996). Distinct cellular and subcellular patterns of expression imply distinct functions for the Drosophila homologues of moesin and the neurofibromatosis 2 tumor suppressor, merlin. J Cell Biol *133*, 843-852.

McNally, J. G., Karpova, T., Cooper, J., and Conchello, J. A. (1999). Three-dimensional imaging by deconvolution microscopy. Methods *19*, 373-385.

Medina, M. A., and Schwille, P. (2002). Fluorescence correlation spectroscopy for the detection and study of single molecules in biology. Bioessays *24*, 758-764.

Meinhardt, H. (1999). Orientation of chemotactic cells and growth cones: models and mechanisms. J Cell Sci *112 (Pt 17)*, 2867-2874.

Metzger, R. J., and Krasnow, M. A. (1999). Genetic control of branching morphogenesis. Science *284*, 1635-1639.

Michelson, A. M., Gisselbrecht, S., Buff, E., and Skeath, J. B. (1998). Heartbroken is a specific downstream mediator of FGF receptor signalling in Drosophila. Development *125*, 4379-4389.

Mlodzik, M. (2002). Planar cell polarization: do the same mechanisms regulate Drosophila tissue polarity and vertebrate gastrulation? Trends Genet *18*, 564-571.

Mochizuki, N., Yamashita, S., Kurokawa, K., Ohba, Y., Nagai, T., Miyawaki, A., and Matsuda, M. (2001). Spatio-temporal images of growth-factor-induced activation of Ras and Rap1. Nature *411*, 1065-1068.

Montalta-He, H., Leemans, R., Loop, T., Strahm, M., Certa, U., Primig, M., Acampora, D., Simeone, A., and Reichert, H. (2002). Evolutionary conservation of otd/Otx2 transcription factor action: a genome-wide microarray analysis in Drosophila. Genome Biol *3*, RESEARCH0015.

Montell, D. J. (1999). The genetics of cell migration in Drosophila melanogaster and Caenorhabditis elegans development. Development *126*, 3035-3046.

Montell, D. J. (2001). Command and control: regulatory pathways controlling invasive behavior of the border cells. Mech Dev *105*, 19-25.

Montell, D. J., Rorth, P., and Spradling, A. C. (1992). slow border cells, a locus required for a developmentally regulated cell migration during oogenesis, encodes Drosophila C/EBP. Cell *71*, 51-62.

Morgan, T. H. (1934). The relation of genetics to physiology and medicine. Nobel lecture, presented in Stockholm on June 4, 1934.

Morin, X., Daneman, R., Zavortink, M., and Chia, W. (2001). A protein trap strategy to detect GFP-tagged proteins expressed from their endogenous loci in Drosophila. Proc Natl Acad Sci U S A *98*, 15050-15055.

Murphy, A. M., and Montell, D. J. (1996). Cell type-specific roles for Cdc42, Rac, and RhoL in Drosophila oogenesis. J Cell Biol *133*, 617-630.

Nagafuchi, A. (2001). Molecular architecture of adherens junctions. Curr Opin Cell Biol *13*, 600-603.

Nakai, J., Ohkura, M., and Imoto, K. (2001). A high signal-to-noise Ca(2+) probe composed of a single green fluorescent protein. Nat Biotechnol *19*, 137-141.

Nakano, A. (2002). Spinning-disk Confocal Microscopy - A Cutting-Edge Tool for Imaging of Membrane Traffic. Cell Struct Funct *27*, 349-355.

Nehls, S., Snapp, E. L., Cole, N. B., Zaal, K. J., Kenworthy, A. K., Roberts, T. H., Ellenberg, J., Presley, J. F., Siggia, E., and Lippincott-Schwartz, J. (2000). Dynamics and retention of misfolded proteins in native ER membranes. Nat Cell Biol *2*, 288-295.

Neufeld, T. P., de la Cruz, A. F., Johnston, L. A., and Edgar, B. A. (1998). Coordination of growth and cell division in the Drosophila wing. Cell *93*, 1183-1193.

Newsome, T. P., Schmidt, S., Dietzl, G., Keleman, K., Asling, B., Debant, A., and Dickson, B. J. (2000). Trio combines with dock to regulate Pak activity during photoreceptor axon pathfinding in Drosophila. Cell *101*, 283-294.

Nieto, M. A. (2001). The early steps of neural crest development. Mech Dev *105*, 27-35.

Niewiadomska, P., Godt, D., and Tepass, U. (1999). DE-Cadherin is required for intercellular motility during Drosophila oogenesis. J Cell Biol *144*, 533-547.

Nobes, C. D., and Hall, A. (1999). Rho GTPases control polarity, protrusion, and adhesion during cell movement. J Cell Biol *144*, 1235-1244.

Noselli, S. (2002). Drosophila, actin and videotape -- new insights in wound healing. Nat Cell Biol *4*, E251-253.

Noselli, S., and Agnes, F. (1999). Roles of the JNK signaling pathway in Drosophila morphogenesis. Curr Opin Genet Dev *9*, 466-472.

Nusslein-Volhard, C., and Wieschaus, E. (1980). Mutations affecting segment number and polarity in Drosophila. Nature *287*, 795-801.

Obermeier, A., Ahmed, S., Manser, E., Yen, S. C., Hall, C., and Lim, L. (1998). PAK promotes morphological changes by acting upstream of Rac. Embo J *17*, 4328-4339.

Oda, H., and Tsukita, S. (1999a). Dynamic features of adherens junctions during Drosophila embryonic epithelial morphogenesis revealed by a Dalpha-catenin-GFP fusion protein. Dev Genes Evol *209*, 218-225.

Oda, H., and Tsukita, S. (1999b). Nonchordate classic cadherins have a structurally and functionally unique domain that is absent from chordate classic cadherins. Dev Biol *216*, 406-422.

Ohshiro, T., Emori, Y., and Saigo, K. (2002). Ligand-dependent activation of breathless FGF receptor gene in Drosophila developing trachea. Mech Dev *114*, 3-11.

Ohshiro, T., and Saigo, K. (1997). Transcriptional regulation of breathless FGF receptor gene by binding of TRACHEALESS/dARNT heterodimers to three central midline elements in Drosophila developing trachea. Development *124*, 3975-3986.

O'Kane, C. J., and Gehring, W. J. (1987). Detection in situ of genomic regulatory elements in Drosophila. Proc Natl Acad Sci U S A *84*, 9123-9127.

Ormo, M., Cubitt, A. B., Kallio, K., Gross, L. A., Tsien, R. Y., and Remington, S. J. (1996). Crystal structure of the Aequorea victoria green fluorescent protein. Science *273*, 1392-1395.

Palecek, S. P., Huttenlocher, A., Horwitz, A. F., and Lauffenburger, D. A. (1998). Physical and biochemical regulation of integrin release during rear detachment of migrating cells. J Cell Sci *111*, 929-940.

Palecek, S. P., Loftus, J. C., Ginsberg, M. H., Lauffenburger, D. A., and Horwitz, A. F. (1997). Integrin-ligand binding properties govern cell migration speed through cell-substratum adhesiveness. Nature *385*, 537-540.

Palecek, S. P., Schmidt, C. E., Lauffenburger, D. A., and Horwitz, A. F. (1996). Integrin dynamics on the tail region of migrating fibroblasts. J Cell Sci *109*, 941-952.

Pantaloni, D., Boujemaa, R., Didry, D., Gounon, P., and Carlier, M. F. (2000). The Arp2/3 complex branches filament barbed ends: functional antagonism with capping proteins. Nat Cell Biol *2*, 385-391.

Pantaloni, D., Le Clainche, C., and Carlier, M. F. (2001). Mechanism of actin-based motility. Science *292*, 1502-1506.

Patel, N. H. (1994). Imaging neuronal subsets and other cell types in whole-mount Drosophila embryos and larvae using antibody probes. Methods Cell Biol *44*, 445-487.

Peifer, M., and Wieschaus, E. (1990). The segment polarity gene armadillo encodes a functionally modular protein that is the Drosophila homolog of human plakoglobin. Cell *63*, 1167-1176.

Perez, F., Diamantopoulos, G. S., Stalder, R., and Kreis, T. E. (1999). CLIP-170 highlights growing microtubule ends in vivo. Cell *96*, 517-527.

Perrimon, N., Noll, E., McCall, K., and Brand, A. (1991). Generating lineage-specific markers to study Drosophila development. Dev Genet *12*, 238-252.

Petit, V., Ribeiro, C., Ebner, A., and Affolter, M. (2002). Regulation of cell migration during tracheal development in Drosophila melanogaster. Int J Dev Biol *46*, 125-132.

Petit, V., and Thiery, J. P. (2000). Focal adhesions: structure and dynamics. Biol Cell *92*, 477-494.

Polesello, C., Delon, I., Valenti, P., Ferrer, P., and Payre, F. (2002). Dmoesin controls actin-based cell shape and polarity during Drosophila melanogaster oogenesis. Nat Cell Biol *4*, 782-789.

Ramirez-Weber, F. A., and Kornberg, T. B. (1999). Cytonemes: cellular processes that project to the principal signaling center in Drosophila imaginal discs. Cell *97*, 599-607.

Reichman-Fried, M., Dickson, B., Hafen, E., and Shilo, B. Z. (1994). Elucidation of the role of breathless, a Drosophila FGF receptor homolog, in tracheal cell migration. Genes Dev *8*, 428-439.

Reichman-Fried, M., and Shilo, B. Z. (1995). Breathless, a Drosophila FGF receptor homolog, is required for the onset of tracheal cell migration and tracheole formation. Mech Dev *52*, 265-273.

Ribeiro, C. (1998). Keeping the public informed about science--lessons from the Swiss gene protection initiative [letter]. Mol Med Today *4*, 14.

Ribeiro, C., Ebner, A., and Affolter, M. (2002). In vivo imaging reveals different cellular functions for FGF and Dpp signaling in tracheal branching morphogenesis. Dev Cell *2*, 677-683.

Ridley, A. J., and Hall, A. (1992). The small GTP-binding protein rho regulates the assembly of focal adhesions and actin stress fibers in response to growth factors. Cell *70*, 389-399.

Riesgo-Escovar, J. R., and Hafen, E. (1997). Common and distinct roles of DFos and DJun during Drosophila development. Science *278*, 669-672.

Rohatgi, R., Ma, L., Miki, H., Lopez, M., Kirchhausen, T., Takenawa, T., and Kirschner, M. W. (1999). The interaction between N-WASP and the Arp2/3 complex links Cdc42-dependent signals to actin assembly. Cell *97*, 221-231.

Rorth, P. (2002). Initiating and guiding migration: lessons from border cells. Trends Cell Biol *12*, 325-331.

Ruberte, E., Marty, T., Nellen, D., Affolter, M., and Basler, K. (1995). An absolute requirement for both the type II and type I receptors, punt and thick veins, for dpp signaling in vivo. Cell *80*, 889-897.

Rubin, G. M., Yandell, M. D., Wortman, J. R., Gabor Miklos, G. L., Nelson, C. R., Hariharan, I. K., Fortini, M. E., Li, P. W., Apweiler, R., Fleischmann, W.*, et al.* (2000). Comparative genomics of the eukaryotes. Science *287*, 2204-2215.

Rusch, J., and Levine, M. (1996). Threshold responses to the dorsal regulatory gradient and the subdivision of primary tissue territories in the Drosophila embryo. Curr Opin Genet Dev *6*, 416-423.

Samakovlis, C., Hacohen, N., Manning, G., Sutherland, D. C., Guillemin, K., and Krasnow, M. A. (1996). Development of the Drosophila tracheal system occurs by a series of morphologically distinct but genetically coupled branching events. Development *122*, 1395-1407.

Sanchez-Madrid, F., and del Pozo, M. A. (1999). Leukocyte polarization in cell migration and immune interactions. Embo J *18*, 501-511.

Sanders, L. C., Matsumura, F., Bokoch, G. M., and de Lanerolle, P. (1999). Inhibition of myosin light chain kinase by p21-activated kinase. Science *283*, 2083-2085.

Sato, M., and Kornberg, T. B. (2002). FGF is an essential mitogen and chemoattractant for the air sacs of the drosophila tracheal system. Dev Cell *3*, 195-207.

Schlessinger, J., Plotnikov, A. N., Ibrahimi, O. A., Eliseenkova, A. V., Yeh, B. K., Yayon, A., Linhardt, R. J., and Mohammadi, M. (2000). Crystal structure of a ternary FGF-FGFR-heparin complex reveals a dual role for heparin in FGFR binding and dimerization. Mol Cell *6*, 743-750.

Schneitz, K., Spielmann, P., and Noll, M. (1993). Molecular genetics of aristaless, a prd-type homeo box gene involved in the morphogenesis of proximal and distal pattern elements in a subset of appendages in Drosophila. Genes Dev *7*, 114-129.

Schober, M., and Perrimon, N. (2002). Unconventional ways to travel. Nat Cell Biol *4*, E211-212.

Schock, F., and Perrimon, N. (2002). Molecular mechanisms of epithelial morphogenesis. Annu Rev Cell Dev Biol *18*, 463-493.

Schoenwaelder, S. M., and Burridge, K. (1999). Bidirectional signaling between the cytoskeleton and integrins. Curr Opin Cell Biol *11*, 274-286.

Scholz, H., Deatrick, J., Klaes, A., and Klambt, C. (1993). Genetic dissection of pointed, a Drosophila gene encoding two ETS-related proteins. Genetics *135*, 455-468.

Schwann, T. (1847). Animal and plant cells drawn to show their similar nature and origin.

Sells, M. A., Knaus, U. G., Bagrodia, S., Ambrose, D. M., Bokoch, G. M., and Chernoff, J. (1997). Human p21-activated kinase (Pak1) regulates actin organization in mammalian cells. Curr Biol *7*, 202-210.

Shaw, L. M., Rabinovitz, I., Wang, H. H., Toker, A., and Mercurio, A. M. (1997). Activation of phosphoinositide 3-OH kinase by the alpha6beta4 integrin promotes carcinoma invasion. Cell *91*, 949-960.

Sheetz, M. P., Felsenfeld, D., Galbraith, C. G., and Choquet, D. (1999). Cell migration as a five-step cycle. Biochem Soc Symp *65*, 233-243.

Shiga, Y., Tanaka-Matakatsu, M., and Hayashi, S. (1996). A nuclear GFP beta-galactosidase fusion protein as a marker for morphogenesis in living *Drosophila*. Dev Growth Differ *38*, 99-106.

Shilo, B. Z., Gabay, L., Glazer, L., Reichman-Fried, M., Wappner, P., Wilk, R., and Zelzer, E. (1997). Branching morphogenesis in the Drosophila tracheal system. Cold Spring Harb Symp Quant Biol *62*, 241-247.

Shim, K., Blake, K. J., Jack, J., and Krasnow, M. A. (2001). The Drosophila ribbon gene encodes a nuclear BTB domain protein that promotes epithelial migration and morphogenesis. Development *128*, 4923-4933.

Silver, D. L., and Montell, D. J. (2001). Paracrine signaling through the JAK/STAT pathway activates invasive behavior of ovarian epithelial cells in Drosophila. Cell *107*, 831-841.

Small, J. V., Geiger, B., Kaverina, I., and Bershadsky, A. (2002). Opinion: How do microtubules guide migrating cells? Nat Rev Mol Cell Biol *3*, 957-964.

St Johnston, D. (2002). The art and design of genetic screens: Drosophila melanogaster. Nat Rev Genet *3*, 176-188.

Starz-Gaiano, M., and Lehmann, R. (2001). Moving towards the next generation. Mech Dev *105*, 5-18.

Steyer, J. A., and Almers, W. (2001). A real-time view of life within 100 nm of the plasma membrane. Nat Rev Mol Cell Biol *2*, 268-275.

Strutt, D. I., Weber, U., and Mlodzik, M. (1997). The role of RhoA in tissue polarity and Frizzled signalling. Nature *387*, 292-295.

Sutherland, D., Samakovlis, C., and Krasnow, M. A. (1996). branchless encodes a Drosophila FGF homolog that controls tracheal cell migration and the pattern of branching. Cell *87*, 1091-1101.

Tanaka-Matakatsu, M., Uemura, T., Oda, H., Takeichi, M., and Hayashi, S. (1996). Cadherin-mediated cell adhesion and cell motility in Drosophila trachea regulated by the transcription factor Escargot. Development *122*, 3697-3705.

Tautz, D., and Pfeifle, C. (1989). A non-radioactive in situ hybridization method for the localization of specific RNAs in Drosophila embryos reveals translational control of the segmentation gene hunchback. Chromosoma *98*, 81-85.

Tepass, U., Fessler, L. I., Aziz, A., and Hartenstein, V. (1994). Embryonic origin of hemocytes and their relationship to cell death in Drosophila. Development *120*, 1829-1837.

Tepass, U., Godt, D., and Winklbauer, R. (2002). Cell sorting in animal development: signalling and adhesive mechanisms in the formation of tissue boundaries. Curr Opin Genet Dev *12*, 572-582.

Tepass, U., Tanentzapf, G., Ward, R., and Fehon, R. (2001). Epithelial cell polarity and cell junctions in Drosophila. Annu Rev Genet *35*, 747-784.

Tepass, U., Truong, K., Godt, D., Ikura, M., and Peifer, M. (2000). Cadherins in embryonic and neural morphogenesis. Nat Rev Mol Cell Biol *1*, 91-100.

Teruel, M. N., and Meyer, T. (2000). Translocation and reversible localization of signaling proteins: a dynamic future for signal transduction. Cell *103*, 181-184.

Thiery, J. P. (2002). Epithelial-mesenchymal transitions in tumour progression. Nat Rev Cancer *2*, 442-454.

Toker, A. (1998). The synthesis and cellular roles of phosphatidylinositol 4,5-bisphosphate. Curr Opin Cell Biol *10*, 254-261.

Tsien, R. Y. (1998). The green fluorescent protein. Annu Rev Biochem *67*, 509-544.

Tsuneizumi, K., Nakayama, T., Kamoshida, Y., Kornberg, T. B., Christian, J. L., and Tabata, T. (1997). Daughters against dpp modulates dpp organizing activity in Drosophila wing development. Nature *389*, 627-631.

Van Aelst, L., and D'Souza-Schorey, C. (1997). Rho GTPases and signaling networks. Genes Dev *11*, 2295-2322.

Van Doren, M., Broihier, H. T., Moore, L. A., and Lehmann, R. (1998). HMG-CoA reductase guides migrating primordial germ cells. Nature *396*, 466-469.

van Roessel, P., and Brand, A. H. (2002). Imaging into the future: visualizing gene expression and protein interactions with fluorescent proteins. Nat Cell Biol *4*, E15-20.

Verkhusha, V. V., Tsukita, S., and Oda, H. (1999). Actin dynamics in lamellipodia of migrating border cells in the Drosophila ovary revealed by a GFP-actin fusion protein. FEBS Lett *445*, 395-401.

Vincent, S., Ruberte, E., Grieder, N. C., Chen, C. K., Haerry, T., Schuh, R., and Affolter, M. (1997). DPP controls tracheal cell migration along the dorsoventral body axis of the Drosophila embryo. Development *124*, 2741-2750.

Vincent, S., Wilson, R., Coelho, C., Affolter, M., and Leptin, M. (1998). The Drosophila protein Dof is specifically required for FGF signaling. Mol Cell *2*, 515-525.

Wallingford, J. B., Fraser, S. E., and Harland, R. M. (2002). Convergent extension: the molecular control of polarized cell movement during embryonic development. Dev Cell *2*, 695-706.

Wappner, P., Gabay, L., and Shilo, B. Z. (1997). Interactions between the EGF receptor and DPP pathways establish distinct cell fates in the tracheal placodes. Development *124*, 4707-4716.

White, J., and Stelzer, E. (1999). Photobleaching GFP reveals protein dynamics inside live cells. Trends Cell Biol *9*, 61-65.

Wilk, R., Weizman, I., and Shilo, B. Z. (1996). trachealess encodes a bHLH-PAS protein that is an inducer of tracheal cell fates in Drosophila. Genes Dev *10*, 93-102.

Wolf, C., and Schuh, R. (2000). Single mesodermal cells guide outgrowth of ectodermal tubular structures in Drosophila. Genes Dev *14*, 2140-2145.

Wood, W., Jacinto, A., Grose, R., Woolner, S., Gale, J., Wilson, C., and Martin, P. (2002). Wound healing recapitulates morphogenesis in Drosophila embryos. Nat Cell Biol *4*, 907-912.

Yamada, K. M., and Geiger, B. (1997). Molecular interactions in cell adhesion complexes. Curr Opin Cell Biol *9*, 76-85.

Zeitlinger, J., Kockel, L., Peverali, F. A., Jackson, D. B., Mlodzik, M., and Bohmann, D. (1997). Defective dorsal closure and loss of epidermal decapentaplegic expression in Drosophila fos mutants. Embo J *16*, 7393-7401.

Zelzer, E., and Shilo, B. Z. (2000a). Cell fate choices in Drosophila tracheal morphogenesis. Bioessays *22*, 219-226.

Zelzer, E., and Shilo, B. Z. (2000b). Interaction between the bHLH-PAS protein Trachealess and the POU-domain protein Drifter, specifies tracheal cell fates. Mech Dev *91*, 163-173.

Zhang, J., Campbell, R. E., Ting, A. Y., and Tsien, R. Y. (2002). Creating new fluorescent probes for cell biology. Nat Rev Mol Cell Biol *3*, 906-918.

Zhang, N., Zhang, J., Cheng, Y., and Howard, K. (1996). Identification and genetic analysis of wunen, a gene guiding Drosophila melanogaster germ cell migration. Genetics *143*, 1231-1241.

Zhang, N., Zhang, J., Purcell, K. J., Cheng, Y., and Howard, K. (1997). The Drosophila protein Wunen repels migrating germ cells. Nature *385*, 64-67.

Zhao, Z. S., Manser, E., Chen, X. Q., Chong, C., Leung, T., and Lim, L. (1998). A conserved negative regulatory region in alphaPAK: inhibition of PAK kinases reveals their morphological roles downstream of Cdc42 and Rac1. Mol Cell Biol *18*, 2153-2163.

Zigmond, S. H. (2000). How WASP regulates actin polymerization. J Cell Biol *150*, 117-120.

Appendix

Ich erkläre, dass ich die Dissertation, **Cellular and molecular analysis of branching morphogenesis in *Drosophila melanogaster***, nur mit der darin angegebenen Hilfe verfasst und bei keiner anderen Fakultät eingereicht habe.

CURRICULUM VITAE

Name: Ribeiro

First name: Carlos

Date of birth: November 10th, 1975

Place of birth: Basel, Switzerland

Citizenship: Portuguese

Marital status: unmarried

Private address:	Rasumofskygasse 1/10 A-1030 Wien, Austria	Phone: +43/1/9435262
Institute address:	Institute of Molecular Biotechnology (IMBA) Austrian Academy of Sciences Dr. Bohr-Gasse 3-5 A-1030 Wien, Austria	Phone: +43/1/79730423 Fax: +43/1/79730459
Email address:	Carlos.Ribeiro@imba.oeaw.ac.at	

Education and Research Experience:

1982-1986	Primary school, Basel, Switzerland
1986-1994	Gymnasium Bäumlihof, Basel, Switzerland
1994	Matur nach Typus B (Graduation)
1994-1999	Biozentrum, University of Basel, Switzerland Diploma studies in biology II
1997-1999	Biozentrum, University of Basel, Switzerland Diploma thesis under Prof. Dr. W. J. Gehring and Dr. M. Affolter **Topic:** *Molecular and genetic analysis of the requirement of the Mad binding sites for the Dpp responsiveness of the* labial *homeotic response element*
1999	Graduation as “dipl. biologie 2” (Master of Science)

1999-2003	Biozentrum, University of Basel, Switzerland PhD thesis in Prof. M. Affolter's group **Topic:** *Cellular and molecular analysis of branching morphogenesis in* Drosophila melanogaster
2003	Graduation as "Dr. phil." with *summa cum laude*
2003-2004	Biozentrum, University of Basel, Switzerland Postdoc in Prof. M. Affolter's group
2004-present	Institute of Molecular Biotechnology (IMBA) of the Austrian Academy of Sciences, Vienna, Austria EMBO postdoctoral fellow in Barry J. Dickson's group

---

Courses:

1998	EMBO Practical Course in "Genome Sequencing and Differential Gene Expression Analysis" at the EMBL, Heidelberg, Germany

0 Cold Spring Harbor Summer Advanced Course in "Advanced Drosophila Genetics" at the Cold Spring Harbor Laboratories, Cold Spring Harbor, NY, USA

Fellowships:

2004-present	EMBO long term fellowship

Publications

Ribeiro, C. (1998). Keeping the public informed about science - lessons from the Swiss gene protection initiative [letter]. **Mol Med Today** *4*, 14.

Marty, T., Vigano, M. A., **Ribeiro, C.**, Nussbaumer, U., Grieder N. C. and Affolter, M. (2001). A HOX complex, a repressor element and a 50 bp sequence confer regional specificity to a DPP-responsive enhancer. **Development** *128*, 2833-2845.

Ebner, A., Kiefer, F. N., **Ribeiro, C.**, Petit, V., Nussbaumer, U., and Affolter, M. (2002). Tracheal development in Drosophila melanogaster as a model system for studying the development of a branched organ. **Gene** *287*, 55-66.

Petit, V., **Ribeiro, C.**, Ebner, A. and Affolter, M. (2002). Regulation of cell migration during tracheal development in Drosophila melanogaster. **Int. J. Dev. Biol.** *46*, 125-132.

Ribeiro, C., Ebner, A. and Affolter, M. (2002). In vivo imaging reveals different cellular functions for FGF and Dpp signaling in tracheal branching morphogenesis. **Dev. Cell.** *2*, 677-683.

Ribeiro, C., Petit, V. and Affolter, M. (2003). Signaling systems, guided cell migration and organogenesis: insights from genetic studies in Drosophila. **Dev. Biol.**, *260(1)*, 1-8

Jazwinska, A., **Ribeiro, C.** and Affolter, M. (2003). Epithelial tube morphogenesis during Drosophila tracheal development requires Piopio, a luminal ZP protein. **Nat. Cell. Biol.**, *5(10),* 895-901.

Ribeiro, C., Neumann, M., Affolter, M. (2004). Genetic control of cell intercalation during tracheal morphogenesis in *Drosophila*. **Curr. Biol.**, *14(24)*, 2197-2207.